

PHASE 2 REPORT - REVIEW COPY
FURTHER SITE CHARACTERIZATION AND ANALYSIS
VOLUME 2B - PRELIMINARY MODEL CALIBRATION REPORT
HUDSON RIVER PCBs REASSESSMENT RI/FS

OCTOBER 1996



for
U.S. Environmental Protection Agency
Region II

Volume 2B
Book 1 of 2

Limno-Tech, Inc.
and
Menzie Cura & Associates, Inc.
and
The CADMUS Group, Inc.



UNITED STATES ENVIRONMENTAL PROTECTION AGENCY

REGION 2
290 BROADWAY
NEW YORK, NY 10007-1866

OCT 11 1996

To All Interested Parties:

The U.S. Environmental Protection Agency (EPA) is pleased to release the Preliminary Model Calibration Report for the Hudson River PCBs Superfund site. This report, the second in a series of six reports that will make up the Phase 2 Report, presents preliminary or interim findings about the modeling effort that is being conducted as part of the Reassessment RI/FS for the Hudson River PCBs Superfund site. EPA decided, based on extensive public comment, that it was important to share with those interested in the Reassessment the assumptions and data sets that would be used in the models, prior to using the models, even though this meant issuing a report on a work in progress. In order to determine the most appropriate data sets and assumptions for the models selected, EPA needed to do a significant amount of the modeling effort before this report could be issued.

Much of the data used in the Preliminary Model Calibration Report is from EPA's Phase 2 investigation, although data from numerous other sources have also been used. Although some of the data used in this report had not been validated, EPA believes it is important to provide the findings of the models in this preliminary report so that interested parties can fully evaluate the implications of the assumptions used within the models. Since the time the work for this report was conducted, the validation of the Phase 2 data has been completed, and the validated data are contained in the database that EPA released in March 1996. Any remedial decision for the site will be based upon validated data.

EPA would appreciate receiving comments on the Preliminary Model Calibration Report by November 22, 1996, so that any changes in the scope of the modeling effort can be made without delay to the Reassessment. It should be recognized that several significant assumptions in this report are based on findings which will be reported on in the Data Evaluation and Interpretation Report. That report, the third in the series of six Phase 2 reports, will be issued within the next several months. As such, EPA will accept comments on the Preliminary Model Calibration Report that are related to the Data Evaluation and Interpretation Report during the comment period for the latter report. Please refer to the report section and page number in each comment. Comments should be sent to:

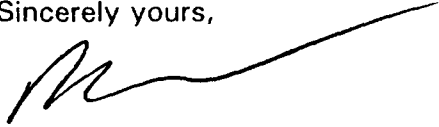
Douglas Tomchuk
US EPA - Region 2
290 Broadway - 20th Floor
New York, NY 10007-1866

Attn: PMCR Comments

A joint liaison group meeting will be held to discuss the Preliminary Model Calibration Report on Monday, October 28, 1996, at 7:30 p.m. at the Best Western Hotel at 200 Wolf Road in Albany.

We look forward to your involvement on the Preliminary Model Calibration Report and throughout the Reassessment. If you have any questions, please contact Ann Rychlenski, the Community Relations Coordinator for the Hudson River PCBs site Reassessment at (212) 637-3672.

Sincerely yours,

A handwritten signature in black ink, appearing to be 'R. Caspe', with a long, sweeping horizontal line extending to the right.

Richard L. Caspe, Director
Emergency and Remedial Response Division

CONTENTS

EXECUTIVE SUMMARY	E-1
1. INTRODUCTION	1-1
1.1 BACKGROUND	1-1
1.2 PURPOSE OF REPORT	1-1
1.3 REPORT FORMAT AND ORGANIZATION	1-3
2. SUMMARY AND PRELIMINARY CONCLUSIONS	2-1
2.1 SUMMARY.....	2-1
2.1.1 <i>Overall Approach</i>	2-1
2.1.2 <i>Water Column and Sediment Models</i>	2-1
2.1.3 <i>Fish Body Burden Models</i>	2-2
2.2 PRELIMINARY CONCLUSIONS	2-3
2.2.1 <i>Upper Hudson River PCB Mass Balance</i>	2-3
2.2.2 <i>Thompson Island Pool Hydrodynamics and Sediment Erosion</i>	2-6
2.2.3 <i>Upper Hudson River Fish Body Burdens</i>	2-7
2.2.4 <i>Lower Hudson PCB Mass Balance and Striped Bass Bioaccumulation</i>	2-9
3. MODELING APPROACH: TRANSPORT AND FATE.....	3-1
3.1 INTRODUCTION	3-1
3.2 MODELING GOALS AND OBJECTIVES	3-1
3.3 CONCEPTUAL APPROACH.....	3-2
3.4 HUDSON RIVER DATABASE.....	3-3
3.5 UPPER HUDSON RIVER MASS BALANCE MODEL.....	3-4
3.5.1 <i>Introduction</i>	3-4
3.5.2 <i>State Variables and Process Kinetics</i>	3-5
3.5.3 <i>Spatial-Temporal Scales</i>	3-7
3.5.4 <i>Application Framework</i>	3-9
3.6 THOMPSON ISLAND POOL HYDRODYNAMIC MODEL	3-9
3.6.1 <i>Introduction</i>	3-9
3.6.2 <i>State Variables and Process Mechanisms</i>	3-10
3.6.3 <i>Spatial-Temporal Scales</i>	3-12
3.6.4 <i>Application Framework</i>	3-12
3.7 THOMPSON ISLAND POOL DEPTH OF SCOUR MODEL	3-13
3.7.1 <i>Introduction</i>	3-13
3.7.2 <i>Process Representation</i>	3-14
3.7.3 <i>Spatial Temporal Scales</i>	3-16
3.7.4 <i>Applications Framework</i>	3-16
3.8 LOWER HUDSON RIVER PCB TRANSPORT AND FATE MODEL	3-16
3.8.1 <i>Introduction</i>	3-16
3.8.2 <i>State Variables and Process Kinetics</i>	3-17
3.8.3 <i>Spatial-Temporal Scales</i>	3-21
3.8.4 <i>Applications Framework</i>	3-21

4. CALIBRATION OF UPPER HUDSON RIVER PCB MODEL	4-1
4.1 INTRODUCTION	4-1
4.2 HISTORICAL TRENDS IN WATER QUALITY OBSERVATIONS.....	4-1
4.3 OVERVIEW OF PRELIMINARY CALIBRATION DATASET	4-2
4.4 MODEL INPUT DATA.....	4-4
4.4.1 <i>System-Specific Physical Data</i>	4-4
4.4.2 <i>External Loadings</i>	4-5
4.4.3 <i>Forcing Functions</i>	4-10
4.4.4 <i>Boundary Conditions</i>	4-11
4.4.5 <i>Initial Conditions</i>	4-12
4.5 INTERNAL MODEL PARAMETERS.....	4-14
4.5.1 <i>Solids Model Parameters</i>	4-14
4.5.2 <i>PCB Model Parameters</i>	4-14
4.6 CALIBRATION APPROACH.....	4-14
4.6.1 <i>Transport Model (Water Balance) Specification</i>	4-15
4.6.2 <i>Solids Model</i>	4-15
4.6.3 <i>PCB Model</i>	4-16
4.7 CALIBRATION RESULTS	4-18
4.7.1 <i>Solids Model</i>	4-18
4.7.2 <i>PCB Model</i>	4-20
4.8 MASS BALANCE COMPONENT ANALYSIS	4-23
4.9 PCB MODEL CALIBRATION SENSITIVITY ANALYSIS.....	4-27
5. CALIBRATION OF THOMPSON ISLAND POOL HYDRODYNAMIC MODEL	5-1
5.1 INTRODUCTION	5-1
5.2 MODEL INPUT DATA.....	5-1
5.2.1 <i>System-Specific Physical Data</i>	5-1
5.2.2 <i>Forcing Functions</i>	5-2
5.2.3 <i>Boundary Conditions</i>	5-3
5.3 INTERNAL MODEL PARAMETERS	5-3
5.4 CALIBRATION APPROACH.....	5-4
5.5 CALIBRATION RESULTS	5-4
5.6 MODEL VALIDATION.....	5-5
5.6.1 <i>Rating Curve Velocity Measurements</i>	5-5
5.6.2 <i>FEMA Flood Studies</i>	5-5
5.7 100 YEAR FLOOD MODEL RESULTS.....	5-6
5.8 SENSITIVITY ANALYSES.....	5-6
5.8.1 <i>Manning's 'n'</i>	5-6
5.8.2 <i>Turbulent Exchange Coefficient</i>	5-7
5.9 CONVERSION OF FLOW VELOCITY TO SHEAR STRESS	5-7
5.9.1 <i>Results</i>	5-9
5.10 DISCUSSION.....	5-9
6. APPLICATION OF THOMPSON ISLAND POOL DEPTH OF SCOUR MODEL	6-1

6.1 INTRODUCTION	6-1
6.2 AVAILABLE DATA	6-1
6.2.1 <i>Bottom Sediment Distribution</i>	6-2
6.2.2 <i>Resuspension Experiments</i>	6-2
6.3 MODEL PARAMETERIZATION AND UNCERTAINTY	6-3
6.3.1 <i>Rearrangement of Erosion Equation</i>	6-3
6.3.2 <i>Parameter Estimation</i>	6-4
6.3.3 <i>Prediction Limits</i>	6-5
6.4 DEPTH OF SCOUR PREDICTIONS AT SELECTED LOCATIONS IN COHESIVE SEDIMENT AREAS	6-5
6.5 GLOBAL RESULTS FOR COHESIVE SEDIMENT AREAS	6-7
7. APPLICATION OF LOWER HUDSON RIVER PCB TRANSPORT AND FATE MODEL	7-1
7.1 INTRODUCTION	7-1
7.2 MODEL INPUT DATA	7-1
7.2.1 <i>System-Specific Physical Data</i>	7-1
7.2.2 <i>External Loadings</i>	7-2
7.2.3 <i>Forcing Functions</i>	7-3
7.2.4 <i>Boundary Conditions</i>	7-4
7.2.5 <i>Initial Conditions</i>	7-4
7.3 INTERNAL MODEL PARAMETERS	7-4
7.4 APPLICATION APPROACH	7-6
7.5 APPLICATION RESULTS	7-7
7.6 DIAGNOSTIC ANALYSES	7-8
7.6.1 <i>Component Analysis</i>	7-8
7.6.2 <i>Sensitivity Analysis</i>	7-9
7.7 DISCUSSION	7-10
8. MODELING APPROACH: FISH BODY BURDENS	8-1
8.1 MODELING GOALS AND OBJECTIVES	8-1
8.2 BACKGROUND	8-3
8.2.1 <i>PCB Compounds</i>	8-3
8.2.2 <i>PCB Accumulation Routes</i>	8-4
8.3 THEORY FOR MODELS OF PCB BIOACCUMULATION	8-7
8.4 BIVARIATE STATISTICAL MODEL FOR FISH BODY BURDENS	8-10
8.4.1 <i>Rationale and Limitations for Bivariate Statistical Model</i>	8-10
8.4.2 <i>Theory for Bivariate Statistical Models of PCB Bioaccumulation</i>	8-10
8.5 PROBABILISTIC BIOACCUMULATION FOOD CHAIN MODEL	8-12
8.5.1 <i>Rationale and Limitations</i>	8-12
8.5.2 <i>Model Structure</i>	8-14
8.5.3 <i>Spatial Scale for Model Application</i>	8-16
8.5.4 <i>Temporal Scales for Estimating Exposure to Fish</i>	8-16
8.5.5 <i>Characterizing Model Compartments</i>	8-16

9. CALIBRATION OF BIVARIATE STATISTICAL MODEL FOR FISH BODY BURDENS	9-1
9.1 DATA USED FOR DEVELOPMENT OF BIVARIATE BAF MODELS	9-1
9.1.1 <i>Fish Data</i>	9-1
9.1.2 <i>Standardization of PCB Results for NYSDEC Fish Analyses</i>	9-3
9.1.3 <i>Water Column Data</i>	9-7
9.1.4 <i>Sediment Data</i>	9-8
9.1.5 <i>Functional Grouping of Sample Locations for Analysis</i>	9-10
9.2 RESULTS OF BIVARIATE BAF ANALYSIS	9-11
9.3 DISCUSSION OF BIVARIATE BAF RESULTS	9-13
9.4 SUMMARY.....	9-15
10. CALIBRATION OF PROBABILISTIC BIOACCUMULATION FOOD CHAIN MODEL	10-1
10.1 OVERVIEW OF DATA USED TO DERIVE BAFs	10-1
10.1.1 <i>Benthic Invertebrates</i>	10-1
10.1.2 <i>Water Column Invertebrates</i>	10-2
10.1.3 <i>Fish</i>	10-2
10.1.4 <i>Literature Values</i>	10-3
10.2 BENTHIC INVERTEBRATE:SEDIMENT ACCUMULATION FACTORS (BSAF)	10-3
10.2.1 <i>Sediment Concentrations</i>	10-3
10.2.2 <i>Approach</i>	10-4
10.2.3 <i>Calculations of BSAF Values for Benthic Invertebrates</i>	10-6
10.3 WATER COLUMN INVERTEBRATE:WATER ACCUMULATION FACTORS (BAFs)	10-12
10.3.1 <i>Approach</i>	10-12
10.3.2 <i>Calculation of BAF_{water} for Water Column Invertebrates</i>	10-15
10.3.3 <i>Alternative Approaches</i>	10-16
10.4 FORAGE FISH:DIET ACCUMULATION FACTORS (FFBAFs)	10-18
10.4.1 <i>Approach</i>	10-19
10.4.2 <i>Water Column Concentrations Used to Derive FFBAF Values</i>	10-20
10.4.3 <i>Forage Fish Body Burdens Used to Derive FFBAF Values</i>	10-20
10.4.4 <i>Calculation of FFBAF Values for Forage Fish</i>	10-23
10.4.5 <i>Calculation of FFBAFs for Small Pumpkinseed Sunfish</i>	10-24
10.5 PISCIVOROUS FISH:DIET ACCUMULATION FACTORS (PFBAF)	10-25
10.5.1 <i>Approach Used for Yellow Perch</i>	10-25
10.5.2 <i>Approach Used for Largemouth Bass</i>	10-25
10.5.3 <i>Approach Used for White Perch</i>	10-26
10.6 DEMERSAL FISH:SEDIMENT RELATIONSHIPS	10-27
10.6.1 <i>Approach and Calculations of BAF Values</i>	10-27
10.7 SUMMARY OF PROBABILISTIC FOOD CHAIN MODELS	10-27
10.8 ILLUSTRATION OF FOOD CHAIN MODEL APPLICATION	10-28
10.9 COMPARISON OF BIVARIATE STATISTICAL AND FOOD CHAIN MODELS	10-28
REFERENCES.....	R-1

EXECUTIVE SUMMARY

The U.S. Environmental Protection Agency (USEPA) is currently conducting a study of the Hudson River PCB Superfund Site, reassessing the interim No Action decision that the Agency made in 1984. The purpose of the Reassessment is to determine an appropriate course of action for the PCB-contaminated sediments in the Upper Hudson River in order to protect human health and the environment. PCBs (polychlorinated biphenyls) were discharged into the Upper Hudson River from two capacitor plants in Hudson Falls and Fort Edward, New York. The Superfund Site extends from Hudson Falls to the Battery in New York City, a distance of approximately 200 river miles. Unacceptable levels of PCBs in fish tissue have resulted in fishing bans and fishing restrictions throughout the river.

This report provides an update on the mathematical modeling efforts being conducted as part of the Reassessment. It is meant as a preliminary or interim report, in that the purpose of the report is to provide interested parties with information about the data and assumptions that are being used in the models, prior to completion of the actual modeling work. Therefore, many of the conclusions are preliminary and may change as the models are further refined and calibrated. When the models are completed, the modeling results will be presented in the Baseline Modeling Report and model predictions for various remedial alternatives will be included in the Phase 3 Report (Feasibility Study).

Study Objectives

The models described in this Preliminary Model Calibration Report were designed to answer the following questions:

1. When will PCB levels in the fish population recover to levels meeting human health and ecological risk criteria under continued No Action?
2. Can remedies other than No Action significantly shorten the time required to achieve acceptable risk levels?
3. Are there contaminated sediments now buried and effectively sequestered from the food chain which are likely to become "reactivated" following a major flood, resulting in an increase in contamination of the fish population?

The overall goal of the modeling analysis is to develop and field validate useful and scientifically credible mass balance models in order to answer these questions. The modeling approach is based on the principle of conservation of mass, that is, the quantity of material that enters a section of the river must be equal to the quantity of material that leaves the section, plus any internal sources or minus any environmental losses.

A large body of information from site-specific field measurements, laboratory experiments and a search of the scientific literature was synthesized within models for the Upper Hudson River and the tidal freshwater portion of the Lower Hudson River. Models were developed for the transport and fate of PCBs in the water column and sediments, and for PCB body burdens in fish. The integration of these different models allows for the simulation of transport and fate of PCBs that enter the river from the upstream boundary at Fort Edward, from various tributaries, across the air-water interface and across the sediment-water interface.

Transport and Fate Model Development

The overall concept involved the development and application of a set of individual models to describe hydrology, solids dynamics and PCB dynamics in the river water and sediments. The principal time frame of interest is from 1983 through 1994. Diverse and extensive data from numerous sources were used in developing and calibrating the models.

The Reassessment database contains information from: USEPA, New York State Department of Environmental Conservation (NYSDEC), U.S. Geological Survey (USGS), General Electric (GE) and private and academic research investigators. The most intensive datasets available are from the USEPA Phase 2 investigations conducted in 1993 and 1994. The USEPA database for the Reassessment is described more fully in the Database Report which was issued in October, 1995. The database itself was issued in March, 1996, and is available on CD-ROM.

Upper Hudson River PCB Model

The Upper Hudson River PCB Model (HUDTOX) is a mass balance model that includes hydrology, solids and PCBs in river water and sediments. HUDTOX was applied to the Upper Hudson River from the northern tip of Rogers Island (upper end of Thompson Island Pool) to Federal Dam at Troy. HUDTOX provides the ability to simulate total PCBs, as well as specific PCB congeners (BZ#4, BZ#28, BZ#52, BZ#[90+101] and BZ#138), based on their particular physical and chemical properties. To date, HUDTOX has been calibrated to field data for the period January 1 through September 30, 1993, coinciding with the USEPA Phase 2 monitoring program.

Thompson Island Pool Hydrodynamic Model

This model computes localized water velocities corresponding to different river flows for areas within Thompson Island Pool (where the contaminated sediments are most concentrated). Results from this model are used as input to the Thompson Island Pool Depth of Scour Model.

Thompson Island Pool Depth of Scour Model

The quantity of sediments likely to become "reactivated" (scoured) following a major flood depends on the velocity of the river flow. River velocities are computed using the Thompson Island Pool Hydrodynamic Model. The Thompson Island Pool Depth of Scour Model is used to determine the range of scour depths and quantities of resuspended (scoured) solids and PCBs during high flow events. The maximum flow simulated using this model corresponds to a 100-year flood.

Lower Hudson River PCB Model

An existing mass balance model developed by Thomann et al., (1989) was used for hydrology, solids and PCBs in Lower Hudson River water and sediments. The Thomann model was applied to the portion of the Hudson River below Federal Dam at Troy. The model represents total PCBs in terms of the sum of individual PCB homologues. The model was validated using revised PCB loads over Federal Dam without the need for re-calibration of the original model parameters.

[Note: EPA understands that as of September 1996, the Thomann model is being updated under a grant from the Hudson River Foundation, and that certain modifications have been made to the published model. EPA is evaluating whether the updated model will be available or appropriate for use in the Reassessment.]

Development of Fish Body Burden Models

The overall concept involved development and application of a set of models for relating body burdens of PCBs (expressed as Aroclor equivalents, individual congeners or total PCBs) in fish to exposure concentrations in Hudson River water and sediments.

Bivariate Statistical Model

The Bivariate Statistical Model relates measured PCB levels in water and sediments (two variables, or "bivariate") to measured PCB levels in fish. This model was applied to the Upper Hudson River and to a segment of the Lower Hudson River near Albany. The Bivariate Statistical Model was developed using the historical PCB Aroclor database.

Probabilistic Bioaccumulation Food Chain Model

The Probabilistic Bioaccumulation Food Chain Model relies upon feeding relationships to link fish body burdens to PCB exposure concentrations in water and sediments. The model combines information from available PCB exposure measurements with knowledge about the ecology of different fish species and the relationships among larger fish, smaller fish, and smaller animals in the water

column and sediments. The Probabilistic Model was developed using both historical and current field data, and was applied to the Upper Hudson River and to a segment of the Lower Hudson River near Albany. In contrast to the Bivariate Statistical Model, which provides average body burden estimates, the Probabilistic Model provides information on uncertainty and variability around these average estimates.

As part of the development of the Probabilistic Model, species-specific profiles (i.e., descriptions of feeding behavior, range and movement) were developed for Yellow Perch, Largemouth Bass, Pumpkinseed Sunfish, Brown Bullhead, White Perch, Spottail Shiner, Shortnose Sturgeon and Striped Bass. These profiles include characteristics that could potentially affect bioaccumulation of PCBs.

Thomann Food Chain Model

The Thomann Food Chain Model is part of the PCB transport and fate model for the Lower Hudson River. The model links PCB exposure concentrations to PCB body burdens in White Perch and Striped Bass. The Thomann model does not explicitly consider the effect of contaminated sediments on accumulation of PCBs in the food chain.

Principal Report Findings

Since this is a preliminary calibration report, it does not present definitive answers to the principal Reassessment questions. However, a number of preliminary conclusions have been drawn based on the work presented here, including:

- The PCB mass balance model for the Upper Hudson River (HUDTOX) provides a reasonable representation of hydraulics, solids dynamics and PCB dynamics for the period of simulation corresponding to the USEPA Phase 2 monitoring program.
- The principal external loadings of total PCBs to the Upper Hudson River during the period of the HUDTOX simulation were across the upstream boundary at Fort Edward (74 percent).
- During the period of the HUDTOX simulation, the model computed a large gain in total PCB mass across Thompson Island Pool between Fort Edward and Thompson Island Dam.
- Large increases in water column concentrations of dissolved phase PCBs, especially for lower-chlorinated congeners, are observed to occur across Thompson Island Pool. These increases appear to be caused by an internal source within Thompson Island Pool.

- The processes controlling PCB dynamics in Thompson Island Pool are not fully understood at the present time. One hypothesis that could explain the large increases in PCB concentrations across the pool is sediment-water advective flux of pore water PCBs due to groundwater inflow. Such a pore water advective flux would be relatively more important for lower-chlorinated PCB congeners due to their greater water solubilities.
- The Thompson Island Pool Hydrodynamic Model produced results that were in good agreement with available information for river flow velocities and water elevations.
- For a 100-year flood event, the Thompson Island Pool Depth of Scour Model predicts that 1,838,600 pounds of solids and 55 pounds of total PCBs will be scoured from the cohesive sediment areas. This mass of PCBs represents less than 1 percent of the total reservoir of PCBs in the cohesive sediment areas of Thompson Island Pool, based on measurements of the in-place reservoir of PCBs from the 1984 NYSDEC survey.
- For a 100-year flood event, the Thompson Island Pool Depth of Scour Model predicts a median depth of scour of 0.41 inches in the cohesive sediment areas. Considering the uncertainty in model predictions, the average depth of scour for this event could range from 0.08 to 2.46 inches.
- The Bivariate Statistical Model for fish body burdens indicates the relative importance of both water column and local sediments as pathways for bioaccumulation of PCBs in Upper Hudson River fish. Reported Aroclor 1016 burdens are mainly attributed to water column concentrations for all species. Reported Aroclor 1254 burdens, which include more highly-chlorinated PCB congeners that tend to accumulate in fat, show a wide range in the relative importance of water column and sediment pathways among different species. Results for Aroclor 1254 are consistent with species feeding behavior: for species that feed in the water column, the water column pathway tends to dominate, while for bottom-feeders, the sediment pathway tends to be dominant. Fish-eating species at higher levels in the food chain appear to accumulate Aroclor 1254 from both water column and sediment pathways.
- The Probabilistic Bioaccumulation Food Chain Model indicates that water pathways contribute significantly to PCB body burdens in forage fish (including Pumpkinseed Sunfish) and Yellow Perch. Water and sediment are both important for Largemouth Bass, and sediment is the main exposure pathway for the bottom-feeding Brown Bullhead. These results compare favorably with results from the Bivariate Statistical Model.

- Results from the original Lower Hudson River modeling effort by Thomann et al., (1989) were successfully reproduced.

Future Baseline Modeling Efforts

The conclusions presented in this Preliminary Model Calibration Report indicate that significant new understanding has been gained about PCB transport, fate and bioaccumulation in the Hudson River. The modeling work for this Reassessment is continuing and more definitive conclusions will be presented in the Baseline Modeling Report. The purpose of this future modeling work is to reduce uncertainties contained in the preliminary models. Future plans include continued development of both the transport and fate mass balance models, and the fish body burden models. They also include applications of these models to additional field data that became available after completion of this preliminary model calibration work.

Future work with the HUDTOX model will include development of a more finely-resolved spatial segmentation grid for Thompson Island Pool, application to daily suspended solids data collected during the Spring 1994 high-flow period and re-calibration using the complete, validated, Phase 2 field data for 1993. Finally, a long-term (1984-1993) hindcasting calibration will be conducted to confirm the predictive capability of the model over a decadal time scale.

Future work with the Thompson Island Pool Depth of Scour Model will include extension of the modeling framework to include both cohesive and non-cohesive sediment areas, and application to the complete, validated, Phase 2 field data for 1993.

Future work with the fish body burden models will include application to NYSDEC 1995 fish data, further analysis of exposure pathways involving water column invertebrates and exploration of patterns of congener uptake between and among different fish species. In addition, use of a model based on fugacity (Gobas, 1993), or chemical potential, will be explored.

The final version of HUDTOX will be used to simulate PCB concentrations in the water column and sediments due to No Action and various flood events. For these simulations, the output of the HUDTOX model for the Upper Hudson River will be linked to the Thomann model for the Lower Hudson River. In turn, the PCB outputs from these Upper and Lower Hudson River models will be linked to the fish body burden models. Finally, predictive modeling simulations to evaluate the effects of various remedial scenarios will be presented as part of the Phase 3 Report (Feasibility Study).

1. INTRODUCTION

1.1 Background

The Hudson River watershed encompasses an area of 13,390 square miles, principally in the eastern portion of New York State (Figure 1-1). The Hudson River PCB Superfund Site extends from Hudson Falls, New York, to the Battery in New York Harbor (River Mile 0), a stretch of almost 200 river miles (Figure 1-2). The Upper Hudson refers to the 40-mile stretch of river upstream of Federal Dam at Troy to Hudson Falls (Figure 1-3). The Lower Hudson refers to the portion of the river downstream of Federal Dam to the Battery (Figure 1-4).

For approximately 30 years, two General Electric (GE) facilities, one in Fort Edward and the other in Hudson Falls (Figure 1-5), used polychlorinated biphenyls (PCBs) to make electrical capacitors. GE discontinued use of PCBs in 1977 when they ceased to be manufactured and sold in the United States. From 1957 through 1975, between 209,000 and 1.3 million pounds of PCBs were discharged from these facilities into the Upper Hudson River. Migration of PCBs downstream was greatly enhanced in 1973 with the removal of Fort Edward Dam and the subsequent release of PCB-contaminated sediments. A region of special concern is the highly-contaminated sediments in Thompson Island Pool (TIP) which is located immediately downstream of the old Fort Edward dam site (Figure 1-5).

In 1976, the New York State Department of Environmental Conservation (NYSDEC) imposed a ban on fishing in the Upper Hudson River due to the potential risk posed by consumption of PCB-contaminated fish. In August 1995, the Upper Hudson was re-opened to fishing, but only on a catch-and-release basis. NYSDEC also imposed a ban on commercial fishing for striped bass in the Lower Hudson River. This ban remains in effect.

In 1984 the U.S. Environmental Protection Agency (USEPA) completed a Feasibility Study on the site that investigated remedial alternatives and issued a Record of Decision (ROD) later that year. The ROD called for: (1) an interim No Action decision concerning river sediments; (2) in-place capping, containment and monitoring of remnant deposit (formerly impounded) sediments; and, (3) a treatability study to evaluate the effectiveness of the Waterford Treatment Plant in removing PCBs from Hudson River water.

1.2 Purpose of Report

In December 1990, USEPA issued a Scope of Work for reassessing the No Action decision for the Hudson River PCB site. The scope of work identified three phases:

- Phase 1 - Interim Characterization and Evaluation
- Phase 2 - Further Site Characterization and Analysis
- Phase 3 - Feasibility Study.

The Phase 1 Report (TAMS/Gradient, 1991) is Volume 1 of the Reassessment documentation and was issued by USEPA in August 1991. It contains a compendium of background material, discussion of findings and preliminary assessment of risks.

The Final Phase 2 Work Plan and Sampling Plan (TAMS/Gradient, 1992) detailed the following main data collection tasks to be completed during Phase 2:

- High- and low-resolution sediment coring
- Geophysical surveying and confirmatory sampling
- Water column sampling (including transects and flow-averaged composites)
- Ecological field program.

The Database Report (Volume 2A in the Phase 2 series of reports; TAMS/Gradient, 1995) and accompanying CD-ROM database issued in March 1996 provides the validated data for the Phase 2 investigation. The Data Evaluation and Interpretation Report (Volume 2C in the Phase 2 series of reports; TAMS/CADMUS/Gradient, 1996 - pending publication) presents results and findings of water column sampling, high-resolution sediment coring, geophysical surveying and confirmatory sampling, geostatistical analysis of 1984 sediment data and PCB fate and transport dynamics.

This Preliminary Model Calibration Report is Volume 2B in the Phase 2 series of reports. It includes descriptions of the transport and fate mass balance models, and the fish body burden models that are being used for this PCB Reassessment RI/FS. All of the work described herein was conducted as part of Task 4 - Preliminary Model Calibration Report. The scope of Task 4 was limited to documentation of the conceptual approaches, databases and preliminary calibration results for each model. With the exception of the Thompson Island Pool Depth of Scour Model, no results are presented for use of the calibrated models as predictive tools. All results in this report are preliminary results from ongoing investigations and should be considered strictly provisional in nature.

The modeling work for this PCB Reassessment RI/FS is continuing as part of the Baseline Modeling phase of the overall study. To provide a more complete context for the modeling results in the present report, work plans for this Baseline Modeling phase are presented in Appendix B. These plans include continuing development with both the transport and fate mass balance models, and the fish body burden models. They also include applications of these models to additional Phase 2 field data that became available after completion of this preliminary model calibration work.

1.3 Report Format and Organization

Section 2 of this report contains a general summary of the preliminary model calibration work and preliminary conclusions drawn from this work. Section 3 contains a description of the overall approach for the transport and fate models, and descriptions of the individual models for the Upper Hudson River, Thompson Island Pool and the Lower Hudson River. Section 4 contains preliminary model calibration results for the Upper Hudson River PCB Model. Section 5 contains preliminary model calibration results for the Thompson Island Pool Hydrodynamic Model. Section 6 contains preliminary model calibration results for the Thompson Island Pool Depth of Scour Model and predictions from this model for a range of flood events, including the 100-year flood. Section 7 contains application results for the Lower Hudson River PCB Model.

Section 8 of this report contains a description of the overall approach for the fish body burden models and descriptions of the individual models for the Upper and Lower portions of the Hudson River. Section 9 contains preliminary model calibration results for the Bivariate Statistical Model. Section 10 contains preliminary model calibration results for the Probabilistic Bioaccumulation Food Chain Model.

The material in this report has been divided into two separate books. Book 1 contains the report text, a list of references, and a glossary of abbreviations and acronyms. Book 2 contains all tables, figures, plates and appendices. Within Book 2, Appendix A contains ecological profiles for fish species represented in the fish body burden models. Appendix B contains the plans for future modeling work.

2. SUMMARY AND PRELIMINARY CONCLUSIONS

2.1 Summary

The following is a general summary of the modeling work conducted to date under Task 4 of this Hudson River PCB Reassessment RI/FS.

2.1.1 Overall Approach

The overall modeling approach is based on the principle of conservation of mass. A large body of information from site-specific field measurements, laboratory experiments and the scientific literature was synthesized within quantitative models for the Upper Hudson River and the tidal freshwater portion of the Lower Hudson River. Models were developed for the transport and fate of PCBs in the water column and bedded sediments, and for PCB body burdens in fish.

The contents of this report are limited to documentation of the conceptual approaches, databases and preliminary calibration results for each model. With the exception of the Thompson Island Pool Depth of Scour Model, no results are presented for use of the calibrated models as predictive tools. All results in this report are preliminary results from ongoing investigations and should be considered strictly provisional in nature.

2.1.2 Water Column and Sediment Models

1. Three separate mass balances are being conducted for the Hudson River: (a) a water balance; (b) a solids balance; and (c) a PCB balance. Each balance includes specification of external inputs, internal sources and sinks, and system outputs.
2. The PCB mass balance in the Upper Hudson River is being conducted using the HUDTOX model developed as part of this RI/FS. This mass balance includes total PCBs and five separate congeners, or groups of co-eluting congeners, corresponding to BZ#4 (2,2'-dichlorobiphenyl), BZ#28 (2,4,4'-trichlorobiphenyl), BZ#52 (2,2',5,5'-tetrachlorobiphenyl), BZ#[90+101] (2,2',3,4',5-Pentachlorobiphenyl and 2,2',4,5,5'-pentachlorobiphenyl) and BZ#138 (2,2',3,4,4',5'-hexachlorobiphenyl).
3. The PCB mass balance in the Lower Hudson River is being conducted using an existing transport and fate model developed by Thomann et al., (1989). This mass balance includes total PCBs represented as the sum of individual homologues.
4. Bathymetry, delineation of cohesive (fine-grained) and non-cohesive (coarse-grained) sediment areas, and an inventory of sediment PCBs were discretized within a fine-scale, grid-based Geographical Information System (GIS) for

Thompson Island Pool in the Upper Hudson River. The cohesive sediment areas in Thompson Island Pool are considered to encompass most of the known PCB "hotspots".

5. Separate Hydrodynamic and Depth of Scour Models were applied to Thompson Island Pool to estimate the range of scour depths and quantities of solids and PCBs eroded from cohesive sediment areas due to large flood events. The maximum design flow in this investigation was 47,330 cfs at Rogers Island, corresponding to a flow return period of 100 years.

2.1.3 Fish Body Burden Models

1. Three approaches for fish body burdens are being used in this study: (a) a Bivariate Statistical Model; (2) a Probabilistic Bioaccumulation Food Chain Model; and (3) the Thomann food chain model. The Thomann food chain model is part of the transport and fate model for the Lower Hudson River. Each of these approaches provides a different perspective on the question of PCB bioaccumulation in fish.
2. The Bivariate Statistical Model represents PCBs in terms of total PCBs and selected Aroclors. The Probabilistic Bioaccumulation Food Chain Model represents total PCBs, selected Aroclors, and the five congeners used in calibration of the HUDTOX model. The Thomann food chain model represents PCB homologues.
3. The Bivariate Statistical Model for fish body burden in a given species is based on the historical dataset of Aroclor measurements, with corrections for changing quantitation methods. It is designed to provide an empirical, preliminary scoping of the causal relationships described in the Probabilistic Bioaccumulation Food Chain Model. The statistical model relies on a bivariate regression approach which relates fish body burden to concentrations in both water and sediment. This allows for the possibility that water and sediment concentrations are not in equilibrium, as is frequently observed in the Upper Hudson River.
4. The Probabilistic Bioaccumulation Food Chain Model consists of the following biotic compartments: (a) benthic invertebrates; (b) water column invertebrates; (c) forage fish; (d) piscivorous fish; (e) demersal fish; and (f) omnivorous fish. PCB concentrations are expressed as lipid-normalized in biota, total organic carbon normalized in sediments and fraction organic carbon normalized in the particulate phase in the water column. Relationships among compartments are expressed as bioaccumulation factors between the concentration in a given compartment and the expected dietary exposure for that compartment. The dietary exposure is based on a weighted concentration in the diet.

5. Species-specific profiles are presented for Yellow Perch (*Perca flavescens*), Largemouth Bass (*Micropterus salmoides*), Pumpkinseed (*Lepomis gibbosus*), Brown Bullhead (*Ictalurus nebulosus*), White Perch (*Morone americana*), Spottail Shiner (*Notropis hudsonius*), Shortnose Sturgeon (*Acipenser brevirostrum*) and Striped Bass (*Morone saxatilis*). These profiles describe foraging strategies, home-ranges and information on reproduction for each of these species.
6. Several sample look-up tables are provided for the predicted 25th, mean, 75th and 95th percentiles for the yellow perch model. Note that the values in these look-up tables are based on unvalidated data and are subject to change. They are provided in this report strictly for illustrative purposes.
7. Statistical distributions of bioaccumulation factors have been derived to date for:
 - (a) sediments to benthic invertebrates (calibration congeners, Aroclors 1016 and 1254, and total PCBs);
 - (b) particulate phase in the water column to water column invertebrates (total PCBs and Aroclors 1016 and 1254);
 - (c) expected dietary concentrations to composite forage fish (total PCBs and Aroclors 1016 and 1254)
 - (d) expected dietary concentrations to yellow perch (total PCBs);
 - (e) pumpkinseed to largemouth bass (total PCBs and Aroclors 1016 and 1254);
 - (f) sediment to brown bullhead (calibration congeners and total PCBs); and
 - (g) benthic invertebrates to brown bullhead (calibration congeners and total PCBs).

2.2 Preliminary Conclusions

The following preliminary conclusions can be drawn from the modeling work conducted to date under Task 4 of this Hudson River PCB Reassessment RI/FS.

2.2.1 Upper Hudson River PCB Mass Balance

1. The PCB mass balance model for the Upper Hudson River (HUDTOX) provides a reasonable representation of hydraulics, solids dynamics and PCB dynamics during a period of simulation corresponding to the Phase 2 water column monitoring program, January 1 through September 30, 1993.
2. The principal hydraulic inputs to the Upper Hudson River during the period of simulation were inflow across the upstream boundary at Fort Edward (34 percent) and tributary inflow from the Mohawk River near the downstream boundary at Federal Dam (43 percent). The remaining inputs were from smaller tributaries and direct runoff.

3. The principal **external** solids loadings to the Upper Hudson River during the period of simulation were from the Mohawk River (58 percent) and the Hoosic River (20 percent). Solids loadings across the upstream boundary at Fort Edward represented only 8.5 percent of the total **external** solids loadings.
4. The principal **external** loadings of total PCBs to the Upper Hudson River during the period of simulation were across the upstream boundary at Fort Edward (74 percent) and from the Mohawk River (18 percent).
5. Hydraulic inputs and external loadings of solids and total PCBs to the Upper Hudson River during the period of simulation showed a strong seasonal dependence. The spring high flow period (March 26 - May 10), which represents 17 percent of the total period of simulation, was responsible for 56 percent of the hydraulic inputs, 87 percent of the solids loadings and 68 percent of the total PCB loadings to the Upper Hudson River during the total period of simulation.
6. The calibrated HUDTOX model represents the average behavior of water column total PCBs and the five congener groups reasonably well during the simulation period. There were 24 combinations of PCB types and model spatial segments for which field data were available for model calibration. Segment-average values for model output were significantly different ($p < 0.05$) than segment-average observed values in only three of these 24 cases.
7. The calibrated HUDTOX model was also successful in representing the more highly resolved day-to-day variability across all model segments. Regression analyses of model output vs. observations were conducted using paired daily values for total PCBs and each of the five congener groups. Results indicated that the HUDTOX model explained an average of 70 percent of the overall spatial-temporal variability in these more highly resolved field data.
8. During the total period of simulation, there was an 8.1 percent gain in water column solids mass across Thompson Island Pool between the upstream boundary at Fort Edward and Thompson Island Dam. The gain in water column solids mass was 7.8 percent during the spring high flow period and 10 percent during the remaining lower flow period.
9. Over the period of simulation, the total mass of solids input across the upstream boundary at Fort Edward was equal to 92 percent of the solids mass transported across Thompson Island Dam. The corresponding quantities during the spring high flow period and the remaining lower flow period were 93 percent and 91 percent, respectively. The total mass of solids due to gross resuspension from the surface sediment layer in

Thompson Island Pool was equal to 20 percent of the solids mass transported across Thompson Island Dam. The corresponding quantity during the spring high flow period was 16 percent. During the remaining lower flow period, solids in Thompson Island Pool were lost from the water column due to net sedimentation.

10. During the total period of simulation, there was a 102 percent gain in total PCB mass across Thompson Island Pool between the upstream boundary at Fort Edward and Thompson Island Dam. The gain in total PCB mass was 104 percent during the spring high flow period and 100 percent during the remaining lower flow period.
11. During the total period of simulation, the total mass of total PCBs input across the upstream boundary at Fort Edward was equal to 49 percent of the total PCB mass transported across Thompson Island Dam. The corresponding quantities during the spring high flow period and the remaining lower flow period were 49 percent and 50 percent, respectively. The total mass of total PCBs due to gross resuspension from the surface sediment layer in Thompson Island Pool was equal to 57 percent of the total PCB mass transported across Thompson Island Dam. The corresponding quantities during the spring high flow period and the remaining lower flow period were 57 percent and 58 percent, respectively.
12. There were significant differences between the dynamics of total PCBs and the dynamics of lower-chlorinated PCB congeners. For example, during the total period of simulation, there was a 585 percent gain in BZ#4 mass across Thompson Island Pool between the upstream boundary at Fort Edward and Thompson Island Dam. The gain in BZ#4 mass was 1435 percent during the spring high flow period and 278 percent during the remaining lower flow period.
13. During the total period of simulation, the total mass of BZ#4 input across the upstream boundary at Fort Edward was equal to only 15 percent of the total BZ#4 mass transported across Thompson Island Dam. The corresponding quantities during the spring high flow period and the remaining lower flow period were 6.5 and 27 percent, respectively. The total mass of BZ#4 due to gross resuspension from the surface sediment layer in Thompson Island Pool was equal to 80 percent of the total BZ#4 mass transported across Thompson Island Dam. The corresponding quantities during the spring high flow period and the remaining lower flow period were 94 percent and 59 percent, respectively. The principal factor responsible for differences between total PCBs and lower-chlorinated congeners appears to be that sediments in Thompson Island Pool are relatively more contaminated with lower-chlorinated congeners than with total PCBs.

14. Large increases in water column concentrations of apparent dissolved phase (i.e. truly dissolved plus dissolved organic carbon-bound) PCBs, especially for lower-chlorinated congeners, are observed to occur across Thompson Island Pool. These increases appear to be caused by an internal source within Thompson Island Pool. It is not clear whether these increases in PCB concentrations originate from historical sediment sources or from more recent discharges.
15. The physical, chemical and biological processes controlling PCB dynamics in Thompson Island Pool are not fully understood at the present time. One hypothesis that could explain the large increases in PCB concentrations across Thompson Island Pool is sediment-water advective flux of pore water PCBs due to groundwater inflow. Such a pore water advective flux would be relatively more important for lower-chlorinated PCB congeners due to their greater water phase solubilities.
16. Sensitivity analyses were conducted with the calibrated HUDTOX model in which total PCB loadings across the upstream boundary at Fort Edward were varied by plus/minus 30 percent. In response to these variations, the total PCB mass transported across Thompson Island Dam varied by plus/minus 14 percent and total PCB loadings across Federal Dam to the Lower Hudson River varied by plus/minus 7 percent.
17. Sensitivity analyses were conducted with the calibrated HUDTOX model in which initial total PCB concentrations in the sediments were varied by plus/minus 30 percent. In response to these variations, the total PCB mass transported across Thompson Island Dam varied by plus/minus 16 percent and total PCB loadings across Federal Dam to the Lower Hudson River varied by plus/minus 20 percent.

2.2.2 Thompson Island Pool Hydrodynamics and Sediment Erosion

1. The Thompson Island Pool hydrodynamic model (RMA-2V) is a two-dimensional, vertically-averaged, time-variable model. This model was used to predict steady-state velocity distributions in Thompson Island Pool for a range of design flows. Results from the RMA-2V model are in good agreement with available measurements for river flow velocities and water elevations. Results from the model for a 100-year flow were consistent with independent results from a FEMA flood modeling study.
2. For a 100-year flood event (47,330 cfs at Rogers Island), the RMA-2V model predicts a mean river flow velocity of 0.945 fps in Thompson Island Pool. Based on the predicted two-dimensional flow velocity distribution, mean applied shear stress in the cohesive sediment areas of Thompson Island Pool was estimated to be 19.5 dynes/cm² for this event.

3. For a 100-year flood event, the Thompson Island Pool Depth of Scour Model predicts that 834,000 kg of solids and 25 kg of total PCBs will be eroded from the cohesive sediment areas. This mass of PCBs represents less than 1 percent of the total reservoir of PCBs in the cohesive sediment areas of Thompson Island Pool, based on measurements of the in-place reservoir of PCBs from the 1984 NYSDEC survey.
4. For a 100-year flood event, the Thompson Island Pool Depth of Scour Model predicts a median depth of scour of 0.16 cm in the cohesive sediment areas. Considering the uncertainty in model predictions, the average depth of scour for this event could range from 0.03 cm (5th percentile) to 0.97 cm (95th percentile).
5. As part of the Phase 2 high-resolution sediment coring effort, detailed vertical profiles are available at five locations in Thompson Island Pool. At all of these locations, depths of observed PCB concentration peaks were greater than predicted median depths of scour for a 100-year flood event.
6. Analysis of uncertainties in the Thompson Island Pool Depth of Scour Model was conducted at the locations of the five high-resolution sediment cores. At four of these five locations, depths of observed PCB concentration peaks were outside the middle 90 percent certainty ranges around predicted median depths of scour.
7. Results from the Thompson Island Pool Depth of Scour Model represent erosion of solids and PCBs from only the cohesive sediment areas, which are considered to encompass most of the known PCB "hotspots". This model is based on assumptions and governing equations that were developed and validated exclusively for cohesive sediments.

2.2.3 Upper Hudson River Fish Body Burdens

1. The Bivariate Statistical Model provides good explanatory power in predicting annual mean total PCB and Aroclor body burden in fish, based on analysis of NYSDEC samples collected from River Mile 142 to River Mile 193 between 1975 and 1992. This scoping exercise indicates that a steady-state food web model of fish body burden, driven by water column and sediment PCB concentrations, is feasible.
2. The Bivariate Statistical Model for fish body burdens indicates the relative importance of water column and local sediment-derived pathways for bioaccumulation of PCBs in five species of Upper Hudson River fish, measured as Aroclor equivalents. Reported Aroclor 1016 burdens are dominantly attributed to water column inputs in all species. Reported Aroclor 1254 burdens, which include more lipophilic and more highly-chlorinated PCB congeners in the quantitation, show a wide range in the relative importance of sediment and water column pathways among different species. The results for Aroclor 1254 are consistent with species foraging behavior and

trophic position: for species at lower trophic levels which forage in the water column, the water column pathway is dominant, while for bottom-foraging species the sediment pathway is dominant. Piscivorous species at higher trophic levels appear to integrate Aroclor 1254 accumulation from both water column and sediment pathways.

3. Statistical models for fish body burdens based on historical monitoring data are dependent on the manner in which Aroclors were quantified by NYSDEC. Reliability of parameter estimates for the statistical models is also limited by the data on water column concentrations, which are generally available only as total PCBs for the period prior to 1991, and the lack of adequate data on time trends in sediment exposure concentrations. The statistical models also do not attempt to address variability in body burden resulting from age and variations in foraging with size, nor seasonal patterns related to temperature and spawning cycles.
4. Biota body burdens in the Probabilistic Bioaccumulation Food Chain Model are expressed as lognormal distributions in which 90 percent of the predicted concentrations fall within the observed range for the five calibration congeners, Aroclors 1016 and 1254, and total PCBs.
5. The Probabilistic Bioaccumulation Food Chain Model indicates that water pathways contribute significantly to PCB body burdens in forage fish (including pumpkinseed sunfish) and yellow perch. Water and sediment are important for largemouth bass and sediment is the main exposure pathway for brown bullhead. These results compare favorably with the results from the Bivariate Statistical Model.
6. Results from the Probabilistic Bioaccumulation Food Chain Model are sensitive to initial concentrations. Although the relationships among each of the compartments have been well established, the model predictions reflect the underlying variability and uncertainty in the water column and sediment PCB concentrations. Model predictions also reflect uncertainties in inter-compartmental relationships. The model defines the percentage of a fish species population expected to be at or below a given concentration (i.e. at the 90th percentile concentration, 90 percent of that species population will experience PCB body burdens at or below the 90th percentile concentration).
7. The sample look-up tables provide an indication of the expected biota body burdens under different sediment-water concentration combinations. The Probabilistic Bioaccumulation Food Chain Model can be used as a tool to evaluate the change in the ratio between water and sediment concentrations.

2.2.4 Lower Hudson PCB Mass Balance and Striped Bass Bioaccumulation

1. Results from the original Lower Hudson River modeling effort by Thomann et al., (1989) were successfully reproduced in this Hudson River PCB Reassessment RI/FS. The Thomann et al., (1989) model is presently the best available tool for quantifying: (a) PCB transport and fate; and (b) bioaccumulation in striped bass in the Lower Hudson River.
2. Subsequent to the original Thomann et al., (1989) modeling effort, revised estimates were made for PCB loadings across Federal Dam to the Lower Hudson River. Preliminary simulations with the Thomann model using these revised PCB loadings indicate that results are still consistent with the original calibration, due in part to large uncertainties in available field observations in the Lower Hudson River.
3. Results from the Thomann model indicate that under recent historical conditions, the tidal freshwater portion of the Lower Hudson River is influenced primarily by PCB loadings across Federal Dam, and that the estuarine portion of the Lower Hudson River is influenced primarily by direct external loadings and loadings from the vicinity of New York City.
4. Results from the Thomann model indicate that net uptake of PCBs by striped bass occurs primarily in the mid-lower Hudson River between River Miles 18.5 and 78.5, and that net loss of PCBs from striped bass occurs in all spatial segments downstream of this area.

3. MODELING APPROACH: TRANSPORT AND FATE

3.1 Introduction

This section contains a description of the overall approach for the transport and fate models, and descriptions of the individual models for the Upper Hudson River, Thompson Island Pool and the Lower Hudson River. Section 3.2 contains the goals and objectives of the overall modeling work in this Hudson River PCB RI/FS. Section 3.3 contains a discussion of the conceptual approach for the transport and fate, and fish body burden models.

Section 3.4 contains a brief summary of the Hudson River database created to support this RI/FS. Section 3.5 contains a description of the Upper Hudson River Mass Balance Model. Section 3.6 contains a description of the Thompson Island Pool Hydrodynamic Model. Section 3.7 contains a description of the Thompson Island Pool Depth of Scour Model. Section 3.8 contains a description of the Lower Hudson River PCB Transport and Fate Model.

Detailed descriptions of the Bivariate Statistical Model and the Probabilistic Bioaccumulation Food Chain Model are contained in Section 8.

3.2 Modeling Goals and Objectives

The goals and objectives of the modeling work described herein were designed to answer the following principal RI/FS questions:

1. When will PCB levels in fish populations recover to levels meeting human health and ecological risk criteria under continued No Action?
2. Can remedies other than No Action significantly shorten the time required to achieve acceptable risk levels?
3. Are there contaminated sediments now buried and effectively sequestered from the food chain that are likely to become "reactivated" following a major flood, possibly resulting in an increase in contamination of the fish population?

The overall goal of the modeling analysis in the reassessment effort is to develop and field validate scientifically credible mass balance models for evaluating and comparing the impacts of continued No Action, various remedial scenarios and hydrometeorological events in terms of PCB concentrations in the water column and sediment, and PCB body burdens in fish.

The specific objectives of the modeling analysis are the following:

1. Develop and apply a predictive model for PCB levels in water and sediments over long-term (decadal) time scales in the Upper Hudson River;
2. Evaluate the impacts of PCB loadings from the Upper Hudson River on PCB levels in water and sediments in the freshwater portion of the Lower Hudson River;
3. Estimate the risk of resuspension of PCBs from the deeply buried sediments of Thompson Island Pool in response to a "catastrophic" flood event;
4. Estimate the impacts of potential resuspension from a "catastrophic" event in Thompson Island Pool on downstream PCB concentrations in water and sediments;
5. Evaluate and apply quantitative models of the relationships between PCB water and sediment concentrations and fish body burdens in the Upper and Lower Hudson River; and,
6. Apply the Hudson River models to evaluate and compare predicted responses to continued No Action, various remedial scenarios and hydrometeorological events in terms of PCB concentrations in water, sediments and fish.

The principal study areas are the Upper Hudson River from Fort Edward to Federal Dam at Troy (Figure 1-3) and the freshwater portion of the Lower Hudson River from Federal Dam to River Mile 55 (Figure 1-4). More detailed analyses are being conducted in Thompson Island Pool (TIP), a 6-mile portion of the Upper Hudson River between Fort Edward and Thompson Island Dam (Figure 1-5).

3.3 Conceptual Approach

The overall modeling approach in this RI/FS reassessment is based on the principle of conservation of mass. Models are being developed for the transport and fate of PCBs in the water column and bedded sediments, and for PCB body burdens in fish. The principal modeling endpoints in this study are the following:

- PCB concentrations in water, bedded sediments and fish
- Mass of PCBs eroded in Thompson Island pool due to a "catastrophic" flood event
- Mass loading rates of PCBs at Thompson Island Dam due to a "catastrophic" flood event
- Mass loading rates of PCBs at Federal Dam

- Mass loadings rates of PCBs from the freshwater portion of the Lower Hudson River to the estuarine portion.

Three separate mass balances are being conducted for the Hudson River: (1) a water balance; (2) a solids balance; and (3) a PCB mass balance. A water balance is necessary because PCB transport is influenced by river flow rates and mixing rates. A solids balance is necessary because PCB fate is influenced by the tendency of PCBs to sorb, or attach, to both suspended and bedded solids in the river. Finally, a PCB mass balance is necessary to estimate PCB water column and sediment concentrations as a function of external loadings, sediment-water exchanges and air-water exchanges.

Two separate models are being applied to Thompson Island Pool to estimate the mass of PCBs eroded due to large flood events: a hydrodynamic model and a depth of scour model for solids and associated PCBs. The hydrodynamic model is being used to determine flow velocities and shear stresses at the sediment-water interface. The depth of scour model is being used to determine the range of scour depths and quantities of resuspended solids and PCBs in cohesive sediment areas.

Three approaches for fish body burdens are being used in this study: (1) a Bivariate Statistical Model; (2) a Probabilistic Bioaccumulation Food Chain Model; and (3) the Thomann food chain model. Each of these approaches provides a different perspective on the question of PCB bioaccumulation in fish. The Bivariate Statistical and Probabilistic Bioaccumulation Models are presented in Section 8. The Thomann food chain model is part of the transport and fate model for the Lower Hudson River and is presented in Section 3.8.

3.4 Hudson River Database

All modeling work in the present report utilized the extensive database that was created to support this Hudson River PCB RI/FS (TAMS/Gradient, 1995). This database contains information from a large variety of different sources:

- New York State Department of Environmental Conservation (NYSDEC)
- New York State Department of Health (NYSDOH)
- New York State Department of Transportation (NYSDOT)
- General Electric Company (GE)
- Lamont-Doherty Earth Observatory (LDEO)
- United States Geological Survey (USGS)
- National Oceanic and Atmospheric Administration (NOAA)
- United States Environmental Protection Agency (USEPA).

The database contains measurements for sediments, fish and aquatic biota, surface water flow and surface water quality. The database includes a total of approximately 750,000 records. Almost 350,000 of these records contain data acquired as part of the USEPA Phase 2 Work Plan and Sampling Plan (TAMS/Gradient, 1992). The remaining records contain data from a large number of historical and ongoing monitoring efforts in the Hudson River.

All transport and fate modeling work in the present report was conducted using field data contained in Release 2.3 of the TAMS/Gradient Phase 2 database. Release 2.3 was an earlier version of the database that contained much unvalidated data and did not contain results from the Phase 2 low-resolution sediment coring effort or from high-frequency measurements conducted during the Spring 1994 high-flow period. Release 3.1, issued in March 1996, contains the final, validated Phase 2 field data.

3.5 Upper Hudson River Mass Balance Model

3.5.1 Introduction

The mass balance model being used for the Upper Hudson River (HUDTOX) is a modified version of the EPA-supported WASP4 toxic chemical model (Ambrose et al., 1988). Many of the modifications to WASP4 were developed as part of the Green Bay Mass Balance Study (Bierman et al., 1992). The HUDTOX model is designed to accomplish the following modeling objectives:

1. Predict PCB concentrations in the water column and sediments over long-term (decadal) time scales in the Upper Hudson River;
2. Estimate the impacts of potential resuspension from a "catastrophic" event in TIP on downstream PCB concentrations in the water column and sediments; and,
3. Evaluate and compare predicted responses to continued No Action, various remedial scenarios and hydrometeorological events in the Upper Hudson River.

The HUDTOX model includes both water column and sediment compartments, and simultaneous mass balances for water, solids and PCBs. The model is three-dimensional in space and variable in time.

Figure 3-1 contains conceptual representations of the water, solids and PCB mass balances in the HUDTOX model. Mass is balanced in space in terms of a finite number of control volumes, or spatial segments. These spatial segments are linked, as specified by the user, to allow inter-segment transport of water, solids and PCBs through mechanisms such as advective flow, dispersive mixing, particle settling and sediment resuspension. Physical-chemical mechanisms are included to describe the transformation and fate of PCBs within model segments. These

mechanisms include equilibrium partitioning between PCBs and solids, and sediment-water and air-water exchanges.

The HUDTOX model requires a large amount of input data in the form of system-specific physical characteristics, external loadings, forcing functions, boundary conditions and initial conditions. The principal model inputs include the following:

- Geometry for model spatial segmentation grid in water column and bedded sediments
- Advective flow rates and dispersive mixing rates
- External mass loading rates for all model state variables
- Particle gross settling, resuspension and net burial velocities
- Equilibrium partition coefficients for PCBs
- Sediment-water and air-water exchange rates for PCBs
- Atmospheric gas phase PCB concentration
- Initial conditions for all model state variables.

Many of these model inputs, such as geometry and water flow rates, are specified using direct measurements for the Upper Hudson River. Some model inputs, such as sediment-water and air-water exchange rates, are specified using available information from the scientific literature. Finally, model inputs such as gross settling and resuspension velocities are determined through calibration of model output to Upper Hudson River field data.

3.5.2 State Variables and Process Kinetics

The general HUDTOX mass balance equations are fully documented in Ambrose et al., (1988). This reference includes model theory, a user manual and a programmer's guide. Apart from the water balance equations, the HUDTOX model consists of two simultaneous, coupled mass balances for solids and PCBs. These two mass balances can be viewed as submodels within the overall HUDTOX modeling framework.

Solids Submodel

Particle dynamics are important in controlling the transport, transformation and fate of PCBs in aquatic systems due to the tendency of PCBs to sorb, or attach, to both suspended and bedded solids (e.g. Eadie and Robbins, 1987). Karickhoff (1979; 1984) has shown that organic carbon is the principal sorbent compartment for hydrophobic organic chemicals, such as PCBs, in aquatic systems. In addition to organic carbon in particulate form, dissolved organic carbon (DOC) can also be important in the sorption and fate of PCBs (e.g. Eadie et al., 1990; Bierman et al., 1992).

The HUDTOX solids submodel consists of two state variables: total suspended solids (TSS), and DOC. These two state variables represent the sorbent compartments for toxic chemicals within the HUDTOX model framework. Figure 3-2 displays the relationships among these solids state variables in HUDTOX.

All particulate matter, both biotic and abiotic, is represented as TSS in HUDTOX because neither the Phase 2 nor the historical data include sufficient parameter measurements to allow simulation of multiple solids types. To represent particulate organic carbon, a constant organic carbon fraction is assigned to TSS (Thomann and Mueller, 1987). Internal loadings of biotic solids due to primary production are represented in the solids model. These loadings were externally specified using estimates based on field measurements of primary productivity in the freshwater portion of the Lower Hudson River (Cole et al., 1992).

Toxic Chemical Submodel

The principal state variable in the HUDTOX toxic chemical submodel is total chemical concentration. HUDTOX represents the components of total chemical in three phases through the use of equilibrium partitioning relationships. Figure 3-3 illustrates these phases which include: truly dissolved chemical, TSS-sorbed chemical, and DOC-sorbed chemical. The PCB measurements in the Phase 2 database do not distinguish DOC-bound PCBs from truly dissolved PCBs, but measure these phases together as "apparent" dissolved phase PCBs. Nonetheless, it is important to distinguish truly dissolved phase concentrations from DOC-bound concentrations because bioconcentration of PCBs, due to direct uptake from ambient water, is driven by only the truly dissolved phase component (e.g. DiToro et al., 1991).

A schematic diagram of the HUDTOX toxic chemical submodel components and process mechanisms is shown in Figure 3-4. Since the solids and chemical submodels in HUDTOX are fully integrated, they are structurally the same. The toxic chemical submodel includes additional process mechanisms to simulate equilibrium phase partitioning between unbound (or truly dissolved), TSS-sorbed, and DOC-sorbed chemical. In addition, air-water exchange of dissolved chemical,

and sediment-water exchanges of truly dissolved and DOC-sorbed chemical are included.

Two important differences between the HUDTOX and WASP4 toxic chemical kinetics should be noted. First, HUDTOX includes temperature-corrected Henry's Law constants (H) as described in Achman et al., (1993) and shown in Equation 3-1.

$$\log H_T = \log H_{298} * (7.91 - 3414.0 / T) / (7.91 - 3414.0 / 298.15) \quad (3-1)$$

This correction affects air-water exchange to a significant degree for PCBs, since H_T can vary by an order of magnitude for the range of water temperatures (approximately 0 to 30 deg. C) observed in the Upper Hudson River. A second kinetic modification employed in HUDTOX is a temperature correction for PCB partition coefficients (K_p) as proposed by TAMS/CADMUS/Gradient (1996 - pending publication). The form of this empirical relationship is shown in Equation 3-2.

$$\log K_{p,T} = \log K_{p,293.15^\circ K} + TSF * (1/T - 1/293.15) \quad (3-2)$$

where,

- K_p = partition coefficient (L/kg)
- T = water temperature ($^\circ K$)
- TSF = temperature slope factor ($^\circ K$).

Other enhancements which simplify application of the toxic chemical model have also been made and are described by Bierman et al., (1992) for the model application to Green Bay, Lake Michigan.

3.5.3 Spatial-Temporal Scales

The HUDTOX water column geometry was developed with 13 spatial segments to represent the Upper Hudson River. The model segments run from the northern tip of Rogers Island (River Mile 194.6) to Federal Dam (River Mile 153.9) as displayed in Figure 3-5. The resolution of this spatial segmentation grid was determined primarily by the available field data in Release 2.3 of the TAMS/Gradient Phase 2 database. As part of the future modeling work (Appendix B), a more finely-resolved spatial segmentation grid will be developed for TIP. This grid will be two-dimensional in the horizontal and will consist of 10-20 spatial segments.

The period of simulation for the HUDTOX model calibration in the present report was January 1 to September 30, 1993, coinciding with the Phase 2 water column monitoring program. The characteristic time scale for this HUDTOX calibration was monthly to seasonal. As part of the future modeling work (Appendix B), the HUDTOX model will also be calibrated to high-frequency data

collected during the Spring 1994 high-flow period. In addition, a long-term hindcasting calibration will be conducted over a decadal time scale (1984-1993).

The selection criteria for specifying the HUDTOX water column segmentation include the following:

1. The location of major tributaries to the Upper Hudson River;
2. The location of lock and dam structures along the river;
3. The location of any significant sources of direct PCB loading to the river;
4. The location of Phase 2 and historic sampling stations;
5. The location of USGS gaging stations; and,
6. Sediment PCB "hot spot" locations along the river.

The specific water column geometry was determined based upon data collected by the TAMS/Gradient team and General Electric (TAMS/CADMUS/Gradient, 1996 - pending publication). Surficial areas of HUDTOX segments were determined within the ARC/INFO Geographic Information System (GIS) based upon Upper Hudson River shoreline coordinates. Table 3-1 provides a comparison of the HUDTOX segment surface areas with river geometry developed during the 1984 Feasibility Study (NUS, 1984).

Hydrographic survey data collected by General Electric during 1991 (O'Brien and Gere, 1993b) were used to estimate HUDTOX model segment cross-sections. The TAMS/Gradient team also has extensive hydrographic measurements of a portion of the Upper Hudson River, but the General Electric data provide a more complete coverage. No significant differences were found between the two datasets in regions covered by both surveys, including TIP, so the General Electric data were used exclusively in determining cross-section geometry for HUDTOX. The General Electric bathymetric elevation data were processed into distinct river cross-sections. Figure 3-6 displays the approximate locations of the bathymetric data along the length of the river. Water surface elevations representative of average flow conditions in the river were assigned to each bathymetric cross-section to determine average HUDTOX segment cross-sectional areas and depths. Thirteen water column segments (numbered 1 through 13) were constructed to represent the Upper Hudson River. Segments 1, 2 and 3 are used to represent Thompson Island Pool.

The HUDTOX sediment geometry, underlying the water column segmentation, was based upon the only recent, comprehensive sediment information available at the time of this preliminary model calibration work (O'Brien and Gere, 1993a). The General Electric sediment cores are represented in layers of 0-5 cm, 5-10 cm, and 10-25 cm, so HUDTOX was developed with directly corresponding sediment segment layers, plus two additional deep layers representing 25-50 cm and 50-100 cm. Altogether, 65 segments (numbered 14-78) are used to represent the Upper Hudson River sediment within the HUDTOX model framework as shown by Figure 3-7. A non-interacting sediment boundary layer segment (Segment 79) was also used to simplify the tracking of any deep burial of toxic chemical out of the spatial segmentation grid.

The upper 5 cm active sediment layer thickness is consistent with applications of WASP4-based PCB models at other sites. A surficial sediment mixed layer depth of 4 cm was determined for Green Bay, Lake Michigan, based on ²¹⁰Pb sediment profiles (Bierman et al., 1992), while a 10 cm surficial sediment layer was used by Velleux and Endicott (1994) to model PCBs in the Lower Fox River, Wisconsin. The deeper sediment layers of 25 and 50 cm in thickness were incorporated in HUDTOX to ensure that the total sediment PCB reservoir will be represented in future long-term historical hindcasting and decadal projection applications.

3.5.4 Application Framework

The HUDTOX model was developed within the EPA-WASP4 computer coding framework maintained and distributed by the EPA Center for Exposure Assessment Modeling, Athens, Georgia (Ambrose et al., 1988). The model was compiled and run using the FTN77/486 FORTRAN 77 software (Version 2.51) developed by the University of Salford and distributed by OTG Systems, Inc. Model development, testing and applications were conducted on IBM-PC compatible computers with 32 bit, 80486- and Pentium-based microprocessors.

3.6 Thompson Island Pool Hydrodynamic Model

3.6.1 Introduction

The TIP Hydrodynamic Model was developed to provide necessary input information for the TIP Depth of Scour Model. The Depth of Scour Model requires information on shear stresses exerted at the sediment-water interface for a given river flow rate. The TIP Hydrodynamic Model computes river flow fields in terms of water depths and velocities. In turn, these river flow fields are used to compute shear stresses at the sediment-water interface.

The TIP Hydrodynamic Model consists of the RMA-2V finite element model. This hydrodynamic model, developed and used by the U.S. Army Corps of Engineers, is a well-known model which has been applied to many different rivers and estuaries in the United States. In these applications, RMA-2V has been shown to accurately model various flow fields. Also, RMA-2V is the only hydrodynamic model for which commercially available software has been developed for pre- and post-processing the model input and output.

A short summation of the hydrodynamic model is as follows. A finite element grid is first constructed for the TIP section of the river. The RMA-2V finite element model solves for the river's flow field at specified nodes of the elements. The flow field is hydraulically determined by the specified upstream flow, the river's boundary conditions and the river's resistance to flow. The downstream boundary was obtained from a rating curve developed for the stage-discharge gage near the Thompson Island Dam, the downstream boundary. The river's resistance is quantified by the river channel's Manning's 'n'.

This next sections describe the solution variables and equations used to compute the values of these variables, the temporal and spatial scales of the model and the framework in which the model was applied.

3.6.2 State Variables and Process Mechanisms

The model state variables are the velocities of flow in the x and y directions (horizontally), u and v, and the depth of flow, h. To solve for these three variables, three equations are needed. These are as follows:

1. Continuity

$$\frac{\partial h}{\partial t} + \frac{\partial(uh)}{\partial x} + \frac{\partial(vh)}{\partial y} = 0 \quad (3-3)$$

2. Momentum

a. x-direction (longitudinal) momentum

$$\frac{\partial u}{\partial t} + u \frac{\partial u}{\partial x} + v \frac{\partial u}{\partial y} + g \frac{\partial h}{\partial x} + g \frac{\partial a_0}{\partial y} + C_f q \frac{u}{h} = \frac{l}{\rho} \left(E_{xx} \frac{\partial^2 u}{\partial x^2} + E_{yy} \frac{\partial^2 u}{\partial y^2} \right) \quad (3-4)$$

b. y-direction (transverse) momentum

$$\frac{\partial v}{\partial t} + u \frac{\partial v}{\partial x} + v \frac{\partial v}{\partial y} + g \frac{\partial h}{\partial y} + g \frac{\partial a_0}{\partial x} + C_f q \frac{v}{h} = \frac{l}{\rho} \left(E_{xx} \frac{\partial^2 v}{\partial x^2} + E_{yy} \frac{\partial^2 v}{\partial y^2} \right) \quad (3-5)$$

where,

h	=	water depth [L]
u	=	depth - integrated flow velocity in the x-direction (longitudinal) [L/T]
v	=	depth - integrated flow velocity in the y-direction (lateral) [L/T]
x	=	distance in the longitudinal direction [L]
y	=	distance in the lateral direction [L]
t	=	time [L]
g	=	acceleration due to gravity [L/T ²]
a_o	=	bottom elevation [L]
C_f	=	flow roughness coefficient [dimensionless]
n	=	Manning's n channel roughness coefficient [dimensionless]
E_{xx}	=	normal turbulent exchange coefficient in the x direction
E_{xy}	=	tangential turbulent exchange coefficient in the x direction
E_{yy}	=	normal turbulent exchange coefficient in the y direction
E_{yx}	=	tangential turbulent exchange coefficient in the y direction
ρ	=	water density [M/L ³]
q	=	resultant velocity = $(u^2 + v^2)^{1/2}$ [L/T].

Consistent units are used in the above equations, all spatial dimensions in feet, the time dimension in seconds, etc. The flow roughness coefficient C_f is related to the Manning's coefficient by the relation $C_f = (2.22 \cdot g \cdot n^2)/h^{1/3}$.

Because the RMA-2V model was run for steady state conditions, which is explained in the next section, the model actually solved the above equations with the time derivatives equal to zero. Also, two forces that are sometimes included in these equations, the Coriolis force and the wind stress force, have been neglected here. These forces are small compared to the other forces for rivers and can be neglected.

3.6.3 Spatial-Temporal Scales

The RMA-2V model was applied to TIP, the 6-mile portion of the Upper Hudson River between Fort Edward (River Mile 195) and Thompson Island Dam (River Mile 189) (Figure 3-8). The model computes the velocity flow field and depths at nodes of the finite element grid. Figure 3-9 shows the finite element grid used for the TIP. This grid is composed of approximately 3000 elements and 6000 nodes.

The finite element grid in the TIP channels was developed from the extensive river bathymetry measurements conducted by GE in 1991. These measurements included many more data points than actually needed to construct the grid. Only the data points approximately every 50 feet transversely, and every 300 feet longitudinally, were used. The finite element grid in the floodplain was constructed from elevations taken from the USGS topographic maps. As seen in Figure 3-9, the grid in the floodplain is much coarser than in the TIP channels. This is justified because velocities in the floodplain are much smaller than in the TIP channels and do not vary as much.

The spatial scale of the model was largely determined by the resolution needed to adequately define the flow field variations and hence shear stress variation. The shear stresses exerted on the river bottom depend on the magnitude of the vertically averaged velocity and the depth of flow above the bottom. Because both of these quantities can vary significantly across the flow field (transversely), the shear stress will also vary across the river. This variation must be determined because sediment PCB concentrations are not uniformly distributed across the flow field. Therefore the bottom shear stresses must be determined for each point in the river. For this reason primarily, a two dimension model must be used since a one dimensional model does not account for the transverse variation of the velocity and depth of flow and therefore the transverse variation of shear stresses can not be computed.

The hydrodynamic model was applied assuming that the flow through the TIP was at steady state, i.e., the flow did not vary over time. This assumption is justified given that the historical flow record at Fort Edward shows that the Hudson River high flows events occur over an extended time (several days) and for the purposes of computing the velocity field and shear stresses, this time is long enough to establish steady state conditions.

3.6.4 Application Framework

The RMA-2V model was first calibrated to the known hydrodynamic data of the river. The Manning's n for the river is the primary calibration parameter for the model. River data, such as river stage-discharge relations for the upstream (Lock 7) gaging station was used to calibrate the model. Other data, such as velocity

measurements made by the USGS during high flow events, were used to validate the model results.

The RMA-2V model was then applied to the TIP to compute the two dimensional flow field and ultimately the bottom shear stresses which occur during high flow events. The specific steps used in this process are as follows:

1. The flow field velocity and depth was determined using RMA-2V;
2. The river bottom shear velocity for each node was determined from calculated velocity and depth at each node.
3. The bottom shear stresses were then calculated from the bottom shear velocities using the relation $\tau = \rho \cdot u^*{}^2$.

The commercial software, FastTabs by the Boss Corp., was used as a pre- and post-processor for the RMA-2V model. This software enables the user to quickly construct a finite element grid and allows for quick and easy evaluation of the model results.

3.7 Thompson Island Pool Depth of Scour Model

3.7.1 Introduction

The Depth of Scour Model was designed to accomplish the modeling objective of estimating the risk of resuspension of PCBs from the deeply buried sediments of TIP in response to a “catastrophic” flood event. The model provides quantitative and qualitative information to estimate this risk. The Depth of Scour model estimates the total mass of solids and PCBs eroded from cohesive sediments for each high flow event at specified spatial and temporal scales. In addition, more detailed estimates of local scour at selected locations in TIP were conducted. These analyses included an explicit consideration of the uncertainty in the estimates.

It is important to note here that the model has not been designed to simulate the subsequent transport and redistribution of these eroded sediments. The entrainment, deposition, and post-deposition consolidation of sediments is a complex phenomenon and only partially understood at the current time. The evaluation of the dynamic characteristics of the scouring phenomenon is beyond the scope of the current framework. Hence, the model as currently designed evaluates only the mass *remobilized* for each design high-flow event.

In addition to estimating the mass of solids and PCBs eroded from cohesive sediments in TIP, more detailed estimates of the local scour were conducted at selected locations. As part of the Phase 2 monitoring program, sediment cores were taken at six locations in the TIP area and analyzed at a high vertical resolution. Some of these sediment cores show peak PCB concentrations in excess

of 2,000 $\mu\text{g/g}$ (ppm). The vertical resolution of PCB data at these locations allowed a more detailed investigation of the potential risk of scour in response to large events.

The conceptual approach used for the TIP Depth of Scour model is shown in Figure 3-10. To compute the masses of solids and PCBs eroded at a fine spatial scale an ARC/INFO-based Geographical Information System (GIS) was utilized. The site was discretized into a regularly spaced grid of dimensions 10x10 feet. Computations were conducted locally at the nodal locations where flow field information was available from the TIP Hydrodynamic Model. Subsequently results were interpolated to generate individual grids. The sediments were spatially differentiated into cohesive and non-cohesive areas, with analyses restricted to only cohesive sediment areas for this preliminary model calibration effort.

3.7.2 Process Representation

To compute the depth of erosion and total mass of solids eroded from cohesive sediments for a high-flow event two categories of information are necessary. First, the hydrodynamic conditions at the sediment-water interface need to be specified. The primary forcing function for entrainment is the shear stress exerted at the sediment-water interface by flowing water. The TIP Hydrodynamic Model yields estimates of velocities (and bottom shear stress) at a fine spatial resolution. Secondly, the physico-chemical properties of the bedded sediments greatly influence the magnitude (and rate) of entrainment of sediments for a given event, and the resulting depth of scour.

Entrainment mechanisms can be classified into two distinct categories based on sediment bed properties. The main parameters affecting the entrainment of non-cohesive sediments include grain size and shape (and their distributions), the applied shear stress, bed roughness, and specific weight. Bed sediments which are primarily fine grained and/or possess a high clay content exhibit interparticle effects which are cohesive in nature. The resultant entrainment properties are very different from non-cohesive sediment beds (no interparticle interactions). Since the toxic contaminants of interest (PCBs) are associated primarily with fine grained sediments, this distinction is of considerable importance in the TIP area.

The TIP Depth of Scour Model in the present report was developed for only cohesive sediments. As part of the future modeling work (Appendix B), the Depth of Scour Model will be extended to include both cohesive and non-cohesive sediments in TIP.

Cohesive Sediment Erosion

The influence of particle diameter has a significantly lower influence on the entrainment characteristics of cohesive sediments in comparison to electrochemical influences. Relatively small amounts of clay in the sediment-water mixture can

result in critical shear stresses far larger than those in non-cohesive materials of similar size distribution (Raudkivi, 1990).

All previous studies on the entrainment of cohesive sediments hypothesize that the scour magnitude (and rate) is primarily influenced by the excess applied shear stress (i.e. the difference between the applied shear stress and the critical shear stress of the surficial sediments) and the state of consolidation (or age after deposition) of the bed sediments (Partheniades, 1965; Mehta et al., 1989; Xu, 1991). The mass of material resuspended (or rate of entrainment) can be expressed in the following functional form:

$$M = f(\tau - \tau_c; \text{age}; \text{other sediment properties})$$

where, M is the mass (or rate) of material resuspended, and τ is the applied shear stress, and τ_c is the bed critical shear stress. The function f has been expressed in a variety of different forms ranging from linear (e.g. Partheniades, 1965), exponential (e.g. Parchure and Mehta, 1985), and the power relationship developed by Lick and co-workers (e.g. Gailani et al., 1991).

Based on statistical analysis of laboratory and field data Lick et al (1995) proposed an erosion equation of the following form which approximated his experimental data:

$$\varepsilon = \frac{a_0}{t_d^n} \left(\frac{\tau - \tau_c}{\tau_c} \right)^m \quad (3-6)$$

where, ε is the total amount of material resuspended (g/cm^2); t_d is the time after deposition; and a_0 , n , and m are empirical constants.

The depth of scour can be calculated as :

$$Z_{scour} = \frac{\varepsilon}{C_{bulk}} \quad (3-7)$$

where, C_{bulk} is bulk sediment density (g/cm^3). This equation has been applied and results validated to several rivers (e.g. Fox River, Detroit River, and Buffalo River).

The above empirical formulation (Equation 3-6) is not appropriate when the applied shear stresses are greater than about $20 \text{ dynes}/\text{cm}^2$. The erosion rates, however, still exhibit a power relationship. The applied shear stresses rarely exceed $20 \text{ dynes}/\text{cm}^2$ over fine-grained sediments in TIP, even for major storms, thus the above functional form can be utilized. It should be pointed out here that Equation 3-6 has been derived from laboratory experiments and needs to be calibrated for specific sites. A truly fundamental and generic model to characterize event-driven resuspension is beyond the current research state-of-the-art.

3.7.3 Spatial Temporal Scales

The selection of the appropriate spatial scales for the TIP Depth of Scour Model was primarily driven by the extent of variability in the river bed sediment properties and PCB concentrations. Since PCB concentrations can vary by several orders of magnitude across distances as small as a few hundred yards (TAMS/CADMUS/Gradient, 1996 - pending publication), a fine scale Geographical Information System (GIS) based approach has been adopted. The site has been discretized into a uniformly sized grid with cell spacing of 10 feet. This level of spatial resolution should be adequate in capturing the spatial variability in the depth of scour and mass of solids and PCBs eroded from the cohesive areas in TIP.

The cohesive computations result in a mass estimate for the entire event assuming that the event peak shear stress is established instantaneously. Experiments by Lick et al., (1995) indicate that this mass is eroded over the time scale of approximately one hour.

3.7.4 Applications Framework

The TIP Depth of Scour Model is a GIS-based computational framework designed to yield estimates of mass of solids and PCBs eroded for specific design events. All computations were carried out on a grid with ten by ten foot cells. The GIS utilized in the model was ARC/INFO. All computations and processing were carried out on a SUN SPARC-20 workstation. The model as currently designed is operational only on this hardware-software platform.

3.8 Lower Hudson River PCB Transport and Fate Model

3.8.1 Introduction

The modeling approach taken for the Lower Hudson River differs from that for the Upper Hudson in that existing PCB fate/transport and food chain model applications were used. Thomann et al., (1989,1991) developed both a physico-chemical and a food chain model to describe PCB concentrations in Lower Hudson River water, sediments and fish. This existing model was used essentially unchanged for this RI/FS reassessment. The use of the Thomann model is intended to accomplish the following modeling objectives:

1. Evaluate the impacts of PCB loadings from the Upper Hudson River on PCB levels in water and sediments in the freshwater portion of the Lower Hudson River;
2. Provide quantitative relationships between PCB water and sediment concentrations and fish body burdens in the freshwater portion of the Lower Hudson River; and,

3. Evaluate and compare predicted responses to continued No Action, various remedial scenarios and hydrometeorological events in the freshwater portion of the Lower Hudson River.

The remainder of this section provides a summary description of the model framework as described in Thomann et al., (1989, 1991). It is divided into sections describing:

- State Variables and Process Kinetics
- Spatial-Temporal Scales
- Applications Framework

3.8.2 State Variables and Process Kinetics

The Lower Hudson River PCB model consists of linked submodels:

1. Physico-chemical Model: Predicting PCB Concentrations in Water and Sediment; and,
2. Food Chain Model: Predicting PCB Concentrations in White Perch and Striped Bass.

Each submodel is designed to consider a single PCB homologue; results for total PCB concentrations are obtained by summing model results from simulations for each individual homologue. State variable and process kinetics for the two modules will be discussed separately.

Physico-chemical Model

The physico-chemical model used for model calibration contains two state variables: (1) total homologue concentration in the water column; and (2) total homologue concentration in sediments.

Solids concentration in the water column was treated as a forcing function for model calibration. The equation for total (i.e., dissolved plus particulate) PCB homologue concentration in the water column segment i is given in explicit finite difference form as:

$$\begin{aligned}
 V_{li} \frac{dc_{Tl,i}}{dt} = & \sum_j (Q_{ij} c_{Tl,j} - Q_{ji} c_{Tl,i}) + \sum_j E'_j (c_{Tl,j} - c_{Tl,i}) \\
 & + K_{f,i} A_s \left(\frac{f_{d2,i} c_{T2,i}}{\phi_{2,i}} - f_{dl,i} c_{Tl,i} \right) - K_{l,i} V_{li} c_{Tl,i} + k_{ll,i} A_s \left[\left(\frac{C_{g,i}}{H_e} \right) - f_{dl,i} c_{Tl,i} \right] \\
 & - v_{si} A_s f_{p1,i} c_{Tl,i} + v_{ui} A_s f_{p2,i} c_{T2,i} + W_{tl,i}
 \end{aligned} \quad (3-8)$$

where,

V_{1i}	=	volume of water column segment i (L^3) - Note: subscript 1 denotes water column
$c_{T1,i}$	=	total homologue concentration in water column segment i (M/L^3)
Q_{ij}	=	flow from segment i to segment j (L^3/T)
$C_{T1,j}$	=	total homologue concentration in water column segment j (M/L^3)
E_{ij}	=	bulk dispersion between segment i and j (L^3/T)
$K_{f,i}$	=	vertical diffusion rate (L/T)
A_s	=	surface area (L^2)
f_{d2}	=	PCB dissolved fraction in bed sediment segment i - Note: subscript 2 denotes sediments
$c_{T2,i}$	=	total homologue concentration in sediment segment i (M/L^3)
$\phi_{2,i}$	=	porosity of sediment segment i
$f_{d1,i}$	=	PCB dissolved fraction in segment i
$K_{1,i}$	=	PCB decay rate in segment i (T^{-1})
$k_{11,i}$	=	overall volatilization rate in segment i (L/T)
$c_{g,i}$	=	gas phase PCB concentration (M^3/L^3)
H_e	=	Henry's Law constant
v_{si}	=	solids settling velocity in segment i (L/T)
$f_{p1,i}$	=	PCB particulate fraction in water column segment i
$v_{u,i}$	=	solids resuspension velocity in segment i (L/T)
$W_{tl,i}$	=	PCB mass input rate to segment i (M/T).

The terms in Equation 3-8 correspond respectively to: advection, horizontal dispersion, vertical diffusion across the sediment-water interface, decay, volatilization, settling, and resuspension.

The dissolved and particulate fractions of PCBs are estimated from the partition coefficient and solids concentrations by:

$$f_d = \frac{1}{1 + K_p m} \quad (3-9)$$

$$f_p = \frac{K_p m}{1 + K_p m} \quad (3-10)$$

where,

K_p = porosity-corrected partition coefficient (L^3/M).

The mass balance equation for total PCB homologue in the active bed sediment is

$$\begin{aligned} V_{2i} \frac{dc_{T2,i}}{dt} = & -K_{f,i} A_s \left(\frac{f_{d2,i} c_{T2,i}}{\phi_{2,i}} - f_{d1,i} c_{T1,i} \right) - K_{2i} V_{2i} c_{T2,i} + v_{si} A_s f_{p1,i} c_{T1,i} \\ & - v_{u,i} A_s f_{p2,i} c_{T2,i} - v_{d,i} A_s f_{p2,i} c_{T2,i} + K_{f,i} A_s \left(\frac{f_{d3,i} c_{T3,i}}{\phi_{3,i}} - \frac{f_{d2,i} c_{T2,i}}{\phi_{2,i}} \right) \end{aligned} \quad (3-11)$$

where,

$K_{2,i}$ = decay rate in active sediment segment I ($1/T$)

f_{p2} = PCB particulate fraction in active sediment segment I (dimensionless)

f_{d3i} = PCB dissolved fraction in deep sediment segment I (dimensionless)

$c_{T3,i}$ = total homologue concentration in deep sediment segment I (M/L^3)

$\phi_{3,i}$ = porosity of deep sediment segment I (dimensionless).

The terms in Equation 3-11 correspond respectively to: diffusive exchange with the water column, decay, settling, resuspension, net sedimentation, and diffusive exchange with deep sediments.

Food Chain Model

The state variables for the food chain model are the organism weight and whole body burden for each food web compartment. The model does not explicitly consider the effect of contaminated sediments on food chain bioaccumulation. The equation for individual organism weight is:

$$\frac{dw_k}{dt} = (a_{kj} C_{kj} - r_k) w_k \quad (3-12)$$

where,

w_k = organism weight in compartment k (M/L^3)

a_{kj} = mass assimilation efficiency of organism j in compartment k ($M(\text{predator})/M(\text{prey})$)

C_{kj} = weigh specific consumption of organism j in compartment k
(M(predator)/M(preyl)/T)

r_k = respiratory weight loss in compartment k (1/T).

Equation 3-12 states that net weight gain is equal to the difference between food assimilated and respiration losses.

The mass balance equation for whole body burden is:

$$\begin{aligned} dv'_k / dt &= d(vw)_k / dt = w_k dv_k / dt + v_k \frac{dw_k}{dt} \\ &= k_{uk} w_k c - K_k v'_k + \sum_j p_{kj} \alpha_{kj} C_{kj} w_j v_j \end{aligned} \quad (3-13)$$

where,

v'_k = whole body burden in compartment k (M)
 v_k = organism PCB concentration in compartment k (M/L³)
 k_{uk} = contaminant uptake from the water compartment k
(L³/T/M)
 c = dissolved PCB concentration (M/L³)
 K_k = excretion rate for compartment k (T⁻¹)
 p_{kj} = food preference of compartment k on compartment j
 α_{kj} = homologue assimilation efficiency.

Equation 3-13 states that an organism can gain toxicant via uptake from the water column, lose toxicant via excretion, and/or gain toxicant via consumption of contaminated prey.

Equations 3-12 and 3-13 were applied over 27 food chain compartments, comprised of:

- Phytoplankton
- Zooplankton
- Small fish
- White perch: 7 year classes
- Striped bass: 17 year classes.

As seen in Figure 3-11, the first two year classes of striped bass are assumed to feed solely on zooplankton. Intermediate age striped bass feed on small fish and young white perch, while older striped bass feed primarily on intermediate age white perch.

3.8.3 Spatial-Temporal Scales

The spatial and temporal scales represented in the Lower Hudson model were selected to represent the long-term time scale and a broad geographic spatial scale. According to Thomann et al., (1989) the reasons for these coarse scales were as follows:

- Many significant components of the problem are associated with long time and broad space scales, i.e., decadal loading of PCBs, long term "memory" of sediment contamination, long life span and geographic distribution of striped bass
- Construction of a model with more detailed resolution was not feasible due to data availability, computational requirements, and time and funding limits.

The Lower Hudson model operates with a daily time step, with the intended temporal resolution of discerning year to year and decade to decade changes.

The spatial domain of the model extends from Federal Dam as an upstream boundary to the New York Bight and Long Island Sound as a downstream boundary (Figure 3-12). Also shown in Figure 3-12 is the model segmentation. Fifteen segments represent the Hudson River water column from Federal Dam to the Battery. An additional 15 segments are used to represent areas below the Battery, including six segments for the New York Bight and four segments for Long Island Sound. Each water column segment is underlain by from two to fourteen vertical sediment segments. The model contains a total of 120 sediment segments.

3.8.4 Applications Framework

The Lower Hudson River modeling was conducted using the computer program WASTOX (Part 1, Exposure Concentration and Part 2, Food Chain). The WASTOX program provides a framework for modeling the fate of toxic chemicals in aquatic environments. It was developed at Manhattan College, based on a version of the WASP model used there, under cooperative agreements with the Environmental Research Laboratory, Gulf Breeze, Florida, and the Large Lakes and Rivers Research Station of the Environmental Research Laboratory, Duluth, Minnesota.

WASTOX Part 1 was used to generate exposure concentrations. The exposure concentrations were processed using task-specific computer programs to provide inputs for WASTOX Part 2. WASTOX Part 2 was used to generate food chain concentrations.

The specific WASTOX executables used were WTXSS3.EXE (1-26-88) for Part 1 and FCHN2-C.EXE (11-4-88) for Part 2. These files were provided to LTI by Dr. Robert V. Thomann, who had primary responsibility for the Lower Hudson model application. These were run on IBM PC-compatible computers.

4. CALIBRATION OF UPPER HUDSON RIVER PCB MODEL

4.1 Introduction

A complete description of the Upper Hudson River PCB Model is contained in Section 3.5. The present section contains preliminary calibration results for this model for a period of simulation from January 1 to September 30, 1993. The calibration was conducted for total PCBs and five separate PCB congeners, or groups of co-eluting congeners, corresponding to BZ#4, BZ#28, BZ#52, BZ#90 + 101 and BZ#138.

Consideration of total PCBs is necessary in order to represent a complete mass balance for all of the individual PCB congeners. In addition, the USEPA currently uses total PCBs as the exposure concentration for estimating human cancer risk. The five calibration congeners, or groups of co-eluting congeners, represent a wide range of physical-chemical properties that influence PCB environmental transport and fate. These congeners were used for model calibration in order to establish the technical credibility of the model over a range of different conditions.

Section 4.2 contains a summary of historical trends in flow, TSS and total PCBs in the Upper Hudson River. Section 4.3 contains an overview of Release 2.3 of the TAMS/Gradient database that was used for this preliminary model calibration. Section 4.4 contains descriptions of model input data. Section 4.5 contains descriptions of internal model parameters. Section 4.6 discusses the calibration approach used for water, solids and PCBs. Section 4.7 contains model calibration results. Section 4.8 contains results from a diagnostic and components analysis conducted with the calibrated model. Section 4.9 contains results from a limited set of sensitivity analyses conducted with the calibrated model.

4.2 Historical Trends in Water Quality Observations

From 1957 through 1975, between 209,000 and 1.3 million pounds of PCBs were discharged to the Upper Hudson River from two GE facilities, one in Fort Edward and the other in Hudson Falls (Figure 1-5). GE discontinued use of PCBs in 1977 when they ceased to be manufactured and sold in the United States. Migration of PCBs downstream was greatly enhanced in 1973 with the removal of Fort Edward Dam and the subsequent release of PCB-contaminated sediments.

Figure 4-1 illustrates historical trends in USGS field data for flow, TSS and total PCBs at Fort Edward from 1977 through 1992. In general, peak annual flows tend to occur in spring, accompanied by large increases in TSS concentrations. Trends in total PCB concentrations are confounded, in part, by changes in analytical methods and detection limits over this historical period. Nonetheless, it appears that total PCB concentrations were at maximum values during the late-1970s and

early-1980s and then declined substantially in the mid- to late-1980s. Note that these PCB data are plotted on a log scale.

Figure 4-2 illustrates trends in these same parameters at both Fort Edward and Thompson Island Dam from 1991 through 1993. Although the magnitudes of peak annual flows differ among years, they still tend to occur in spring, accompanied by large increases in TSS concentrations. An exception to this association between high flows and increases in TSS concentrations appears to occur in fall of 1991. At this time large increases in TSS concentrations do not appear to be associated with high flows.

In an apparent reversal of an earlier trend, total PCB concentrations in fall of 1991 increased beyond 1,000 ng/l for the first time since 1983. Total PCB concentrations continued to remain at relatively high levels during 1992 and 1993. TAMS/CADMUS/Gradient (1996 - pending publication) contains a discussion of possible sources of PCBs that could be responsible for these observations.

A curious phenomenon is that there appear to be substantial differences in total PCB concentrations between Fort Edward and Thompson Island Dam, a distance of only 6 miles. The reason for these differences is not clear because there are no large tributary inputs to TIP between these two locations. In particular, it is not clear whether this apparent increase in PCB load originates from historical sediment sources or from more recent discharges.

It is important to recognize that the physical, chemical and biological processes controlling PCB dynamics in the Upper Hudson River, especially in TIP, are not fully understood at the present time. Furthermore, the HUDTOX model calibration in the present report is limited to a period of simulation from January 1 to September 30, 1993. It is not yet clear whether the PCB dynamics operative during this simulation period are fully representative of historical PCB dynamics, or whether they will be representative of PCB dynamics under future conditions. The long-term (1984-1993) hindcasting calibration to be conducted as part of the future modeling work (Appendix B) will provide more information on historical PCB dynamics.

4.3 Overview of Preliminary Calibration Dataset

Daily USGS flow data were available at four mainstem Upper Hudson River stations: Fort Edward, Stillwater, Waterford, and Green Island (Figure 1-3). Other estimates of daily flow, at Schuylerville, Stillwater and Waterford, were also developed as part of the Phase 2 monitoring effort (TAMS/CADMUS/Gradient, 1996 - pending publication). These estimates were developed prior to release of Water Year (WY) 1993 data from USGS, and are based on least-squares fit regression models of historical NYSDOT staff-gauge height and USGS flow records. The 1993 USGS daily flows were chosen over the Phase 2 estimates for use in the HUDTOX calibration for two reasons: first, a consistent source of data for

upstream, mainstem, and tributaries could be used for developing the flow fields; and second, the USGS data are the official flow records for the river.

There are four major tributaries flowing into the Upper Hudson River: Batten Kill, Fish Creek, Hoosic River, and Mohawk River. Daily flows were recorded by the USGS on Hoosic and Mohawk Rivers. These gaged flow data formed the basis in estimating ungaged flows for the Upper Hudson River. Figure 4-3 shows the variation of daily flows at the upstream boundary, Hoosic River, and Mohawk River for the preliminary model calibration period. Figure 4-4 shows daily flows and available USGS TSS data at Fort Edward.

The Phase 2 water column monitoring program included 12 PCB samples from the Hudson River at Fort Edward, 6 samples from the Hoosic River, and 6 samples from the Mohawk River during the preliminary model calibration period. Six of the 12 PCB measurements at Fort Edward were instantaneous (transect) samples and 6 were flow averaged samples, each composited over a period of about 2 weeks. The GE 1993 water column dataset included larger numbers of samples, taken at both Fort Edward and Thompson Island Dam. Figure 4-5 shows total PCB concentrations at Fort Edward for both the Phase 2 and GE datasets, along with daily river flows.

The Phase 2 database contains values for total PCBs and congener concentrations in two different formats (TAMS/CADMUS/Gradient, 1996 - pending publication). Value 1 reports the quantitation limits for non-detected PCB congeners; however, zero values are used for summing these congeners when deriving total PCB concentrations. Value 2 contains non-detected congener concentrations that are set to zero or one-half the quantitation limits, depending on the frequency of non-detected results within a sample grouping. In most cases, differences between these two values were minimal and could not be distinguished graphically. Therefore, only Value 2 was used for model inputs and for comparison with model output during this preliminary model calibration.

The GE PCB database included measurements of individual capillary column peak values instead of PCB congener concentrations (O'Brien and Gere, 1993a, 1993c, 1993d, 1994). The TAMS/Gradient Team investigated the relationship between these data and the PCB congener measurements in the Phase 2 database for the Rogers Island sampling station. This analysis determined that total PCBs, Peak#24, Peak#31 and Peak#82 in the GE database correspond well to total PCBs, BZ#28, BZ#52 and BZ#138, respectively, in the Phase 2 database. The correspondence between the GE capillary column peak measurements is documented in Release 3.1 of the TAMS/Gradient Phase 2 database (TAMS/Gradient, 1995). On the basis of direct data comparisons, however, there were significant discrepancies between the two datasets for BZ#138. Consequently, it was decided that both GE and Phase 2 data would be used in

computing loadings for total PCBs, BZ#28 and BZ#52. Only Phase 2 data were used for congeners BZ#4, BZ#101 + 90 and BZ#138.

The only available sediment data contained in Release 2.3 of the TAMS/Gradient Phase 2 database for the calibration period are for nine high resolution sediment cores. These data are not sufficient to provide representative estimates of average sediment concentrations for the HUDTOX sediment segments. These high resolution cores are limited in number and are specifically located in depositional areas of the river. The GE 1991 sediment survey data (O'Brien and Gere, 1993a) provide a more extensive coverage of bottom sediments and were used to specify HUDTOX sediment conditions in the present calibration. At the time of this preliminary model calibration work, this was the only recent dataset that provided a comprehensive picture of sediment conditions, including both solids and congener-specific PCB characterizations.

4.4 Model Input Data

Three distinct types of model inputs are necessary to apply the HUDTOX mass balance model:

1. System-specific physical data;
2. External loadings, forcing functions, boundary and initial conditions; and,
3. Process-related parameters.

The following subsections describe these model inputs for the present HUDTOX calibration. Two transient events complicated the model calibration for this period: first, 100-year floods in the Mohawk and Hoosic Rivers from spring snowmelt in 1993; and second, large sediment solids releases from spring construction activities on Hudson River Lock No. 1 just upstream from Waterford (Figure 1-3). An additional source of uncertainty is the unknown amounts of upstream loadings due to migration of PCBs from the overburden and bedrock at the GE facilities in Hudson Falls and Fort Edward (Figure 1-5) (TAMS/CADMUS/Gradient, 1996 - pending publication).

4.4.1 System-Specific Physical Data

HUDTOX employs the water column and sediment segmentation described in Section 3.5.3. Figures 3-5 and 3-7 provide a map of the water column segmentation, and a schematic of the water and sediment segmentation, respectively. The specific geometry of the model segmentation is presented in Table 4-1. The water column is represented by a single vertically-mixed layer, while five different layers represent the vertical profile of the Upper Hudson River sediment physical and chemical properties. Thus, a total of 13 water column, and 65 sediment segments represent the river from the northern tip of Rogers Island to

Federal Dam. As discussed in Section 3.5.3, a non-interacting sediment segment is used to accumulate any chemical burial out of the system, so that a total of 79 segments is simulated within the HUDTOX model framework.

4.4.2 External Loadings

Upstream, Tributary and Ungaged Flows

To develop a better understanding of load-response dynamics, a spring high-flow period was operationally defined to encompass the period from March 26 through May 10, 1993. Flood conditions occurred throughout the Upper Hudson River Basin between these dates. USGS daily flow measurements at Green Island during this period were always above 15,000 cfs, and were generally above 7,000 cfs at the Fort Edward gauging station.

Figure 4-6(a) summarizes external water inputs and shows the dominance of upstream and Mohawk River flows in the Upper Hudson River water balance. Upstream flow into Segment 1 was specified from USGS daily records at Fort Edward. Similarly, USGS flow records were used to specify Hoosic River (Segment 9) and Mohawk River (Segment 13) inflows on a daily basis. Appropriate corrections were applied to account for any drainage area increases between gaging stations, and for inflows from smaller tributaries.

Ungaged flows were estimated on a monthly basis using Water Year (WY) 1993 USGS daily flow records at Hudson River mainstem stations (Fort Edward, Stillwater, and Waterford) and available information on ungaged tributary drainage areas. As discussed in Section 4.3, the NYSDOT staff-gauge vs. flow relationships developed by TAMS were not used to specify Hudson River flows because WY1993 USGS data for Stillwater and Waterford stations became available in time for this model calibration.

When using the USGS flow measurements and the estimated flow from Batten Kill and Fish Creek to conduct a water balance for the Upper Hudson River, there was a residual amount of unbalanced water. This extra flow was presumed to result from other ungaged minor tributaries, direct runoff, and non-point sources. The amount of residual flow each model segment receives was assumed to be proportional to the longitudinal length of that segment. Estimation of daily flows using this method was not appropriate due to reasons such as time lags in hydrographs between upstream and downstream stations. Therefore, these minor ungaged flows were estimated on a monthly average basis.

Batten Kill and Fish Creek discharge into the same HUDTOX model segment. Therefore, the flow from these two tributaries was estimated as a single ungaged point source based on the increase in flow magnitude and drainage area from Fort Edward to Stillwater USGS stations. The ratio of these two values represents the flow yield per unit drainage area. This yield was assumed to be applicable to

Batten Kill and Fish Creek. Thus the total discharge from Batten Kill and Fish Creek was estimated by applying this yield to their total drainage areas.

Initial solids modeling efforts indicated that ungaged tributary solids loads between Fort Edward and the Hoosic River were substantially underestimated. The combined drainage areas of the ungaged Batten Kill (394 mi²) and Fish Creek (90 mi²) tributaries constitute approximately 94 percent of the Hoosic River drainage area (510 mi²), so daily flow and TSS loads were estimated based upon Hoosic River data and the limited available data for Batten Kill.

Table 4-2 is a summary of average flows over the calibration period from January 1 to September 30, 1993. It can be seen that ungaged minor tributary or non-point flows account for less than 10 percent of all inflows to the Upper Hudson River for the 272-day preliminary model calibration period.

Solids Loads

Tributary loading estimation methods usually take advantage of the correlation between constituent concentrations and flow so that a complete concentration time series can be constructed from the more readily available flow data. Various methods of loading estimation were examined by Preston et al., (1989), including averaging estimators, ratio estimators, and regression methods. Regression methods usually exploit the correlation between log-transformed constituent concentration and flow. A bias is introduced when constituent concentrations are estimated from this type of log-transformed correlations. The minimum variance unbiased estimator (MVUE) developed by Cohn et al., (1989) employs corrections to eliminate this bias.

Daily TSS loads were estimated for Fort Edward, Hoosic River, and Mohawk River using the MVUE method. Statistical distributions of TSS and flows, as well as correlations between them, were examined for the USGS, Phase 2 water column monitoring program, and GE datasets. Flow data collected by the USGS approximated log-normal distributions. With TSS concentrations, USGS data resembled log-normal distributions, while the GE data did not. There were insufficient data points in the Phase 2 water column monitoring program to draw a definitive conclusion in this regard.

Good correlations between TSS and flow were generally observed with the USGS and Phase 2 data, while poor correlations were found with the GE data. To avoid the complications of a possible underlying, long-term trend in TSS concentrations, only 1993 data were considered for use estimating upstream boundary TSS loading. Since there were only six instantaneous TSS measurements at the upstream boundary in the Phase 2 database, they were excluded from regression analysis for the sake of internal consistency. As a result, only the 1993 USGS measurements were used in the final regression analysis to define the

upstream boundary condition for TSS during the preliminary model calibration period.

For loadings from the Hoosic and Mohawk Rivers, 1993 USGS TSS data were not available at the time of this work and historical records were used to conduct regressions. Consequently, while the 1993 USGS data were used in the MVUE regressions for computing daily TSS load estimates at the HUDTOX model upstream boundary (i.e. Fort Edward), the historic USGS data were used for the Hoosic and Mohawk Rivers. This approach improved the reliability of estimated loads because it eliminated the potential incompatibilities among different TSS datasets, and resulted in improved log-normal distributions and better correlations between TSS and flow.

Estimated daily loads for the upstream boundary, Hoosic River, and Mohawk River are shown in Figure 4-7. It should be noted that total TSS loads during the model calibration period and TSS loads during high flow events from the Hoosic River were greater than those from the upstream boundary, even though the magnitude of flow in the Hoosic is typically lower (Figure 4-3).

The Hoosic River discharge measured at the Eagle Bridge USGS gage station corresponds to a drainage area of 512 mi², while the total drainage area of Hoosic River is 710 mi² (TAMS/Gradient, 1992). To correct for this difference, all Hoosic flow data were increased by the same percentage of the drainage area increase, while TSS concentrations remained the same. This constituted a 39 percent increase in flow and TSS loadings from the Hoosic River between the gage and the confluence with the Upper Hudson River.

The Phase 2 water column monitoring program collected six TSS measurements from Batten Kill during 1993. These limited measurements were insufficient to define a time series of TSS concentrations for the modeling period and therefore were averaged to yield a median TSS of 5.0 mg/l. This value was adopted for Batten Kill, Fish Creek, and all other ungaged sources. These ungaged sources did not contribute significantly to the overall mass balance of water or TSS as shown by Tables 4-2 and 4-3.

Initial modeling of TSS as a tracer during low flow conditions revealed that Batten Kill and Fish Creek were probably contributing significant solids loads to the Upper Hudson River. Subsequently, daily flow and TSS loading estimates were developed for these tributaries based on available, but limited, information. Daily combined Batten Kill and Fish Creek solids loading was estimated based on an average ratio of Batten Kill to Hoosic River TSS concentrations (64 percent for combined Phase 2 and GE data) and tributary drainage areas (94 percent).

Figure 4-6(b) illustrates that the principal external solids loadings to the Upper Hudson River during the calibration period were from the Mohawk River (58 percent) and the Hoosic River (20 percent). Solids loadings across the upstream boundary at Fort Edward represented only a small fraction (8.5 percent) of total external solids loadings. Also, approximately 56 percent of the upstream and tributary hydraulic inputs and 87 percent of the external solids loading occurred during the spring high flow period which represents just 17 percent of the total period of simulation.

Internal solids loading due to primary production is often a significant source of solids in aquatic systems (e.g., Bierman et al., 1992). The Phase 2 monitoring program did not include measurements of primary production or measurements of the water quality constituents needed to apply a primary production model. To represent solids dynamics as accurately as possible in the HUDTOX model, an estimated primary production rate equivalent to 1.2 g TSS/m²-day (at 20°C) was used, based on field measurements by Cole et al., (1992) in the tidal freshwater portion of the Lower Hudson River. An Arrhenius temperature correction factor of 1.066 (Ambrose et al., 1988) was used to correct the rate due to the lower temperatures of the Upper Hudson River and to represent the variation in primary production due to seasonal (and daily) changes in ambient river temperatures. At 20°C, this rate is equivalent to 175 g carbon/m²-year, assuming that the organic carbon content of phytoplankton solids (measured by dry weight) is 40 percent. The total solids load contribution of this internal source is presented in Table 4-3.

The Phase 2 database contains insufficient field measurements to reliably specify external loadings for calibration of DOC in the HUDTOX model. The available data indicate that DOC levels are relatively stable throughout the Upper Hudson River. Consequently, DOC dynamics in HUDTOX were represented within the solids submodel in a simplified fashion. DOC was represented as a model state variable, but it was not used as a calibration target. Instead, constant DOC concentrations for external inflows were specified to maintain water column concentrations close to 4.83 mg/l, the average level measured during the Phase 2 sampling program (TAMS/CADMUS/Gradient, 1996 - pending publication). The dominance of upstream and Mohawk River DOC loads is seen in Figure 4-6(c), while Figure 4-6(b) indicates the relatively greater significance of TSS loads from other tributaries.

PCB Loads

To evaluate the feasibility of using a regression method to estimate PCB loading time series, correlations between PCB and flow, as well as between PCB and TSS were examined. It was found from the Phase 2 database that PCBs are generally better correlated with TSS than with flow, and that higher chlorinated congeners correlated with TSS better than lower chlorinated congeners. No correlation between PCB and flow or between PCB and TSS was observed in the

more frequently measured GE 1993 data. Therefore, only the Phase 2 dataset could possibly be used in MVUE or other regression methods. However, the quantity of Phase 2 data was insufficient to construct reliable correlations for estimating the time series of external PCB loads to the Upper Hudson River.

As a result, linear interpolation of PCB concentrations was used to compute the HUDTOX upstream boundary PCB loads for this preliminary model calibration period. To illustrate temporal coverage of available PCB data, Figure 4-5 shows total PCB concentrations at the upstream boundary from both Phase 2 and GE datasets along with daily Upper Hudson River flows at Fort Edward. As seen from Figure 4-5, there was an apparent outlier in the GE 1993 PCB dataset collected in January. Consistent with recommendations by TAMS/CADMUS/Gradient (1996 - pending publication), this data point was excluded from all PCB loading estimations.

Only 6 instantaneous water column PCB samples from the 1993 Phase 2 water column monitoring program were available for estimating loads from the Hoosic River, Mohawk River and Batten Kill. This was an insufficient quantity for generating a reliable time series to represent dynamic PCB loading conditions for the modeling period. Therefore, these data were simply averaged to yield constant PCB concentrations for these three tributaries. The average PCB concentration in Batten Kill was applied to both Batten Kill and Fish Creek. A small PCB concentration of 10 ng/L was assumed for other direct minor tributaries and direct runoff since field data were not available to better quantify these loads, and also because water quality monitoring in the Upper Hudson River does not indicate a presence of any other significant incremental PCB loads (TAMS/CADMUS/Gradient, 1996b - pending publication). PCB congener fractions for these minor sources were estimated based on the data collected for Batten Kill.

Loads from these minor sources constitute only a small fraction of the overall PCB loads and do not significantly affect the HUDTOX model results. Table 4-4 summarizes the accumulated total PCB loads for the Upper Hudson River preliminary model calibration period. Estimated daily total PCB loads entering the HUDTOX upstream boundary at Fort Edward, and from the Hoosic and Mohawk Rivers, are shown in Figure 4-8.

Table 4-5 summarizes all of the constituent mass loadings from the different external sources for the 1993 HUDTOX calibration. The upstream PCB loads are generally dominant, with 74 percent of the total external PCB load passing by Fort Edward as indicated by Figure 4-9(a). Figures 4-9(b-f) summarize the external loadings for the remainder of the selected PCB calibration congeners. The effect of high spring flows in the Upper Hudson River on the external PCB loads is also illustrated by these figures. With the exception of BZ#4, greater than 70 percent of the upstream PCB loads occur during the spring high flow period. The BZ#4 load shows the opposite behavior with just 27 percent of the upstream load occurring during the spring high flow period, reflecting this congener's relative low affinity for

sorbing onto solids. Overall, 68 percent of the total PCB external loading to the Upper Hudson River occurs during the spring high flow period.

The Mohawk River is the second largest external source of PCBs to the river (17 percent) and even surpasses upstream boundary loads for PCB congener BZ#138 (58 percent for Mohawk River versus 29 percent across the upstream boundary (Figure 4-9) during both spring high flow and lower flow conditions. However, there is much uncertainty in the tributary PCB loadings for the HUDTOX calibration period because they are based on the average of just 6 sample collections over the 9-month 1993 Phase 2 water column monitoring program. For example, 100 year floods occurred during 1993 spring runoff in the Mohawk River, while the Hudson River above Schuylerville experienced at most once in 5 year flooding. Therefore, the relative magnitudes of the external PCB and TSS loads during the calibration period may not represent long-term average conditions.

An additional source of uncertainty is the unknown amounts of upstream loadings due to migration of PCBs from the overburden and bedrock at the GE facilities in Hudson Falls and Fort Edward (TAMS/CADMUS/Gradient, 1996 - pending publication). These sources are upstream of the HUDTOX model boundary at Fort Edward. It is impossible to determine what portion of the actual upstream PCB loadings were captured by the Phase 2 water column monitoring program.

Direct atmospheric PCB loads to the Upper Hudson River are assumed to be negligible for the 1993 HUDTOX calibration period. This assumption is reasonable since the water surface area available for direct deposition is negligible in comparison to the drainage area of the watershed.

4.4.3 Forcing Functions

Ambient environmental conditions can significantly affect the kinetic processes which determine the fate of PCBs in the Upper Hudson River. The HUDTOX model framework includes time variable forcing functions for sediment, water, and air temperatures. In the water column, temperature affects the partitioning of PCBs and air-water gas exchange which may lead to volatilization of PCBs. Time series forcing functions for water temperature, measured at three stations during the Phase 2 monitoring program, were constructed and assigned to represent conditions in nearby HUDTOX model segments. Table 4-6 presents the water temperature time series developed from field measurements at Phase 2 Upper Hudson River water quality sampling stations 4, 5, and 8.

Sediment temperatures are not typically measured, so active sediment layer segment temperatures were assumed to be the same as the overlying surface waters. A constant temperature of 7 °C was used in the HUDTOX calibration for all lower sediment layers. The air temperature time series was developed based on 1993 mean monthly measurements at Albany, New York available from the NOAA

National Climatic Data Center. Volatilization losses of PCB through air-water exchange in the WASP-based HUDTOX model are controlled by the shear-induced turbulence of the river hydraulics, so air temperature has no effect on the present model formulation.

Two other environmental forcing functions are also incorporated in the HUDTOX framework, but these are not significant to the present PCB calibration. Wind speed and ice cover can both affect air-water gas exchange. In a highly advective river system such as the Upper Hudson River, hydraulic considerations (i.e. water velocity and depth) and temperature typically drive atmospheric exchange more than wind. Relationships describing gas exchange due to wind-driven shear are usually applied to open waters such as lakes, embayments and large estuarine systems.

4.4.4 Boundary Conditions

Upstream Hudson River and major tributary boundary conditions were incorporated in the model calibration through use of external loading functions described in Section 4.4.2. Boundary conditions were used in HUDTOX to specify state-variable constituent concentrations for the smaller ungaged tributary and non-point source inflows along the length of the river. Figure 4-6, Figure 4-9 and Table 4-5 summarize external loads for the calibration period. Non-point source loads were not significant for either solids (0.6 percent) or any PCB types (0.4 percent to 2.3 percent) represented in the HUDTOX model.

HUDTOX also requires that the atmospheric boundary gas phase concentration of toxic chemical state variables be specified in order to predict atmospheric exchange at the air-water interface. No recent site-specific atmospheric PCB measurements in the Hudson River vicinity were available for this HUDTOX calibration. Historical atmospheric PCB data in the Upper Hudson River indicate a large variation in concentration, with higher levels localized to landfill and remnant areas (TAMS/Gradient, 1991). GE 1989 air sampling near remnant areas show PCB concentrations up to 230 ng/m^3 . However, the detection limits were high (50 ng/m^3) and the vast majority of the air PCB measurements were below detection (246 out of 252 samples at three locations). For lack of more representative, site-specific atmospheric data, a gas phase concentration of 0.77 ng/m^3 for total PCBs was employed based on measurements from the Green Bay Mass Balance Study (Bierman, et al., 1992). Gas phase concentrations for individual PCB congeners were estimated based upon the ratio of water column congener to total PCB concentrations measured at Upper Hudson River tributary stations during the 1993 Phase 2 monitoring program. The resulting atmospheric concentrations used in the HUDTOX calibration for PCB congener BZ#s 4, 28, 52, 101+90, and 138 were: 0.0952, 0.0195, 0.0357, 0.0205, and 0.0113 ng/m^3 , respectively.

4.4.5 Initial Conditions

Bottom sediment properties and PCB concentrations are needed by HUDTOX to simulate sediment-water interactions. The only sediment data in Release 2.3 of the TAMS/Gradient Phase 2 database were for nine high resolution sediment cores. These data were not sufficient to provide representative estimates of average concentrations for HUDTOX sediment segments. The GE 1991 sediment survey data (O'Brien and Gere, 1993a) provided a more extensive coverage of bottom sediments and were therefore used instead to represent initial sediment conditions for this preliminary HUDTOX model calibration.

The GE 1991 sediment survey data are composites of individual samples taken from different locations within a river stretch. The composite measurements represent the average of all these individual samples within a vertical sediment layer. An approximate river mile was assigned to each composite sample. To estimate average concentrations for model segments, the GE composite samples were assigned to each HUDTOX segment based on their river mile locations. Composite samples within the same model segment and same sediment depth range were processed to estimate mean sediment solids and PCB concentrations. This processing involved assigning the GE composites to either a coarse or fine sediment category, based on the physical characterizations of individual samples within each composite group. Weighted solids and PCB concentrations were then computed based upon the areal distribution of sediment solids types determined for the TIP (approximately 20 percent fine and 80 percent coarse - see Section 6).

A solids mass density (ρ_s) of 2.67 g/cm^3 was chosen for model calibration as a median value based on an analysis of solids from the High Resolution Coring Program (TAMS/CADMUS/Gradient, 1996 - pending publication). The mean initial sediment solids concentration (or bulk density) was 1.1 g/cm^3 (or $1.1 \times 10^6 \text{ g/m}^3$) across all sediment segments, based on the 1991 GE sediment survey data. This value corresponds reasonably well with the median value of 1.3 g/cm^3 determined from the Phase 2 high resolution sediment cores (TAMS/CADMUS/Gradient, 1996 - pending publication). Table 4-7 presents the specific initial sediment solids concentrations used for the HUDTOX solids model calibration.

The GE 1991 sediment data include PCBs sorbed to sediment and PCBs dissolved in pore water (apparent dissolved concentrations). While the number of sediment bound PCB samples was significantly greater than that of pore water samples, more than 80 pairs of sediment and pore water samples were matched from the database. Total PCB concentrations were estimated by combining the solid sorbed and pore water dissolved fractions from these pairs. It was found that the solid sorbed PCBs account for more than 98 percent of total PCB concentrations in all cases. Therefore, the pore water fraction was neglected and only the solid-bound fraction was included in estimating total PCB concentrations in the sediments for the HUDTOX model initial conditions.

Another complication was that the GE dataset contains reported PCB capillary column peak measurements instead of the specific PCB congener concentrations reported in the Phase 2 database. These peak values were converted to congener concentrations in accordance with a TAMS/Gradient Team investigation of the comparability between the GE and Phase 2 datasets. A memorandum by Cook (1994) describes factors for estimating individual PCB congener values from the GE PCB peak measurements. More specifically, GE Peak#24, Peak#31, Peak#82 and total PCB measurements were found to be directly comparable to the Phase 2 BZ#28, BZ#52, BZ#138 and total PCB data, and required no conversions. The analysis found that comparable BZ#4 + 10 values were consistently estimated by multiplying GE Peak#5 measurements by a factor of five. PCB congener BZ#101 + 90 values, comparable to those in the Phase 2 data, were estimated by doubling the GE Peak#53 measurements.

Because PCB congener BZ#4 was a model calibration target, the TAMS/Gradient Team extracted concentration values for this congener from BZ#4 + 10 water column measurements using results from a statistical regression analysis applied to the Phase 2 high resolution core data. From more than 440 pairs of BZ#4 and BZ#10 data, the ratio of BZ#4 to BZ#4 + 10 had an average value of 0.7842 and a standard deviation of 0.227. This indicated that the relative compositions of BZ#4 and BZ#10 were stable in the bottom sediments. Thus, BZ#4 was initially computed from the BZ#4 + 10 values using this ratio.

It was later found that BZ#4 concentrations estimated using this method were greater than total PCBs concentrations in some instances, thus necessitating a different approach. The percentage of BZ#4 in total PCBs was computed using Phase 2 high resolution core data for each model segment where data were available. BZ#4 concentrations in each individual model segment were then estimated using this percentage value or a value interpolated based on adjacent upstream and downstream segments. These percentages ranged from 0.07 to 0.12 derived from a total number of 148 samples. Estimated initial PCB concentrations in the sediments for each upper layer HUDTOX model segment (0-5 cm) are listed in Table 4-8.

The GE composited sediment core samples were analyzed for 3 distinct vertical sediment layers: 0-5 cm, 5-10 cm, and 10-25 cm deep. These layers correspond directly to the top 3 sediment layers in HUDTOX sediment segmentation grid (Figure 3-7). There are two additional sediment layers in the model: 25-50 cm and 50-100 cm. Sediment properties and PCB concentrations need to be specified for these model segments as well. Because data were not available and these layers will not have any significant impact on the model results for the 9-month calibration period, data for the 10-25 cm layer were assumed to also be representative of the corresponding deeper sediment layers.

4.5 Internal Model Parameters

The conceptualized mass transport and kinetic structure of HUDTOX contains a number of internal model parameters. Figures 3-2 and 3-4, respectively, illustrate the HUDTOX solids and toxic chemical model structures. Beyond advective flow, longitudinal dispersion (D_L) is common to both the HUDTOX solids and PCB models. However, D_L is not significant to the mass transport processes in the model since the Upper Hudson River is highly advective. Also, many of the interfaces between model segments are located at lock and dam structures along the river (see Figure 3-5), effectively preventing large-scale mixing between these segments.

4.5.1 Solids Model Parameters

The process parameters affecting solids transport and transformation within the HUDTOX framework (Figure 3-2) are presented in Table 4-9. The solids mass balance was conducted for both TSS and DOC. A small degree of solids degradation in the sediment, with DOC as a by-product, was required to maintain an approximately constant DOC concentration gradient between the sediment and water column. This degradation approximates the mineralization of particulate detrital carbon in the sediment.

4.5.2 PCB Model Parameters

The toxic chemical fate and transport mechanisms within the HUDTOX model framework are depicted by Figure 3-4. The required process parameters used to describe these PCB dynamics are presented in Table 4-10. Each of the model parameters is defined in the table along with the appropriate units for use in HUDTOX. The sources used to derive each parameter are also listed in Table 4-10. Note that all of the parameters used in calibrating HUDTOX are congener-specific and are based upon either an *a priori* analysis of Phase 2 water column monitoring data (TAMS/CADMUS/Gradient, 1996 - pending publication) or on values from the scientific literature. Parameters for total PCBs were estimated by using median values from the ranges of values for individual congeners.

4.6 Calibration Approach

In mass balance modeling, spatial averaging of measured water quality constituents is commonly employed to estimate constituent concentrations that are representative of individual model segments. Model simulations can then be compared with these average concentration values and their variability to evaluate model performance. In this preliminary model calibration, the Upper Hudson River water column was divided into 13 longitudinal segments (Figure 3-5), but there were only 6 water column sampling stations in the Phase 2 water column monitoring program. Also, the sampling stations were located far apart, so that no more than one station could be assigned within a single model segment. Therefore,

it was not possible to actually estimate average water quality parameter concentrations for individual model segments. Instead, water quality parameters simulated by the model were compared directly with the time series of data measurements from single sampling stations located within the appropriate model segments.

The Phase 2 water column monitoring program included 6 stations over the section of the Upper Hudson River being modeled, as shown in Table 4-11. For the TSS calibration, additional daily measurements collected by the Rensselaer Polytechnic Institute (RPI) at stations located in HUDTOX Segments 10 and 11, and the USGS data were also used.

4.6.1 Transport Model (Water Balance) Specification

The first step in developing a calibration of HUDTOX for the 1993 simulation period involved specifying external advective flows and their respective routing schemes through the model segmentation to form a mass balance for water. As discussed in Section 4.4.2, these include upstream, tributary, and ungaged (including nonpoint) flows. Only surface water flows were included in the present calibration of HUDTOX. This calibration of HUDTOX does not include potential groundwater inflows to the Upper Hudson River, since the information needed to spatially and temporally estimate these sources does not exist at this time. The potential effect of groundwater inflow (also termed pore water advection) on water column PCB levels in TIP is examined, however, as part of the HUDTOX model calibration diagnostics in Section 4.8.

The bulk mixing among surface water segments in HUDTOX must also be specified as part of the transport conditions in the HUDTOX calibration. Since HUDTOX is one-dimensional in this respect, a longitudinal dispersion (D_L) coefficient was used. The limited number of mainstem water quality stations in the Phase 2 monitoring program, and the lack of a good natural tracer prevent calibration of D_L within HUDTOX. Instead, the value of D_L used for model calibration was estimated from data generated during a 1967 USGS dye study conducted in the Upper Hudson River near Fort Edward (Shindel, 1969). Also note that D_L is set to zero for 7 of the 12 HUDTOX segment interfaces because they are located at dams along the river.

4.6.2 Solids Model

The HUDTOX solids model is specified in terms of two constituent state variables: particulate solids (total suspended solids in the water column and bedded solids in the sediment), and dissolved organic carbon (DOC). As discussed in Section 4.4.2, DOC is not a calibration target for this preliminary model application. Instead, DOC is simulated as a state variable to distinctly represent the transport and transformation of DOC-bound components within the PCB mass balance. The

approach used for the particulate solids calibration of HUDTOX for the calibration period was the following:

1. As a screening-level check on the consistency between external loadings and observed water column concentrations, TSS was first simulated as a conservative tracer;
2. Internal solids loadings due to primary production were added to the model;
3. A constant gross settling velocity for water column TSS was specified, based on ranges of values used in similar model applications to other systems;
4. Solids resuspension velocities during non-event conditions were determined by calibrating model output to observed TSS values;
5. Solids resuspension velocities during high flow events were increased so that model output represented observed increases in TSS during these events;
6. Final calibration of solids resuspension velocities was conducted by ensuring that model output for cumulative solids transport fluxes matched observed solids fluxes at Stillwater and Waterford. These observed fluxes were derived using the MVUE loading method and available USGS field measurements for river flow and TSS at these two locations; and,
7. Solids kinetic processes in HUDTOX were adjusted to maintain an approximately constant DOC concentration gradient between the sediment and water column. To accomplish this, a small degree of sediment solids mineralization to DOC was required.

4.6.3 PCB Model

The PCB calibration was built upon the above hydraulic and solids mass balances. Emphasis was placed on specification of site-specific external PCB loadings, and independent specification of PCB process-related parameters using site-specific measurements or values from the scientific literature. The PCB calibration was not arbitrarily "tuned" to match model output with observed concentration values. This calibration approach served as a good test of the underlying hydraulic and solids mass balances. The specific steps in the HUDTOX calibration for total PCBs and the five calibration congeners were the following:

1. Using Phase 2 sampling program data (TAMS/CADMUS/Gradient, 1996 - pending publication), a constant fraction of organic carbon (f_{oc}) on TSS was determined and specified for the water column. GE data from 1991 were

used to estimate constant f_{oc} values in bedded sediments on a segment-specific basis;

2. Values for the partition coefficients, K_{poc} and K_{doc} were fixed based upon a three-phase partitioning analysis of the Phase 2 water column monitoring data (TAMS/CADMUS/Gradient, 1996 - pending publication). Median values (at 20°C) determined from this data analysis were specified for each of the five selected PCB congeners. Values for total PCBs were estimated based upon the distributions of partition coefficients for the individual congeners;
3. Congener-specific temperature slope factors (tsf) were used to represent seasonal variation of PCB partition coefficients. This effect is described by Equation 3-2. Estimates of tsf values for each calibration congener were generated as part of the Phase 2 data analysis (TAMS/CADMUS/Gradient, 1996 - pending publication);
4. The chemical diffusion coefficient (D_{ci}) between sediment layers was fixed at the level of molecular diffusion. D_{si} was then adjusted on a PCB congener-specific basis for differences in molecular weight (O'Connor, 1985);
5. The chemical diffusion coefficient (D_{swi}) between the active sediment layer and the water column was increased to 10 times the molecular diffusion rate to account for the influences of bioturbation and water currents (DiToro and Fitzpatrick, 1993);
6. Congener-specific Henry's Law constants (H at 25 °C) were specified based on a literature compilation developed as part of the Green Bay Mass Balance Study (Bierman et al., 1992). The correction to ambient river temperature for H is shown by Equation 3-1 in Section 3.5.2; and,
7. Air-water gas exchange (volatilization) of dissolved phase PCBs was internally calculated based upon hydraulic conditions and chemical-specific characteristics as implemented in the standard WASP4 toxic chemical model (Ambrose et al., 1988). A standard reaeration temperature correction factor (θ) of 1.024 was employed. Note that enhanced gas exchange over dams was not included in HUDTOX for this preliminary model calibration. This phenomenon has little effect on the PCB modeling for the January-September 1993 preliminary model calibration period, but it may be a significant factor for long-term predictions.

4.7 Calibration Results

4.7.1 Solids Model

The values of the model parameters used to calibrate the HUDTOX solids model are presented in Table 4-12. The basis for the selection of the calibration values and the solids modeling results are discussed in the following paragraphs.

The HUDTOX solids model calibration strategy required first that an assessment of any potentially significant unmeasured sources of solids loads to the Upper Hudson River be evaluated. Initial simulations using TSS as a conservative tracer indicated that significant external solids loads were likely entering the river between Fort Edward and the confluence with the Hoosic River, and that primary production might be a significant internal source of solids during summer low-flow conditions. Section 4.4.2 discusses how these solids loads were estimated for inclusion in the HUDTOX solids model calibration. Calibration of the solids settling and resuspension rates were undertaken once these unmeasured loads were estimated.

A constant solids gross settling velocity (V_s) of 2.0 m/day was used in the model calibration. This value is consistent with the range of gross solids settling velocities used in other relevant mass balance modeling studies. Thomann et al., (1989, 1991) used a value of 3.05 m/day in a model of PCB homologues in the Lower Hudson River. LTI (1992) used a value of 2.0 m/day in a model for TCDD (dioxin) in the Columbia River Basin. Bierman et al., (1992) used a value of 2.5 m/day in a model of total PCBs and PCB congeners in Green Bay, Lake Michigan. USEPA (1984) used values ranging from 0.25 to 0.80 m/day, depending on river flow, in a model of four heavy metals in the Flint River, Michigan.

Much of the Phase 2 water column monitoring program during 1993 occurred during lower-flow, non-event conditions. The TSS concentrations measured during these periods provided a set of data for calibrating a baseline solids resuspension velocity for Upper Hudson River. A spatially variable V_r was used, with higher values specified at downstream model segments to better represent observed water column TSS concentrations. The required increase in V_r may be due in part to an increase in the actual proportion of sediment area subject to resuspension in downstream segments. During high-flow events, a multiplying factor was applied to V_r to empirically represent the influence of increased sediment scour on water column TSS concentrations. A value of 60 for this factor was determined by calibrating model output for cumulative solids flux to observed cumulative solids fluxes at Stillwater and Waterford. The factor was applied when the mean ambient velocity exceeded 3.0 ft/sec.

Analysis of the Phase 2 high resolution sediment cores indicated that long-term solids deposition rates ranged between 0.5 and 5.0 cm/year (TAMS/CADMUS/Gradient, 1996 - pending publication). Also, some of the cores could not be dated, suggesting that settling and resuspension may be at near-equilibrium in portions of river. The results could not be used to specify solids burial velocity (V_b) in the HUDTOX model because the sediment cores were taken in depositional areas of the river and do not necessarily represent the segment-average spatial scale of the HUDTOX model. For solids in this preliminary model calibration, a constant burial velocity of 6.0×10^{-6} m/day (or 0.22 cm/yr) was assigned on the basis of best professional judgment.

Model results for the preliminary model calibration period are not sensitive to changes in this solids burial velocity; however, decadal-scale predictive results for PCBs are expected to be very sensitive to specification of the solids burial velocity. Consequently, prior to use of the HUDTOX model for such predictive simulations, a long-term (1984-1993) hindcasting calibration will be conducted (Appendix B) to ensure that the model accurately represents observations of solids and PCB dynamics in the Upper Hudson River.

Figure 4-10 presents the solids model calibration results for the period of simulation. Phase 2 data from transect and flow averaged sampling events are plotted against computed TSS for model Segments 3, 6, 8 and 12. USGS data are plotted for model Segments 8 and 12, while the nearly-daily TSS measurements taken by Bopp at two stations in the Upper Hudson River are plotted in Segments 10 and 11. The ability of the model to capture some of the TSS variation over the course of the spring snowmelt event is evident during April 1993 (Julian days 90 to 120). TSS levels in the river are generally low and flat during non-event conditions, providing data for calibrating baseline resuspension rates in the river.

A comparison of the computed cumulative TSS flux with that generated through MVUE regression of the USGS TSS data is shown in Figures 4-11 and 4-12. The cumulative TSS fluxes at Stillwater are comparable. Differences in cumulative fluxes occur at Waterford, probably due in part to springtime construction activities at Lock 1. It is possible that large amounts of solids were released from the lock during this period, and these would not be accounted for in the HUDTOX solids model.

It should be noted that much of the dynamic variation in computed TSS concentrations is driven by external solids loadings from upstream and from tributaries. Consequently, further adjustments in settling and resuspension rates in the HUDTOX model result in only marginal improvements in the overall TSS calibration.

Two simple goodness-of-fit tests were conducted to quantitatively evaluate the TSS calibration. Figure 4-13 plots the computed vs. observed TSS concentrations for the preliminary model calibration period. A large degree of scatter is evident, but the regression line falls along a near one-to-one slope, and the correlation coefficient (R^2) of 0.69 is relatively high. The results from a set of Student's t-tests comparing computed versus observed mean TSS concentrations for individual model segments are shown in Table 4-13. Segment-mean values for model output were significantly different ($p < 0.05$) than segment-mean observed values in just one of six cases. Failure to pass the t-test in downstream model segment 11 indicates that uncertainties remain in the present model calibration. Some of these uncertainties are due to insufficient data for specification of external solids loadings from downstream tributaries and sediment solids concentrations. Some uncertainty is also due to the fact that the preliminary HUDTOX model is not an "event" model designed to represent day-to-day variability, but instead is designed to represent variability on weekly to monthly time scales, depending on the time scales of the external forcing functions.

A final aspect of the solids model calibration involved the selection of a sediment solids degradation rate to maintain near-constant dissolved organic carbon (DOC) levels in the sediments. Since organic carbon is not modeled as a state variable in HUDTOX, this degradation represents the mineralization of particulate detrital carbon (PDC) in the sediments. DOC is a by-product of this degradation process, which allows a significant DOC concentration gradient to exist from the sediments to the water column. The selected solids degradation rate of $1.1 \times 10^{-6} \text{ day}^{-1}$ maintains an appropriate DOC concentration gradient and has a negligible effect on sediment solids levels.

4.7.2 PCB Model

The chemical-specific HUDTOX parameters for total PCBs and the five calibration congeners are presented in Table 4-14. Figure 4-14 presents the calibration results for water column total PCBs (particulate plus dissolved) in selected model segments. GE PCB data are shown in Segment 3 (at Thompson Island Dam), while the Phase 2 data (Transect and Flow-Average sampling events) are shown in Segments 3, 6, 8, and 12. Note that an apparent increase in PCB levels from approximately Julian Day 160 to 180 (June 9-29, 1993) is due to the upstream boundary conditions at Rogers Island.

Results in Figures 4-14 through 4-19 present the preliminary HUDTOX model calibration (solid lines) for total PCBs, and total concentrations of the five congeners, respectively. In general, the model output provides a good representation of the temporal structure of the PCB data. Model output is lower than field observations in TIP; however, a significant increase in PCB concentration between the upstream boundary shown in the Segment 1 plot and Segment 3 is

demonstrated. This is consistent with the observed net gain of PCBs in the water column across TIP (TAMS/CADMUS/Gradient 1996 - pending publication).

The actual causal mechanism(s) for the observed PCB gain across TIP is not yet fully understood. Some of this effect is probably due to higher concentrations of lower chlorinated PCB congeners (e.g. BZ#4) in TIP sediments, relative to concentrations of higher chlorinated congeners. Because lower chlorinated congeners tend to have lower partition coefficients, TIP sediments are relatively enriched with both particulate and dissolved phases of these lower chlorinated congeners. Consequently, sediment-water PCB fluxes due to pore water advection, resuspension or diffusion will tend to be relatively enriched with lower chlorinated congeners. A comparison between BZ#4 (Figure 4-15) and BZ#138 (Figure 4-19) illustrates this behavior when upstream boundary conditions are compared to HUDTOX results (solid lines) for Segments 1 and 3, which are located in TIP.

This preliminary HUDTOX model was used to test the hypothesis that PCB gains across TIP might be consistent with advective flux of pore water PCBs due to groundwater inflow. This evaluation was conducted for total PCBs and BZ#4, the calibration target with the lowest partition coefficient (Table 4-14). If this sediment-water exchange mechanism is important, then the flux for BZ#4 would be expected to be larger than fluxes for total PCBs and any of the other target congeners.

Potential groundwater inflow to TIP was estimated using two independent methods. First, Darcy's law (Equation 4-1) was applied to estimate groundwater flow velocity using estimates of hydraulic conductivity (k) and the groundwater hydraulic gradient (j):

$$u = k * j \quad (4-1)$$

where,

- u = Darcy velocity [L/T]
- k = hydraulic conductivity [L/T]
- j = hydraulic gradient [L/L].

Groundwater flow into TIP was estimated by multiplying the Darcy velocity by the bottom area of the pool. The pool is approximately 6 miles long and 800 feet wide, a bottom surface area of $2.53 \times 10^7 \text{ ft}^2$ ($= 2.35 \times 10^6 \text{ m}^2$).

The hydraulic gradient was estimated from land surface topography using USGS quadrangle maps. The measured land surface slope ranges between 0.01 and 0.03, averaging approximately 0.02 along the length of the TIP river reach. A relatively low hydraulic conductivity of $6 \times 10^{-4} \text{ cm/sec}$ was applied to represent an

average silty-sand content in TIP sediments (Freeze and Cherry, 1979). This results in an estimated 10 cfs of groundwater inflow to TIP. Note that hydraulic conductivity for primarily sandy sediments is on the order of 1×10^{-2} cm/sec. A hydraulic conductivity of 2×10^{-3} cm/sec, representative of a more heterogeneous (e.g. gravel, sand, and silt) sediment, produces an estimated groundwater inflow to TIP of 30 cfs.

Second, an analysis of gains in Hudson River flow between USGS gages at Hadley and Fort Edward was conducted. Average annual flow increases by approximately 120 cfs over this 30 mile section of river. No major tributaries enter the river between these two stations, while the drainage basin area increases by approximately 100 mi². If all of the increase in flow was attributed to groundwater, then the maximum likely groundwater inflow over the 6 mile reach of TIP would be 24 cfs. Accounting for surface runoff over the reach reduces this estimate, but it still provides a reasonable approximation of groundwater inflow to TIP. In addition, evaluation of the flow differences between Hadley and Fort Edward on an annual basis may underestimate the actual groundwater inflow during summer low flow periods if river levels fall in relation to nearby groundwater levels. It should also be noted that observed increases in PCBs across TIP are at a maximum during summer low flow periods.

Based on the above analyses, a value of 30 cfs for total groundwater inflow to TIP was chosen for evaluating the effect of potential pore water advection. Dashed lines in Figures 4-14 and 4-15 show the results for the HUDTOX calibration parameterization for total PCBs and BZ#4, but include an assumed pore water inflow of 30 cfs across TIP. Results indicate that porewater advection is potentially of sufficient magnitude to influence total PCB concentrations in TIP; however, information is not available to quantify the temporal and spatial variability of potential groundwater inflows to TIP. Furthermore, the present analyses are based on sediment PCB concentrations as reported in the GE 1991 sediment survey data. The surficial (0-5 cm) sediment PCB concentration measured during 1991 may not fully represent 1993 conditions.

More detailed calibration results for total PCBs and the five calibration congeners are presented in Figures 4-20 through 4-31. These temporal profiles provide a comparison of model results with available data for both apparent dissolved and particulate phase PCBs in the water column. In general, the HUDTOX model represents the mean behavior of water column total PCBs and the five congener groups reasonably well. Variability in the relative influence of porewater inflows across different PCB congeners is evident by the dashed lines in the plots of total PCBs and BZ#4, which represent the computed PCB concentrations with constant porewater advection into TIP model segments. Total PCBs and BZ#4 water column concentrations increase significantly when porewater advection is included in the HUDTOX model. The other four PCB congeners have higher partition coefficients than BZ#4, consequently, porewater advection would

be expected to be less important for these calibration targets than for BZ#4. Porewater advection was not evaluated for any of these other four congeners.

A set of t-tests was also conducted to provide a quantitative evaluation of the PCB model calibration (without porewater advection). These tests demonstrated the ability of the model to represent the mean behavior of PCBs among the individual model segments. Tables 4-15 through 4-17 contain results from these tests for total, dissolved, and particulate phase PCBs. For 88 percent of the comparisons across all calibration targets and model spatial segments, there were no significant differences ($p < 0.05$) between segment-mean values for model output and segment-mean observed values for total PCBs. Corresponding results for dissolved and particulate phase PCBs were 79 percent and 71 percent, respectively.

Regression analyses were conducted to provide additional quantitative evaluation of the HUDTOX model calibration. Model output is plotted versus observed data for each of the PCB calibration targets in Figures 4-32 through 4-34 for total, dissolved and particulate phase PCBs, respectively. Only Phase 2 transect data are included in these plots, since the flow-averaged PCB data cannot be compared on a point-to-point basis with the model output values.

The calibrated HUDTOX model was successful in representing day-to-day variability across all model spatial segments. Although scatter is evident in these comparisons and there are several apparent outlying data points, the calibrated model explained an average of 70 percent of the overall spatial-temporal variability in these day-to-day field data. HUDTOX was also successful in representing the average behavior of water column total PCBs and congener groups within each model spatial segment.

4.8 Mass Balance Component Analysis

As part of the HUDTOX modeling effort, a mass balance component analysis was developed for the solids and PCB calibrations. This type of evaluation focuses on the significance of the various sources, sinks and mass reservoirs for each state variable within the modeling framework. The entire Upper Hudson River model segmentation and the TIP were analyzed for the 9-month preliminary model calibration period. In addition, the 1993 spring high flow period was examined separately from the rest of the model simulation period. This high flow period was defined for the mass balance analysis as extending from March 26 through May 10, 1993 in order to capture spring flooding conditions occurring throughout the entire Upper Hudson River.

For the entire model calibration period, Figures 4-35 and 4-36 present the mass balance component diagrams for the solids calibration in TIP and the Upper Hudson River, respectively. Upstream Hudson River solids loads dominate both sediment resuspension and primary production sources in TIP, but solids loads from

downstream tributaries and sediment solids dynamics are more dominant for the Upper Hudson River as a whole. The principal external solids loadings to the Upper Hudson River during the simulation period were from the Mohawk River (59 percent) and the Hoosic River (20 percent). Solids loadings from the upstream boundary at Fort Edward represented only 8.5 percent of the total external solids loadings. The minimal effect of the solids degradation (i.e. mineralization) required to maintain near-constant sediment DOC concentrations is also evident from the solids mass balance component diagrams.

The effect of the 1993 spring high flow period on the components of the solids mass balance is shown in Figure 4-37. Approximately 85 percent of the solids load across the upstream boundary, and 87 percent of the tributary solids load, enters the Upper Hudson River during the spring high flow period. Also, the bulk of the computed sediment solids resuspension, in both TIP (70 percent) and the entire Upper Hudson (78 percent), occurs during the spring high flow period. However, it should be noted that the TSS gain across TIP is just 8 percent during the spring high flow period because the upstream boundary condition dominates the solids load to this section of the river. Only 5 percent of the solids mass passing over Thompson Island Dam is due to net resuspension within TIP over the entire 1993 calibration period. During the lower flow periods, the gross settling flux of TSS exceeds sediment solids resuspension, and a net settling of TSS occurs throughout the Upper Hudson, including Thompson Island Pool. A net 10 percent TSS gain across TIP occurs during the lower flow period, primarily due to internal solids load generation through primary production.

Mass balance diagrams for the HUDTOX model calibration of total PCBs are shown in Figure 4-38 and 4-39. These diagrams summarize results for the entire 9-month preliminary model calibration period. Note that these diagrams are not a representation of the mass balance for a complete year, and should not be construed to indicate river characteristics outside of the period simulated.

The principal sources of total PCBs to the water column of the Upper Hudson River during the entire 9-month period of simulation were internal loadings due to resuspension from the surface sediment layer (859 kg) and external loadings across the upstream boundary at Fort Edward (352 kg). The principal losses of total PCBs from the water column were outflow at Federal Dam (985 kg) and gross settling of particulate phase PCBs (311 kg). Volatilization losses (53 kg) for total PCBs were nearly an order-of-magnitude lower than other loss processes.

The principal source of total PCBs to the surface sediment layer of the Upper Hudson River during the period of simulation was gross settling of particulate phase PCBs (311 kg). The principal losses of total PCBs from the surface sediment layer were resuspension to the water column (859 kg) and net burial to deeper sediment layers (418 kg).

The principal sources of total PCBs to the water column of TIP during the period of simulation were internal loadings due to resuspension from the surface sediment layer (406 kg) and external loadings across the upstream boundary at Fort Edward (352 kg). The principal losses of total PCBs from the water column were outflow at Thompson Island Dam (712 kg) and gross settling of particulate phase PCBs (46 kg). Overall, net resuspension in TIP (i.e. resuspension minus gross settling) represent 51 percent (360 kg) of the total PCB mass transported across Thompson Island Dam.

The principal source of total PCBs to the surface sediment layer in TIP during the period of simulation was gross settling of particulate phase PCBs (46 kg). The principal losses of total PCBs from the surface sediment layer were resuspension to the water column (406 kg) and net burial to deeper sediment layers (194 kg). In TIP (Figure 4-38) the resuspension of total PCBs is relatively more important than in the Upper Hudson River as a whole. The PCB mass flux from resuspension was nearly 10 times greater than PCB gross settling in TIP, while it was less than a factor of 3 greater over the entire Upper Hudson River.

Figure 4-40 displays the PCB mass balance components for the 9-month 1993 calibration period for both (a) Upper Hudson River; and (b) TIP. Stacked bars are used to show the effect of the 1993 spring high flow period relative to the total simulation period. The 45-day spring high flow period dominates both the external and internal (i.e. resuspension) loading sources of PCBs to the water column for the simulation period. Approximately 70 percent (247 kg) of the total PCB loading across the upstream boundary occurs during the spring high flow period. Also, more than 70 percent of the computed resuspension of total PCBs from the sediment, in both TIP (73 percent or 285 kg) and the entire Upper Hudson River (70 percent or 628 kg), occurs during the spring high-flow period.

Figure 4-40b also shows the greater than two-fold net gain of total PCBs across TIP during both spring high flow (104 percent or 256 kg) and lower flow (100 percent or 104 kg) conditions. This is in contrast to the small 8 percent net gain of TSS across the pool during the spring high flow period, and a 10 percent gain during the remaining lower flow period (see Figure 4-37). These results point out that relatively high PCB concentrations in the sediments of TIP have a significant effect on Upper Hudson River PCB dynamics. Even low rates of solids exchange between the sediment and water column can transfer significant quantities of PCBs into the water column. In fact, the model results indicate that TIP contributes 52 percent (121 kg) of the total PCB (231 kg) resuspension load to the Upper Hudson River during the lower flow period of the 1993 calibration.

The importance of TIP as a source of PCBs to the Upper Hudson River is illustrated by Figures 4-41 through 4-45 which show the mass balance over the HUDTOX calibration period for congeners BZ#4, BZ#28, BZ#52, BZ#101 + 90 and BZ#138, respectively. The differences in the dynamics of total PCBs and BZ#4 are

demonstrated by the 585 percent (79 kg) gain in BZ#4 mass across TIP during the calibration period versus the 102 percent (361 kg) gain for total PCBs. During the spring high flow period, BZ#4 shows a 1435 percent (51 kg) gain across TIP and a gain of only 278 percent (27 kg) during the lower flow periods of the model calibration period.

These results illustrate the variations in relative importance of different fate and transport mechanisms across the range of PCB congeners simulated. For example, dissolved and DOC-bound diffusive transport from the sediment transfers a greater proportion of BZ#4 into the water column than it does for the other congeners. Also, the mass balance results show that the relative loss of BZ#4 due to volatilization is significantly greater than for other congeners. These findings are not unexpected because BZ#4 has the lowest partition coefficient ($\log K_{poc} = 5.108$, see Table 6-9) among the PCB congeners simulated. These factors, along with the relatively high percentage of lower-chlorinated congeners in TIP sediments, are the principal reasons responsible for the large computed differences in PCB dynamics across the range of PCB congeners included in this preliminary model calibration.

The influence of potential porewater PCB fluxes was examined in the component mass balances for TIP for BZ#4 (Figures 4-46 and 4-47). For the entire preliminary model calibration period, an assumed, constant 30 cfs of porewater advection into TIP caused a 34 percent increase (92 kg to 124 kg) in the outflow of PCB congener BZ#4 at Thompson Island Dam. Figure 4-48 shows the mass balance for the BZ#4 simulation with the inclusion of pore water advection. Approximately 30 percent of the sediment BZ#4 load from TIP was due to pore water advection for this particular simulation. The corresponding increase in total PCB mass outflow from TIP was less than 6 percent (712 kg to 753 kg) as shown in Figures 4-49 and 4-50. Higher-chlorinated PCB congeners show minimal water column increases due to porewater advection, a modeling result which is consistent with field observations.

It should be noted that all results from these component analyses are premised on the HUDTOX preliminary model calibration for the period of January 1 through September 30, 1993. This calibration contains many sources of uncertainty. The principal uncertainties in the HUDTOX calibration at the present time are the following:

1. Suspended solids loads from tributaries downstream of Thompson Island Dam (91 percent of total external solids loadings) are uncertain due to the limited number of field measurements, for both TSS and flow, in the tributaries;
2. PCB loads across the upstream boundary of the model at Fort Edward, the principal source, are uncertain due to unknown amounts of PCB loadings from the GE facilities at Hudson Falls and Fort Edward, and the limited number of field measurements;

3. Large uncertainties in specification of the three-dimensional sediment physical properties and sediment PCB concentrations;
4. Uncertainties in specification of solids settling and resuspension velocities, and the potential dependence of these rates on river flow; and
5. Uncertainties due to an incomplete understanding of the causative mechanism(s) for observed increases in water column concentrations of lower-chlorinated congeners across TIP.

Plans for future modeling work (Appendix B) contain elements that will address some of these uncertainties. The more finely-resolved spatial segmentation grid for TIP will better represent horizontal differences in sediment-water interactions. In conjunction with use of data from the Phase 2 low-resolution sediment coring effort, this grid will allow more accurate specification of sediment physical properties and sediment PCB initial concentrations. Calibration of HUDTOX to high-frequency TSS data for Spring 1994 will reduce uncertainties in solids settling and resuspension velocities. Additional hypothesis testing and sensitivity analyses will lead to better understanding of the causative mechanism(s) for observed increases in PCB concentrations across TIP.

4.9 PCB Model Calibration Sensitivity Analysis

To provide additional insight into the parameterization of this preliminary HUDTOX calibration, a limited sensitivity analysis was conducted. Two of the HUDTOX model inputs have been identified as having a large degree of uncertainty: sediment PCB initial conditions and upstream PCB boundary conditions. To evaluate responses of the model to changes in these conditions, sensitivity analyses were conducted with the calibrated HUDTOX model in which sediment initial conditions and upstream PCB loadings were varied by plus/minus 30 percent. A total of four independent simulations was conducted to produce sensitivity results for total PCBs and the five selected PCB congeners used for the HUDTOX calibration.

The sensitivity results for the 30 percent variation in sediment PCB initial conditions are presented in Figures 4-51 through 4-56 for total PCBs, and congeners BZ#4, BZ#28, BZ#52, BZ#101 + 90 and BZ#138, respectively. These time series plots illustrate that water column PCB levels are very sensitive to the sediment conditions during transient flood events when a greater exchange of solids between sediment and water is occurring. Figure 4-52 shows that computed BZ#4 concentrations exhibit greater sensitivity to sediment conditions than other congeners during the lower flow period in summer of 1993 (after May 10th or Day 130).

The model results for a 30 percent variation in upstream boundary PCB loads were less sensitive than to a 30 percent change in sediment initial conditions. Model results are presented in Figures 4-57 through 4-62 for total PCBs, and congeners BZ#4, BZ#28, BZ#52, BZ#101+90 and BZ#138, respectively. As expected, the results show a trend of decreasing sensitivity to the upstream boundary moving downstream, as sediment-water interactions and other external sources affect PCB levels in the water column. The sensitivity of computed PCB concentrations to transient spikes of upstream PCBs during lower flow periods is also very apparent during June 1993 (Julian Days 153 to 181).

The results of the sensitivity simulations are summarized by the total PCBs mass balances shown in Figures 4-63 and 4-64. For analyses in which initial total PCB concentrations in the sediments were varied by plus/minus 30 percent, total PCB mass transported across Thompson Island Dam varied by plus/minus 16 percent, and total PCB loadings across Federal Dam to the Lower Hudson River varied by plus/minus 20 percent. For analyses in which total PCB loadings across the upstream boundary at Fort Edward were varied by plus/minus 30 percent, total PCB mass transported across Thompson Island Dam varied by plus/minus 14 percent, and total PCB loadings across Federal Dam varied by plus/minus 7 percent.

5. CALIBRATION OF THOMPSON ISLAND POOL HYDRODYNAMIC MODEL

5.1 Introduction

Estimation of resuspension of bottom sediments containing PCBs in the Thompson Island Pool (TIP) as a result of high river flows requires a hydrodynamic model to represent the flow conditions of interest. The calibration of the hydrodynamic model, RMA-2V, as applied to the TIP, is described in this section. RMA-2V is a finite element model, primarily developed for and maintained by the U. S. Army Corps of Engineers. The purpose of the hydrodynamic modeling is to calculate a two-dimensional (longitudinally and laterally), vertically-averaged, velocity field in TIP for various flows of interest. By knowing the two-dimensional flow field, the two-dimensional shear stresses exerted on the bottom of the river can be calculated. From the two-dimensional shear stresses, the mass of river bed sediment eroded during the various flows of interest can be calculated with the TIP Depth of Scour Model (Section 6).

The description of the TIP hydrodynamic modeling effort is divided into 10 sections. Section 5.2 describes the input data required by the model to simulate TIP. Section 5.3 describes the internal model parameters used in the calibration. Section 5.4 describes the calibration approach. Section 5.5 provides the calibration results. Section 5.6 describes additional, separate sources of information used to validate the model calibration results. Section 5.7 describes predictive results for the 100-year flood event. Section 5.8 describes model sensitivity in response to changes in various model inputs. Section 5.9 describes the conversion of the vertically-averaged velocities computed by the model to the corresponding bed shear stresses. Finally, Section 5.10 contains a discussion of the model results.

5.2 Model Input Data

A hydrodynamic model requires specific input data describing the hydraulic conditions of the system chosen for simulation. These input data consist of the system specific physical data, the forcing functions or upstream boundary conditions, and the downstream and side channel boundary conditions. These are described below.

5.2.1 System-Specific Physical Data

The system specific physical data consists of the river dimensions used to develop the model's segmentation and the river's resistance to flow, which is expressed in terms of the Manning's 'n'. Manning's 'n' is a calibration parameter derived from comparing the model output to river observations for a range of flows.

Model Segmentation

The RMA-2V model uses a six-node triangular element scheme to describe the physiography of the target system. The model segmentation consists of approximately 6000 nodes defining 3000 elements. Each node is defined by an x-y coordinate and its corresponding elevation. The vertically averaged velocity vector is calculated at each of these nodes for a given flow condition. Figure 5-1 shows the river segmentation used in the model calibration.

The model segmentation or model grid for the main channel is based on the bathymetric survey performed by General Electric in 1991 (O'Brien and Gere, 1993b). The model grid for the adjacent floodplain is based on the USGS topographic maps. Smaller elements are used in the main channel where changes in velocity can be large and larger elements were used in the floodplain where the velocity and its changes are relatively small. The nodes of the finite element grid in the main channel are located approximately every 50 feet across the river and approximately 300 feet along the channel.

Manning's 'n'

The input parameter, Manning's 'n', expresses the river's hydraulic resistance to flow. Conceptually, resistance to flow reflects the character of the sediments and the nature of the flow pathways. This parameter is commonly a calibration parameter since its value cannot be predicted accurately from a measurement of the physical dimensions of the river or from a description of the sediment type. Two site specific flow modeling studies, Zimmie (1985) and FEMA (1982) had been conducted previously and the Manning's 'n' values can be expected to be near the values used in these studies. Table 5-1 contains the Manning 'n' values used in these two studies.

For this study, the values of Zimmie were used initially and then subsequently calibrated to best fit the recorded observations of the river, especially those at high flow. The sensitivity of the model to changes in this parameter is discussed below in Section 5.8.

5.2.2 Forcing Functions

The principal forcing function of the model consists of the upstream boundary condition, which is the specified flow. The model was run for a total of eight different flows (Table 5-2). The first four flows are of interest because the concentration of suspended sediment in the river was sampled when they occurred. The suspended sediment concentration data taken during these flows will be used to help calibrate the TIP Depth of Scour Model. Recall that the Depth of Scour Model requires the shear stresses computed from the velocities calculated in the hydrodynamic model calibrated here. The fifth flow is of interest because it is the highest flow recorded in TIP after the Fort Edward dam was removed in 1973. The

final three flows are of interest because they represent high flow events with a specified return period.

The model results for these eight design flows will be used in the TIP Depth of Scour Model to evaluate the risk of resuspension of PCBs from the deeply buried sediments. These design flows were specified at the most upstream transect of the model grid. This transect is approximately 500 feet upstream of Rogers Island.

5.2.3 Boundary Conditions

The boundary conditions of the model consist of the side channel boundary condition and the downstream boundary condition. The side channel boundary condition is the requirement that the velocity normal to the sides of the channel is zero. This is implicitly performed in the RMA-2V model. The downstream boundary condition consists of specifying the water surface elevation at the most downstream transect, which is the Thompson Island Dam. This water surface elevation was taken from the rating curve for Gauge 118, which is located just above Thompson Island Dam. The rating curve was developed from a regression analysis performed on the discharge-water level data accumulated during the 11 year period of 1983 to 1993 (TAMS/CADMUS/Gradient, 1996 - pending publication). Examination of this rating curve showed that the regression is good for flows up to 30,000 cfs; however, the third-order polynomial developed in the regression fails to accurately predict increasing river elevations for flows above 30,000 cfs. Refined extrapolation using engineering best judgment and a theoretical rating curve (Zimmie, 1985) was used to determine the water levels at Thompson Island Dam above these flows.

The downstream boundary must be specified as an elevation since if a flow is specified, there would not be a way to incorporate the backwater effects of the dam into the model.

5.3 Internal Model Parameters

There are two internal model parameters, the Manning's 'n' for the river and the turbulent exchange coefficients. Only the Manning's 'n', one for the main channel and one for the floodplain, were used as calibration parameters. The other main input parameter, the turbulent exchange coefficient, is not a true physical parameter since it reflects the flow field, the model grid, and the numerical solution technique of RMA-2V. Therefore, values were assigned for the turbulent exchange coefficients based on guidelines in the literature (Thomas and McNally, 1990) and not changed in the calibration procedure. Moreover, changes in this parameter do not significantly affect the model's results and model sensitivity to changes in this parameter is discussed in Section 5.8.

5.4 Calibration Approach

The calibration approach consists of determining an appropriate value for the turbulent exchange coefficients and then varying the Manning's 'n' so that the river levels computed by the model agree well with the river levels predicted by the upstream rating curve for each flow input at the upstream transect of the grid. Note that only one value of Manning's 'n' was used for the entire length of the main channel since there is no physical data on which to base a variation.

The upstream rating curve used for comparing to model output during calibration was Gauge 119, near Lock Number 7, which is near the southern tip of Rogers Island (Figure 5-2). The Gauge 119 rating curve is similar to the Gauge 118 in that they are both third-order polynomial regressions on data from 1983 to 1993 and these regressions are only fully valid for flows less than 30,000 cfs. As with Gauge 118, the Gauge 119 water levels for flows above 30,000 cfs were determined using best engineering judgment.

Because this component of the study is primarily interested in higher Hudson River flows, those conditions above 30,000 cfs for the rating curves for both Gauge 119 (upstream) and Gauge 118 (downstream) are unsubstantiated. Therefore, the calibration first focused on the flow of 30,000 cfs. The Manning's 'n' values were calibrated for 30,000 cfs and were then used in the model to predict water elevations for lesser flows. These predicted water elevations were then compared with the elevations from the Gauge 119 elevations.

The turbulent exchange coefficients were determined to be well-represented by 100 lb-sec/ft². This determination is based on the guidelines given in the RMA-2V manual (Thomas and McNally, 1990). Specifically, the guidelines given in the manual suggest a range of values from 50 to 200 lb-sec/ft², and the model results proved to be relatively insensitive within this range of values.

5.5 Calibration Results

As described above, the model was primarily calibrated for the flow of 30,000 cfs. The Manning's 'n' for the final calibration were 0.020 for the main channel and 0.060 for the floodplain. The model computed the same river water surface elevation as observed at Gauge 119 using these calibration values. Table 5-3 shows this result along with the comparison of model output vs. rating curve water levels for lesser flows. Although the calibrated Manning's 'n' appears to be somewhat low, it was judged that a higher value could not be justified given the model's results especially those at low flows.

As seen when comparing the last two columns in Table 5-3, the model's results are slightly higher than the rating curve for the smaller flows. However, for the calibration flow of 30,000 cfs, the model result for river water elevation at Gauge 119, was the same as the rating curve. This observation of excellent model

fit at the upper limit of the river observations is helpful for examining the critical flows above 30,000 cfs.

5.6 Model Validation

There were two additional and separate sources of information used to validate the calibration results. The first source is Hudson River velocity measurements made in the TIP by the USGS. The second source is the flood study conducted by FEMA. A comparison between model results with these sources of information are discussed below.

5.6.1 Rating Curve Velocity Measurements

The USGS periodically measures the flow in the Hudson River in TIP to develop and update the river's rating curves. For the rating curve located at Scott's Paper upstream of Rogers Island, the flow is measured by measuring the depth and velocity at numerous points over the cross-section of the river at Rogers Island. These data are taken at the bridges over the Hudson River on both sides of Rogers Island. Figure 5-3 shows the location in the Hudson River where the velocities were taken. Using these data, the model's simulated velocities can be compared to the measured velocities as a check on the accuracy of the model.

The model was run for the same discharge (29,800 cfs) as measured on 18 April 1993. The model computed velocities approximately the same or in places slightly lower than measured. For example, the river velocities measured in the middle of the channel by the USGS were approximately 4.3 feet per second (fps) while the model computed velocities of approximately 4.1 fps. Even though these values are sufficiently close for validation, it should be noted that these measured velocities should be slightly higher since the bridges from which the velocity measurements are taken constrict the flow, causing localized higher velocities. The model does not include the localized effect of the bridges and, therefore, no constriction is accounted for in the model.

5.6.2 FEMA Flood Studies

The Federal Emergency Management Agency regularly conducts studies on rivers to predict the flood elevations in rivers for various frequencies of flows. The results of the study conducted by FEMA in 1984 were used as an additional check on the reasonableness of the model. The 100 year flow used by FEMA (52,400 cfs) is greater than the 100 year flow used in this study (47,330 cfs) so that a direct comparison of 100 year flood elevations was not initially possible. However, the model was eventually run for the 100 year FEMA flow of 52,400 cfs, and the model predicted a river elevation at Fort Edward of 130.4 ft. NGVD (National Geodetic Vertical Datum, formerly Sea Level Datum of 1929). The FEMA flood study using the HEC-2 program (with the higher Manning 'n' values) predicted a river elevation of 130.7 ft. NGVD. These results are very comparable and each

model reflects a slightly different representation of the river hydraulics. The RMA-2V model developed here was also run for 52,400 cfs with a Manning's 'n' of 0.030 for the main channel and 0.075 for the floodplain (approximately the same as the FEMA study). This resulted in a predicted river elevation of 131.7. More importantly, the river velocities do not vary appreciably for the various representations. Given this comparison, the model results are judged to be comparable to the FEMA flood studies.

5.7 100 Year Flood Model Results

The model was run for the 100 year flood of 47,330 cfs and the predicted river elevation at the downstream tip of Rogers Island was 128.6 ft. This elevation is slightly lower than the extrapolated rating curve's elevation of 129.1. Again, the model's predicted velocities would not be appreciably effected by the difference observed between the model results and the extrapolated rating curve. This model run was used as the baseline run for testing the model sensitivity which is discussed in the next section. Figure 5-4 shows the model grid along with the computed velocity vectors.

5.8 Sensitivity Analyses

The sensitivity of the model to the principal inputs was evaluated by varying the finite element grid size, the Manning's 'n', and the turbulent exchange coefficient. The model's sensitivity to the grid size was checked by running the model with a finite element grid with approximately two times the number of elements as the finite element grid used. The results obtained with the larger grid resolution were the same as the smaller grid and, therefore, it was concluded that the finite element grid used here was of sufficient resolution to simulate the river flow.

The sensitivity of the model to the Manning's 'n' and the turbulent exchange coefficient was measured by the effect on the predicted water elevations for the 100 year flood at the downstream tip of Rogers Island (Gauge 119). The sensitivity results are presented in the following discussion.

5.8.1 Manning's 'n'

The Manning's 'n' was varied over a reasonable range for the main channel and the floodplain. The model was run for the 100-year flood of 47,330 cfs and the results are contained in Table 5-4. These results indicate that changes in Manning's 'n' do not significantly affect results from the calibrated model. It is also evident that the main channel Manning's 'n' generally affects the results much more than the floodplain's Manning's 'n', as would be expected since higher velocities and most of the flow occur in the main channel.

5.8.2 Turbulent Exchange Coefficient

There are four turbulent exchange coefficients (E) and all four were set to 100 lb-sec/ft² in the baseline run. The TABS-2 (RMA-2V) manual provides guidelines in choosing values for these coefficients. These guidelines are: (1) in general, there is a tendency for these coefficients to be assigned at values that are too high rather than too low; and (2) most rivers without flow reversal will have coefficients in the range of 10 to 100 lb-sec/ft². Table 5-5 shows the effects of varying these turbulent exchange coefficient values in the calibrated model.

It can be concluded that the high values of E do not affect the river elevation dramatically, especially evidenced by the small increase in the river elevation for doubling the coefficients. Also, the model predicts higher elevations for higher turbulent exchange coefficients. This means that if higher turbulent exchange coefficients were used in the calibration, then a lower Manning's 'n' would have to be used to obtain equally good agreement with the observed rating curve. Given these results, it was judged that a turbulent exchange coefficient of 100 was indeed reasonable and that further calibration was not required.

5.9 Conversion of Flow Velocity to Shear Stress

The conversion of the vertically-averaged river velocities obtained from the RMA-2V model to shear stresses is required to compute the resuspension of bed sediments in the TIP. Several candidate conversion formulations were investigated. The four methods, with a short description of each, are presented below.

1) Smooth wall log velocity profile

This conversion method (Thomas and McNally, 1990, Schlichting, 1979) derives from the assumption that the vertical velocity profile at any point in the river follows the smooth wall log velocity profile. The following equation describes this velocity profile.

$$\frac{u}{u^*} = 2.5 \ln(3.32 u^* d / \nu) \quad (5-1)$$

where,

- u = vertically averaged velocity
- u^* = shear velocity
- d = depth of flow
- ν = kinematic viscosity.

The applicability of this relation to the Hudson River is suspect since it is known that the bottom of the river is not hydraulically smooth and, therefore, it is doubtful whether this expression is applicable to describe the velocity distribution in the channel.

- 2) Method used by Gailani (Gailani et al., 1991), on the Fox River

$$\tau_b = 0.03 \cdot u^2 \quad (5-2)$$

where,

τ_b = bottom shear stress.

This relation is based on empirical evidence obtained in laboratory flumes (personal communication with Gailani, 1994). This relation is somewhat theoretically based since the shear velocity can be approximated by a fixed fraction of the vertically averaged velocity.

- 3) Rough wall log velocity profile

$$\frac{u}{u^*} = 6.25 + 2.5 \ln(d/k) \quad (5-3)$$

where,

u = vertically averaged velocity

u^* = shear velocity

d = depth of flow

k = equivalent Nikuradse roughness.

This relation (Thomas and McNally, 1990) describes the velocity profile for a rough wall river flow, which is typically the condition for all river flows. The only parameter for this equation is k , the roughness factor. This parameter can be estimated from the Manning's roughness (Chow, 1960), and for ' n ' = 0.02, k was determined to be 0.04 feet.

- 4) Manning shear stress equation

$$u^* = \frac{3.81 \cdot u \cdot n}{d^{1/6}} \quad (5-4)$$

This shear stress conversion (Thomas and McNally, 1990) is based on equating the one-dimensional Manning equation with the definition of the cross-sectional average shear stress, which is

$$u^* = (gdS)^{1/2} \quad (5-5)$$

where,

g = acceleration due to gravity
 d = the average depth of flow
 S = the slope of the river.

Note both equations are only valid for the whole cross-section of the river, the depth and velocity in these equations are the cross-sectional averages. Therefore, these equations are not strictly applicable for a vertically averaged point in the cross-section.

5.9.1 Results

Figure 5-5 gives the variation of shear stress with the average vertical velocity for the four different methods. The depth used to calculate the conversion for methods 1, 2 and 4 was 10 feet. As seen in Figure 5-5, Method 1, the smooth wall velocity profile, yields the smallest shear stress, while Method 4, the Manning shear stress equation, yields the highest, while Methods 2 and 3 yield similar shear stresses. Based on theoretical considerations and site specific characteristics, Method 3, the rough wall velocity profile, was selected as the most representative conversion method to use.

5.10 Discussion

The calibrated RMA-2V model is a reasonable representation of TIP hydraulics for various flow regimes. This conclusion is based on the good agreement found between model output for water levels and rating curve results at Lock 7, and the good agreement between model output for velocities and those measured by the USGS. The model is able to simulate flows well above the calibration flow, 30,000 cfs, based on the reasonable agreement between the 100-year flow predictions by this model and the FEMA model, and the lack of sensitivity of high flow results to changes in internal model parameters.

The sensitivity analyses show that the RMA-2V model is not appreciably sensitive to changes in the calibration parameters. However, the analysis on the conversion of the flow field output (vertically averaged velocity and depth) to the river bed shear stress shows that the shear stress can vary significantly depending on the conversion method used. The method chosen in this analysis was judged to be the most firmly-grounded in a theoretical sense, and it gives similar results to a conversion method based on detailed laboratory data.

6. APPLICATION OF THOMPSON ISLAND POOL DEPTH OF SCOUR MODEL

6.1 Introduction

This section describes application of the Depth of Scour Model for the Thompson Island Pool (TIP). The model is based on a statistical fit of observed TIP erosion data to a modified form of the Lick equation discussed in Section 3.7. The model is applied to address the following questions at flood flow conditions:

1. What is the range of expected scour depths at each of five Phase 2 high resolution coring sites in TIP?;
2. How do these depth of scour ranges compare to observed depth profiles of PCB concentrations at these sites?; and
3. What is the expected range of total PCB and solids mass eroded from cohesive sediments throughout TIP?

Section 6.2 describes the data available to support the depth of scour model. Section 6.3 describes how data from resuspension studies of Hudson River sediments were used to define parameter values and characterize uncertainty in the scour predictions. Section 6.4 provides predicted ranges for depth of scour at each of the five Phase 2 high resolution coring sites, and compares these ranges to observed PCB concentration profiles. Section 6.5 provides global computations for total mass of PCBs and solids remobilized from cohesive sediments throughout TIP. This analysis focuses strictly on cohesive sediment areas because: (1) cohesive sediment areas are considered to encompass most of the known PCB "hotspots"; and (2) available Hudson River resuspension experiments (conducted specifically to allow parameterization of Lick's erosion equation for cohesive sediments) allow greater confidence to be placed in resuspension estimates from cohesive areas than from non-cohesive areas.

6.2 Available Data

The construction and application of the TIP Depth of Scour Model requires a wide variety of system-specific data. Table 6-1 contains a detailed description of the data and information requirements for the hydrodynamic and Depth of Scour models for TIP. For each sub-model, Table 6-1 outlines the data requirements, its purpose, origin, form, and availability. For purposes of discussion in this section, the data will be divided into categories of: (1) bottom sediment distribution; and (2) resuspension experiments. It should be noted that Release 2.3 of the TAMS/Gradient database does not include the low resolution core data from TIP or the high-frequency water column TSS data from Spring of 1994.

6.2.1 Bottom Sediment Distribution

The bedded sediments in TIP were delineated as cohesive and non-cohesive based on the side-scan sonar profiles of fine and coarse sediments (TAMS/CADMUS/Gradient, 1996 - pending publication). The area of non-cohesive sediments in TIP is approximately five times that of cohesive sediments. The PCB distributions were obtained from kriging analysis of the 1984 NYSDEC sediment survey data (TAMS/CADMUS/Gradient, 1996 - pending publication). Results of these analyses are available as a surficial coverage and a vertically-integrated coverage. Inventories of PCBs in the cohesive and non-cohesive areas were computed from the vertically integrated coverages. The surficial coverage indicates the average concentration in the top 30 centimeters of the sediments. Values for this surficial coverage were used to specify sediment total PCBs in the TIP depth of scour model.

Based on the vertically-integrated coverage, the inventory of PCBs in the cohesive areas was 3208 kg, as compared to 7974 kg in the non-cohesive areas. These areas represent a total inventory of 11.2 metric tons (MT) of total PCBs in TIP. The total inventory of PCBs in the entire TIP area is approximately 14.5 MT. The difference is due to the fact that the kriging analysis interpolates over the entire TIP area, i.e. areas in addition to that designated as cohesive and non-cohesive. Those areas, primarily rocky and/or unmapped by the side scan sonar, are not planned to be simulated. In addition there are minor differences in the procedures employed in truncating the GIS coverages to the TIP shore line. A discussion of the total PCB inventory of the Thompson Island Pool can be found in the Data Evaluation and Interpretation Report (TAMS/CADMUS/Gradient, 1996 - pending publication).

6.2.2 Resuspension Experiments

The data used to parameterize the Depth of Scour Model for TIP sediments were obtained from resuspension experiments described in HydroQual (1995). This report contained two different sets of experimental data. The first dataset came from an annular flume study, where sediments from three different locations in TIP were transported to a laboratory at the University of California at Santa Barbara and subjected to two types of experiments involving shear stress. Multiple shear stress tests were conducted by filling the flume with sediment, allowing it to compact for 1, 3, or 14 days with the flume at rest, and running (i.e., rotating) the flume at successively higher levels of shear stress, with steady state suspended sediment concentrations achieved (as indicated by concentration measurements at 30 minute intervals) before each shear stress increase. A continuous flow test was conducted by filling the flume with sediment and running it continuously for 47 days at a shear stress of about one dyne/cm², except that on several days the shear stress was increased to 5 dynes/cm² for two hours, and one multiple shear stress test similar to those described above was conducted.

The purpose of these experiments was to investigate the effects of bed compaction and to estimate the value of the critical shear stress. Based upon these laboratory flume experiments, HydroQual (1995) concluded that: the critical shear stress was approximately 1 dyne/cm², the maximum time since deposition (t_d) was 7 days, and the exponent, n , for t_d was 0.5. These parameter values were directly used in the analysis described below.

The second set of sediment resuspension measurements described in HydroQual (1995) consisted of field studies using a portable resuspension device, commonly called a shaker. Surficial sediment cores were collected and brought to shore at 20 locations in TIP and 8 locations downstream; each location had one (TIP) or two (downstream) sets of three cores each. Each core was subjected to a shear stress in the shaker and the resulting resuspension potential was determined. The field study produced 107 resuspension potential-shear stress data pairs for the Hudson River, with 60 measurements specific to TIP. The shear stresses used in the field study ranged from 5 to 11 dynes/cm². Observed sediment erosion rates in TIP ranged from 0.06 to 28.84 mg/cm².

From the TIP-specific data, HydroQual (1995) assumed a TIP-wide constant value of 3 for m , and back-calculated core-specific values for a_0 necessary to produce the observed erosion. The methodology used to determine the value for m was not provided. They reported a mean value and standard deviation for a_0 of 0.071 (in units of mg- day^{1/2}/cm²) and 0.062 respectively, not including some excluded values.

6.3 Model Parameterization and Uncertainty

This section describes how data from resuspension studies of Hudson River sediments were used to define parameter values for the scour equations presented in Section 3.7, and characterize total uncertainty in the scour predictions. It begins with a description of rearrangement of the erosion equation to allow parameter estimation, discusses the parameter values obtained, and concludes with a discussion of prediction uncertainty.

6.3.1 Rearrangement of Erosion Equation

As discussed in Section 3.7.2, a formulation known as Lick's equation (Gailani, et al., 1991) has been used to predict erosion as a function of shear stress for fine-grained cohesive sediments:

$$\varepsilon = \frac{a_0}{t_d^n} \left(\frac{\tau - \tau_c}{\tau_c} \right)^m \quad (6-1)$$

where ε is the total amount of material resuspended (g/cm²); t_d is time after deposition; and a_0 , n , and m are empirical constants.

If the value of τ_c is known or assumed, while the other parameters are unknown, then Lick's equation can be reduced from five parameters to two using a dimensionless shear stress parameter τ' :

$$\varepsilon = A (\tau')^m \quad (6-2)$$

where

$$\tau' = (\tau - \tau_c) / \tau_c,$$

$$A = a_0 / t_d^n$$

Equation 6-2 can be linearized as follows:

$$\ln(\varepsilon) = \ln(A) + (m) \ln(\tau') \quad (6-3)$$

Therefore, a linear regression may be performed to fit a straight line to data for erosion vs. dimensionless shear stress in log-log space. The slope obtained from this regression will correspond to the exponent m from Lick's equation, while the intercept will correspond to the log of the lumped term a_0/t_d^n . Characterization of the distribution of errors around this regression will also provide an estimate of the uncertainty in erosion predictions.

6.3.2 Parameter Estimation

All statistical analyses were conducted using SYSTAT Version 6.0 for Windows, and only data from TIP were considered. A linear regression of natural log erosion (in mg/cm^2) vs. natural log τ' produced a constant (i.e. intercept) value of -3.829 and a slope value of 2.906. Of 60 TIP data points, two outliers were deleted; 58 data points were used. The outliers were identified solely on the basis that their studentized residuals were too large (absolute value greater than 3.0). The outliers were: (1) erosion = 0.06 at shear stress = 5; and (2) erosion = 0.47 at shear stress = 11. The regression R-squared value was 0.541. p-values for both the regression constant and the slope were <0.00001 . An analysis of the residuals strongly indicated that they could be assumed to be normally distributed. It was concluded on the basis of these and other statistical indications that the use of linear regression was supported by the data.

The value of 2.906 obtained for m is similar to the value of 3 reported by HydroQual (1995). Assuming from the flume studies that the maximum time since deposition (t_d) was 7 days, and the exponent, n , for t_d was 0.5, the lumped term corresponds to a value of a_0 of 0.0575. This value is within the uncertainty of the value shown above as reported by HydroQual.

6.3.3 Prediction Limits

Given a regression line with normally distributed residuals, prediction limits for new observations (for a given value of the independent variable) fall on a Student's t-distribution (Neter et al., 1985). For large sample sizes, the Student's t-distribution is approximately normal. Predicted values for new observations were therefore calculated as percentiles of normal distributions, in log-log space. The resulting predicted distribution in ordinary space (again, for given values of shear stress) is log-normal, and is easily calculated. The final step was to divide the erosion (in mg/cm^2) by the bulk density (in mg/cm^3) to get the depth of scour in cm. A value of $1462 \text{ mg}/\text{cm}^3$ was used for the bulk density, based upon observed site data (TAMS/CADMUS/Gradient, 1996 - pending publication).

Predictions based on transformations can be subject to transformation bias when a single number is used to characterize the distribution of values; for example, the mean of logarithmically transformed data is usually not equal to the log of the mean of the data. This model avoids bias by reporting percentiles of the distribution of predicted observations. There is a one-to-one correspondence between the percentiles of a log-normal distribution in normal space and the percentiles of its log-space normal distribution.

There are several assumptions inherent to this analysis. Some of these include:

- The value for critical shear stress and, to a lesser extent, the values for time since deposition and the exponent on time since deposition) observed from the annular flume studies apply throughout TIP
- The statistical model is valid for extrapolation to higher values of shear stress than were used experimentally
- The bulk density, at a specific location, used for converting erosion to depth of scour can be represented as a single number.

In reality, these assumptions are likely to be violated to some extent. They are unavoidable, however, if predictions based upon the data are to be made, regardless of method.

6.4 Depth of Scour Predictions at Selected Locations in Cohesive Sediment Areas

As part of the Phase 2 high resolution sediment coring study, the TAMS/Gradient team collected five sediment cores in TIP. The availability of detailed measurements of sediment physical-chemical properties at these five locations created the opportunity for a finely resolved analysis of resuspension potential in TIP.

Prediction of the expected range of scour depth at each core required a mixture of pool-wide and location-specific data. On a pool-wide basis, the depth of scour model described in Section 6.3 was assumed to apply equally to all five sediment cores. Location-specific inputs consisted of predicted shear stress at each coring location, and sediment bulk density measured for each core. Table 6-2 lists all location-specific input values for each of the five cores.

Table 6-3 contains summary results for each of the five sediment core locations. Results indicate that Core HR-25 is the most likely of the five locations to erode significantly. Cores HR-26 and HR-20 are also susceptible to some erosion, while cores HR-23 and HR-19 are much less susceptible. The predicted median depths of scour for the five locations range from less than 0.03 (HR-23) to approximately 2 cm (HR-25). The third and fourth columns in Table 6-3 show the range of predicted scour depths encompassing the middle 90 percent of expected values (i.e. 5th to 95th percentile) for each core location.

Predicted median depth of scour provides information on quantities of solids that can potentially resuspend during an event; however, it provides incomplete information on quantities of PCBs that can potentially resuspend. The last column in Table 6-3 contains the observed depth of the total PCB peak at each of the five core locations. By comparing predicted median depths of scour and observed depths of PCB peaks, a more complete picture emerges of potential PCB erodability. For example, results indicate that Core HR-25 is likely to experience scour of sufficient magnitude to substantially erode the total PCB peak at that location. Total PCB peaks at the other four locations are predicted to be unscoured; i.e. the total PCB peaks are likely to stay intact after a 100-year flood event.

Figures 6-1 through 6-5 show the observed total PCB profiles with depth for each of the five sediment cores. Three different scour horizons are also depicted on the figures, corresponding to the 5th percentile, median, and 95th percentile. Core HR-25 is the only core location at which the total PCB peak is predicted to be significantly eroded by the 100-year event. Based on the nature of the core profile at this location, this area appears to be a high energy area subject to strong sediment-water interactions. This interpretation is consistent with the incomplete and fractured nature of the core profile. The sediments in this area represent transient rather than old bedded sediments and may contain PCBs from more recent upstream sources. In summary, the above analysis suggests that cohesive sediment areas in TIP are most likely to be depositional areas that remain relatively less disturbed during major flood events.

The above probabilistic analyses are specific to the location of the five Phase 2 high resolution sediment cores, and the 100-year flood event. Results from these analyses do not constitute estimates of uncertainties for other cohesive sediment areas in TIP, or for flood events with different return periods. Figure 6-6 shows the generic envelope of scour predictions based on the Lick resuspension sub-model for

a wide range of applied shear stresses. Figure 6-6 indicates that the 90% prediction interval (i.e. 5th to 95th percentile) provides an envelope spanning somewhat less than two orders of magnitude. Figure 6-6 can be used as a nomograph in interpreting large scale scour projections based on the GIS visualization studies.

Finally, results in Figure 6-7 represent the application of the generic scour predictions in Figure 6-6 to the specific locations of the five Phase 2 high resolution sediment cores for the 100-year flood event. Results in Figures 6-1 to 6-5 correspond to the predicted depth of scour at the 5th, 50th and 95th percentiles for each of the five core locations. Results in Figure 6-7 illustrate the predicted chances of scour over the entire probability range for each of the five cores for the 100-year flood event. Consistent with the above results, Core HR-25 is predicted to be the most susceptible to event-driven erosion, and Core HR-23 is predicted to be the least susceptible.

6.5 Global Results for Cohesive Sediment Areas

Plate 6-1 shows the site map of Thompson Island Pool and is the base map of reference for the GIS-based erodability maps which follow. Plate 6-2 shows the delineation of TIP sediments into cohesive and non-cohesive areas. The potential for erosion of cohesive sediment-associated PCBs in TIP was investigated for a set of five design flows ranging from 8,000 cfs to a maximum of 47,330 cfs, the 100-year flood event. These event flows are based upon the Log Pearson flood frequency analysis for the Fort Edward Gauge conducted by Butcher (1993).

Table 6-4 contains design flows and the mean values of corresponding velocities and shear stresses (cohesive sediments only) predicted by the TIP hydrodynamic model.

Plate 6-3 shows the distribution of steady-state velocities in TIP as predicted by the TIP hydrodynamic model for the 100-year flood event (Section 5.7). Plate 6-3 and subsequent plates depict only the normal river channels, i.e. flood plain conditions are not represented. The nodal values representing the output from the hydrodynamic model were interpolated using a triangulated irregular network (TIN) to yield smoothed estimates of the velocities and shear stresses for display. All computations and intermediate grid calculations were, however, performed at the nodal locations of the hydrodynamic model. This is necessary as the nonlinear nature of the computations result in different mass estimates if the averaging is conducted prior to or subsequent to the computations.

Most of the flow around Rogers Island occurs in the western channel and consequently high velocities are depicted. For the 100-year event, velocities in the eastern channel are less than 2 fps indicating (qualitatively) that the potential for scour is considerably smaller on that side of the island. Velocities are found to be higher in the region spanning Rogers Island to the confluence with Snook Kill as

compared to areas further downstream. Velocities immediately downstream of the Snook Kill confluence show a region with elevated velocities between 3 and 4 fps. Part of the sediments (Plate 6-2) in this region are cohesive and are thus potential regions of high scour. Further downstream the channel east of Billings Island and to the south also shows high velocities ranging up to a maximum of 5 fps. Plate 6-4 shows the corresponding shear stresses (dynes/cm²) for the 100-year event.

For the 100-year event, Plate 6-5 shows the mass of solids eroded from the cohesive sediments in TIP. The numbers represent a total scour for each grid cell (kg/event), normalized to kg/m². Significant scour can be discerned along the shores of the river about a half mile downstream of the southern tip of Rogers Island. Another large scour pocket can be discerned just north of Billings Island on the eastern side of the river channel. Moderately high scour is also visible on the eastern shore of Billings Island near the south end.

Plate 6-6 shows the depth of scour (cm) corresponding to the mass of cohesive solids eroded shown in Plate 6-5. The largest scour depths are approximately 2.5 cm. The influence of tributary flows on sediment water interactions in the main channel in the vicinity of the confluence cannot be estimated since tributary flows were not included in the hydrodynamic model calibration.

For the same 100-year event, Plate 6-7 shows the mass of PCBs eroded from the cohesive sediments in TIP. The numbers represent a total scour for each grid cell (kg/event), normalized to gm/m². Table 6-5 contains results for total masses of solids and PCBs eroded from cohesive sediment areas in TIP. The total reservoir of PCBs in the cohesive areas of TIP was estimated as 3208 kg, based on a kriging analysis of the 1984 NYSDEC sediment survey (TAMS/CADMUS/Gradient, 1996 - pending publication). Table 6-5 indicates that only approximately one percent of this reservoir is predicted to erode for the 100-year event. The predicted median depth of scour for this event is only 0.16 cm. Results in Table 6-5 indicate that the cohesive sediment areas of TIP will experience little, if any, scour even for large events. Since the cohesive sediment areas encompass most known "hot spots" (as defined by 1978 NYSDEC survey), the TIP resuspension model predicts that these localized areas of high contamination will not be affected significantly by large flood events.

It is significant to note that the predicted mass of total PCBs eroded from the cohesive sediment areas of TIP during a 100-year event (25 kg) is less than the total external PCB loading across the upstream boundary of the HUDTOX model at Fort Edward during the entire period of simulation from January 1 to September 30, 1993 (354 kg).

Plates 6-8 to 6-27 show predicted results for the four design flow events other than the 100-year event. For these events, the TIP resuspension model predicts that between 0.001 and 0.3 percent of the total PCB reservoir in the cohesive sediment areas of TIP will be remobilized (Table 6-5).

The mass of PCBs eroded from non-cohesive sediment areas of TIP was not estimated in this preliminary calibration effort for two principal reasons: first, lack of a current spatial inventory of PCBs in the non-cohesive areas; and second, the Lick erosion equation is only applicable to cohesive sediments. At the present time, the most spatially-resolved data for sediment PCBs in TIP are from the 1984 NYSDEC sediment survey. These data were used to specify sediment PCB distributions in both the cohesive and non-cohesive sediment areas. Consequently, all predictions of PCB resuspension in TIP in this report are premised on the assumption that these 1984 sediment PCB distributions are representative of present-day conditions. This assumption is probably more valid for cohesive sediment areas than for non-cohesive sediment areas because, as the above results indicate, lower shear stresses tend to occur in cohesive areas and higher shear stresses tend to occur in non-cohesive areas. Thus it is likely that PCBs associated with non-cohesive sediments in TIP have been more disturbed by high-flow events during the past 10 years than PCBs associated with cohesive sediments.

As part of the future modeling work (Appendix B), the TIP Depth of Scour Model will be expanded to include non-cohesive sediment areas. This task will begin with a detailed characterization of TIP sediments in terms of particle type, particle size distribution, clay content, porosity and total PCB concentration. Results from this characterization will be used to develop a finer-scale horizontal segmentation grid for both cohesive and non-cohesive sediment areas. Each of the sediment segments in this grid will be characterized by a unique set of values for a suite of physical-chemical parameters, including the proportional distribution of total solids mass into multiple particle size classes.

Using the best available information from the scientific literature, critical shear stresses will be estimated as a function of the physical characteristics and particle size classes in each segment. Given a set of segment-specific physical-chemical properties and applied shear stresses, total masses of eroded solids and PCBs, and depths of scour, will be estimated for cohesive and non-cohesive sediment types in each segment. These results will be summed to form cumulative gross erosion estimates for TIP, or they will be used to characterize different sediment areas within TIP with respect to erodability.

7. APPLICATION OF LOWER HUDSON RIVER PCB TRANSPORT AND FATE MODEL

7.1 Introduction

Lower Hudson River modeling was conducted using the existing model application of Thomann et al., (1989, 1991). This section contains a summary description of the model application; a more detailed description is provided in Thomann et al., (1989). The section is divided into sub-sections discussing:

- Model Input Data
- Internal Model Parameters
- Applications Approach
- Diagnostic Analyses
- Sensitivity Analyses
- Discussion.

7.2 Model Input Data

The Lower Hudson River modeling application required model input data describing many characteristics of the site. These consisted of:

- System-specific Physical Data
- External Loadings
- Forcing Functions
- Boundary Conditions
- Initial Conditions.

7.2.1 System-Specific Physical Data

The primary inputs concerning system-specific physical data were model segmentation and geometry. Model segmentation for the physico-chemical and food chain models were discussed previously in Section 3.8.3, with segment maps provided in Figures 3-11 and 3-12. Model segment geometry for physico-chemical model segments one through ten, as well as geometry for the New York Bight and Long Island Sound, was determined from National Ocean Survey charts (Thomann et al., 1989). Geometry for the remaining segments was calculated by aggregating segment geometry for the NYC 208 Model (Hydroscience, Inc. 1978b).

7.2.2 External Loadings

The application of the Lower Hudson model required loading estimates for several parameters, including: cesium, solids, and PCB homologues. Cesium was used during model calibration as a tracer variable to help calibrate solids settling and resuspension velocities. Three sources of cesium loads were considered in the original Lower Hudson application: (1) atmospheric deposition; (2) Indian Point; and (3) river inputs from the Upper Hudson. Atmospheric loads were estimated from ^{90}Sr areal loading rates from Bopp and Simpson (1984), and a $^{137}\text{Cs}:^{90}\text{Sr}$ ratio of 1.59. Indian Point loads were derived from the estimates of Wrenn et al., (1972) and Jinks and Wrenn (date not given). River inputs from the Upper Hudson were estimated from sediment core cesium data from the Albany Turning Basin (to provide an annual estimate of each year's particulate cesium concentration) and a correlation between annual stream flow and solids loading.

Solids loads were estimated from numerous sources. Riverine inputs from Connecticut were taken from Farrow et al., (1986). New York/New Jersey riverine and runoff inputs were based upon a flow-solids correlation for the Hudson River at Waterford. This resulted in an assumed concentration of 150 mg/l. The remaining solids loading estimates were based upon published reports as follows:

- New York/New Jersey Treated Wastewater (Mueller et al., 1982)
- Connecticut Treated Wastewater (Farrow et al., 1986)
- Barged Solids (Mueller et al., 1976)
- Dredge Spoils (Olsen et al., 1984).

PCB loadings were required by the model for each homologue. These were determined by first calculating total PCB loads for each source on an annual basis, then estimating the fraction of the total load comprised by each homologue. Total PCB loads from the Upper Hudson were calculated in three different ways, depending upon the time period of concern: (1) 1946-1959; (2) 1959-1975; and (3) 1976-1987. Loadings for the period 1946 through 1959 were calculated by linearly interpolating between an assumed zero load for 1945 and the loading calculated for 1959. PCB load estimation for 1959 through 1975 followed the same procedure used for cesium. Sediment core data were analyzed to estimate particulate phase PCB concentrations for each year, and total PCB loading was estimated from observed solids loading. PCB loads for the period 1976-1987 were based upon USGS data obtained through NYSDEC.

7.2.3 Forcing Functions

Forcing functions included in the Lower Hudson model application consisted of:

- Advective flows
- Horizontal dispersion coefficients
- Vertical diffusion coefficient
- Fish migration patterns.

Two types of advective flow patterns were used in the Lower Hudson model application: (1) a constant hydrology model using a single long term average circulation pattern; and (2) a variable hydrology model that considers yearly variation in advective transport.

The constant hydrology model used average annual river flows for all tributaries entering the Lower Hudson. A constant 3,348 cfs enters the Hudson River and exits into the Bight, with primary sources being the Upper Hudson, Mohawk, Raritan, and Passaic Rivers. A total of 19,459 cfs enters (and exits) Long Island Sound, of which the primary sources are the Connecticut and Housatonic Rivers. Additional, but smaller, sources of water to the system include urban and rural runoff, sewage treatment plant discharges, and discharges of raw sewage. Reported current measurements are used to define a circulation pattern for the Bight.

Horizontal dispersion coefficients for the Lower Hudson water column were taken from previous model efforts (Hydroscience, Inc. 1975; Hydroscience, Inc., 1978a; Hydroscience, Inc., 1978b). Vertical diffusion of interstitial dissolved PCB concentrations were set to represent assumed molecular diffusivity levels.

The time variable hydrology model categorized the variability of flow conditions as low, average, or high, at any point in time. The transport parameters for the average flow condition were identical to those described above for the constant hydrology model. The low flow condition corresponded to the lowest quartile annual average flow (73 percent of the long term average), while the high flow condition corresponded to the highest quartile. Horizontal dispersion coefficients were adjusted by +/-30 percent in the high and low flow years, respectively.

Since the detailed model segmentation used in the physicochemical model was found to result in excessive computational times, the study area was divided into five regions for the food chain modeling. These were based upon the assumed migration patterns of the striped bass. Region 1 corresponded to the Upper Hudson Estuary from River Miles 153.5 to 78.5, (physicochemical model Segments #1-8).

Region 2 covered River Miles 78.5 to 18.5 (physicochemical Segments #9-14) and was termed the Mid-Lower Estuary. Region 3 corresponded to New York Harbor (Segments 15, 16, 24, 25, 26). Region 4 corresponded to the remaining study area of New York Bight and Long Island Sound. Migration patterns were based upon the work of Waldman (1988a, 1988b). A fifth region was defined to cover the open ocean. PCB concentration was assumed to be zero in this region. The youngest striped bass year classes (0-5) spend the majority of their lives in the Mid-Lower Estuary. Older striped bass (≥ 6 yrs.) reside primarily in the open ocean, with spring time migrations into the Mid-Lower Estuary

7.2.4 Boundary Conditions

The Lower Hudson physicochemical model requires specification of several constituents at the downstream boundary of the model domain. These include salinity, cesium, solids, and PCB homologues. Salinity concentrations were determined from annual mean surface and vertical contours from Bowman (1977). A boundary concentration of zero was used for cesium. Solids boundary conditions were set at 0.5 mg/l in New York Bight (based upon Young and Hillard, 1984; Biscayne and Olsen, 1976) and 1.0 mg/l in Long Island Sound (from Riley and Schurr, 1959). A boundary concentration of zero was used for all PCB homologues.

7.2.5 Initial Conditions

The two primary parameters for which time variable simulations were conducted, cesium and PCBs, assumed initial conditions of zero throughout the study area.

7.3 Internal Model Parameters

The Lower Hudson model required specification of numerous model parameters. These included:

- Solids settling velocity
- Solids sedimentation velocity
- Solids resuspension velocity
- Cesium partition coefficient
- Cesium decay rate
- PCB partition coefficient
- PCB volatilization rate

- PCB decay rate
- Growth and respiration rates
- Bioconcentration feature
- Uptake and excretion rates.

The solids settling velocity was assumed as 10 ft/day throughout the study area. Solids sedimentation velocities were estimated by an areal weighting of the sedimentation regions given in Bopp (1979), and ranged from 0.025-0.5 cm/yr. Net suspension rates were calculated for each segment using the above velocities and the assumption of conservation of mass for the upper sediment layer.

A salinity dependent cesium partition coefficient was used to account for the saturation of sorption sites by potassium in sea water. The cesium partition coefficient was also made solids-dependent, and ranged from 10^3 to 10^5 in the water column and 10^0 to 10^3 in the surface sediments. A cesium decay rate of 0.2295/year was taken from the model of Bopp and Simpson (1984).

PCB partition coefficients in the water column were estimated for each homologue as a function of octanol-water partition coefficients, fraction organic carbon of suspended solids, and solids concentrations using the Particle Interaction Model of DiToro (1985), following Thomann and Salas (1986). PCB partitioning in the sediments include a third phase representing dissolved organic carbon (DOC), such that the partition coefficient can be calculated as f_{oc}/DOC .

Volatilization of PCBs was assumed to be controlled by transfer across the liquid film; such that a constant volatilization rate could be used across all homologues. This volatilization rate of 0.6 m/day was based upon an assumed oxygen transfer rate of 1.0 m/day and consideration of the ratio of the molecular weight of PCBs to that of oxygen.

The PCB decay rate was conservatively set to zero for both the water column and sediments, in light of conflicting data on expected decay. Sensitivity analyses were conducted to determine model response to different assumptions regarding PCB decay rates in sediments. The results of these analyses are discussed in Section 7.6.2.

The food chain model requires specification of growth and respiration rates for each compartment, including: zooplankton, small fish, white perch, and striped bass. Zooplankton growth and respiration rates were based upon published data for *Gammarus*, and correspond to a growth rate of 0.1/day and respiration rate of 0.06/day. The small fish compartment (representing fish of approximately 10g weight, e.g., smelt and pumpkinseed) were based upon generalized weight-

dependent relationships. A value of 0.00631/day was used as the growth rate and 0.0227 for the respiration rate. Age and weight-dependent growth rates were calculated for white perch based upon the work of Mansueti (1957) and Bath and O'Connor (1982). A weight-dependent respiration rate was calculated following the work of Thomann and Connolly (1984) and Connolly and Tonelli (1985).

Age-dependent growth rates for striped bass were calculated from the observed change in average weight class, using the data of Setzler et al., (1980) and Young (1988). Respiration rates were calculated from the equations of Thomann and Connolly (1983) and Connolly and Tonelli (1985).

Bioconcentration factors (BCFs) were required for all of the food chain model compartments discussed above, as well as for phytoplankton. A constant (across homologues) BCF of 30 l/g(w) was used for phytoplankton, based upon the work of Oliver and Niimi (1988). For the remaining compartments, BCFs were calculated based upon the assumption that the lipid-normalized BCF was equal to the octanol-water partition coefficient for each homologue.

Chemical uptake from the water column is calculated as a function of the respiration rate, oxygen concentration, and efficiency of transfer across the gill surface. Homologue-specific transfer efficiencies were based upon the work of Thomann (1989). Excretion rates were calculated as the quotient of the uptake rate from the water column and the BCF.

Chemical assimilation efficiency from food was determined on a homologue-specific basis, following the work of Thomann (1989). These assimilation efficiencies were held constant across all trophic levels.

7.4 Application Approach

The Lower Hudson modeling effort followed a multiphase application approach:

- Salinity Calibration
- Suspended Solids Calibration
- Cesium Model Calibration
- Physicochemical Model Calibration
- Food Chain Model Calibration.

The salinity model application was used to validate model transport processes, including the horizontal dispersion coefficient. The suspended solids model calibration was used to validate solids settling, resuspension, and deposition

velocities. Cesium was used as an additional calibration variable to test the model's ability to simulate the behavior of a particle-based contaminant with a well defined loading history to the Lower Hudson. The physicochemical model calibration was used to test the model's ability to simulate total PCB concentrations in water and sediment. The food chain model calibration was used to test the model's predictive capability of total PCB concentrations in white perch and striped bass.

7.5 Application Results

This section provides a summary description of the results of the applications described above. A more complete description of results is given in Thomann et al., (1989). The transport model was run to steady state using long-term average hydraulic conditions and compared to data from two sources: Hydrosience (1978b) and Olsen (1979). As seen in Figure 7-1, the model compares well to the Olsen (1979) data, but predicts a downstream displacement compared to the Hydrosience (1978b) data. Similar comparisons were also made to the Hydrosience (1978b) data collected in Long Island Sound and the Newark Bay-Arthur Kill-Raritan Bay-Apex transect. The model calibration was judged satisfactory given the paucity of long term data. The suspended solids calibration (Figure 7-2) generally overpredicted the observed data; this was attributed to the fact that sampling data was biased towards exclusion of high flow (and consequently high solids) periods.

The cesium calibration was conducted for the period 1954 to 1983. Model results were compared to annual average data for dissolved cesium in Segment 12 (on a temporal basis) and to the spatial distribution of particulate cesium for the mid- to late-1980s. The model approximately reproduces temporal and spatial trends in the observed data.

The PCB calibration consisted of summing the results of computed concentrations for each homologue and comparing this total to observed total PCB data. Figure 7-3 shows the spatial distribution of model results for 1978 compared to observed data for the period 1977-1979. The model typically falls within the range of the observed data and generally reproduces the observed spatial trends, although the variability in observed data is large. The PCB calibration for sediments consisted of comparison to both surficial and sediment core data. The comparison for spatial sediments is shown in Figure 7-4, and is similar to the water column comparison in that model results fall within a wide range of observed data. Figure 7-4 shows sediment core data for Segments 1-5, compared to two sets of model results which assumed high and low flow hydrology. Model predicted profiles generally fall below the observed core data, although core data were taken from discrete locations that may not represent segment-average conditions.

The food chain model results were compared to white perch and striped bass data collected over time in model Region 2. As seen in Figure 7-5, white perch results for Region 2 were consistent with the limited observed data. A more robust temporal dataset was available for striped bass (Figure 7-6). The model comparison to this data shows the annual average and range of model results, with the model accurately describing temporal trends in data.

7.6 Diagnostic Analyses

Limno-Tech conducted component and sensitivity analyses for the Lower Hudson River model. There are two main purposes for running component and sensitivity analyses on the model. First, the analyses provide increased understanding of model behavior by characterizing the importance of individual model mechanisms. Second, with this understanding, it will be possible to estimate changes in Lower Hudson River water, sediment, and fish PCB concentrations in response to changes in model inputs, without performing additional model simulations.

7.6.1 Component Analysis

An analysis was conducted in which mass balance components for the exposure model and the bioaccumulation model were evaluated in terms of rates of change of total homologues PCB concentration. The exposure model components that were investigated are loading, net advection, net water column dispersion, net settling, and volatilization. Degradation was assumed not to occur, and water-sediment dispersion was assumed to be negligible. Segments 2, 15, 17, and 28 were examined as representative water column segments. Bioaccumulation model components are uptake (water column only), consumption (food only), loss (actual release of PCBs), and total loss (loss including growth dilution). Food chain model Regions 2, 3, 4, and 5 are examined.

The component analysis for the exposure model shows the net settling and volatilization are consistently important components, while loading, net advection, and net dispersion vary widely in importance in different segments. The component analysis for the bioaccumulation model shows that consumption is the dominant component in model Region 2 (upstream) while loss is dominant in Regions 3, 4, and 5 (downstream).

Table 7-1 summarizes the results of the component analysis of the exposure model as the relative magnitudes of the processes of loading, net advection, net dispersion, net settling, and volatilization.

Table 7-2 summarizes the results of the component analysis of the bioaccumulation model as the magnitudes of the processes of uptake, consumption, loss, and total loss. Four example striped bass year classes (0, 2, 6, and 17) are used for each food chain model Region from 1 to 5.

Consumption is the dominant component in Region 2 while loss is dominant in Regions 3, 4, and 5. Uptake is small in all regions. Total loss, which includes growth dilution, is appreciably larger than loss for earlier year classes but not for the later ones.

7.6.2 Sensitivity Analysis

Exposure model sensitivities were computed separately for both dissolved and total PCBs for net settling, biodegradation, external loading, upstream load, and volatilization. All parameters were set to ± 50 percent of baseline values, except for biodegradation. Because biodegradation is zero at baseline, a "high" value and a one-tenth high value were compared to baseline. Segments 2, 15, 17, and 28 were examined as representative water column segments.

Table 7-3 summarizes the results of the exposure model sensitivity analysis. This table shows that the sensitivities of both dissolved and total PCBs are identical. The sensitivity analysis for the exposure model shows that PCB concentrations are not sensitive to settling. Additionally, Segments 2 and 15 were found to be only slightly sensitive to loading, while Segments 17 and 28 were found to be slightly sensitive to the upstream load. PCB concentrations were very sensitive to biodegradation, loadings, upstream load, and volatilization, excepting the segments identified above.,

Bioaccumulation model sensitivities were computed for bioconcentration factors, respiration rates, growth rates, PCB assimilation efficiencies, and dissolved concentrations. Each of these parameters were set to ± 50 percent of baseline value, except for growth rates and assimilation efficiencies. Growth rates were set to ± 10 percent of the baseline value since ± 50 percent would be physically unrealistic, and assimilation efficiency was set to ± 0.2 from the base fraction. Food chain model Regions 2, 3, 4, and 5 were examined and the results are summarized in Table 7-4.

The sensitivity analysis for the bioaccumulation model shows that bioaccumulated PCB concentrations in Regions 2 through 5 are very sensitive to bioconcentration factors and PCB assimilation efficiency, are quite sensitive to respiration and dissolved concentrations. However, PCB concentrations are shown to be only slightly to moderately sensitive to growth rates.

Based on the results of these sensitivity analyses, it appears that in general, the model results will be reliable if accurate data are used for the following inputs: biodegradation, loadings, upstream load, volatilization, bioconcentration factors, PCB assimilation efficiency, respiration and dissolved concentrations. Additionally, since the model is not sensitive to settling and growth rates, it will likely produce reliable results even if these data are uncertain.

7.7 Discussion

The Lower Hudson modeling application was unique in that an existing model application was used in place of new model development for purposes of this study. Subsequent to the original model application, some of the PCB loading estimates to the Lower Hudson were called into question. For example, (TAMS/Gradient, 1991) states that the original modeling likely overestimated the PCB loadings from the Upper to the Lower Hudson. This was due to a claimed high flow bias in using PCB concentration and river discharge measurements taken at the USGS monitoring station in Waterford, New York. The TAMS/Gradient report implies that an estimate of about 13,000 kg transported past Waterford from the Upper to the Lower Hudson for the period 1977-83 is superior to an estimate of about 19,000 kg derived from the Thomann et al., (1989) report. Using the Waterford corrected mean loads for 1977 through 1983 in Table B.4-4 of the TAMS/Gradient report gives a total of 12,400 kg, which is 35 percent below the 19,000 kg estimate. The report also implies that load estimates for years before the 1977-1983 period were overestimated in the Thomann et al., (1989) report, but it does not provide an alternative figure.

Limno-Tech investigated the effect that an upstream loading discrepancy of the magnitude suggested by the TAMS/Gradient report would have on predicted concentration profiles and the validity of the original model calibration. The Lower Hudson model was run with a 35 percent reduction in upstream loading across the board from 1946 to 1983. Figure 7-7 shows the original (Thomann et al., 1989) model results along with model results using the revised loading from the Upper Hudson. Although the revised loading estimates result in a significant change in computed results, both sets of computed results fall within the range of the observed data. Thus, this loading discrepancy does not necessarily invalidate the model calibration.

Other sources of data collected subsequent to the development of the existing Lower Hudson model conflict with some of the assumptions contained in the model. Additionally, regular collections of striped bass by NYSDEC between River Miles 88 and 153 demonstrate that both adults and juveniles migrate into Region 1. Incorporation of these new data into the Lower Hudson modeling framework may improve its predictive ability.

EPA understands that as of September 1996, the Thomann model is being updated under a grant from the Hudson River Foundation, and that certain modifications have been made to the previously-published model. EPA is evaluating whether the updated model will be available or appropriate for use in this Hudson River RI/FS.

8. MODELING APPROACH: FISH BODY BURDENS

8.1 Modeling Goals and Objectives

The goal of this component of the modeling effort is to develop a framework for relating body burdens of PCBs (expressed as Aroclor equivalents, individual congeners or total PCBs) in fish to exposure concentrations in Hudson River water and sediments. This framework is used to understand historical and current relationships as well as to predict fish body burdens for future conditions. Estimates of PCB body burdens in fish are intended to be used for human health and ecological risk assessments and aid in decision making regarding options for addressing PCB-contaminated sediments in the upper Hudson.

The objectives of the body burden modeling effort are based on discussions with the investigators responsible for human health and ecological risk assessments and with the fate and transport modeling team. Because PCB analytical protocols have varied over time, the framework needs to account for historical as well as current data to the extent possible. Accordingly, the framework is structured to meet the following objectives:

1. relate historical body burden data (as PCB Aroclors and Aroclor totals) to exposure concentrations in water and sediments;
2. relate current and future body burdens (as PCB Aroclors, totals, and individual congeners) to exposure concentrations in water and sediments;
3. provide estimates in a form that can be used for human health risk assessments;
4. provide estimates in a form that can be used for ecological risk assessments; and,
5. provide a set of modeling tools that can be coupled with the output from the PCB fate and transport models to evaluate future management goals.

To meet these objectives, two modeling approaches have been developed to relate body burdens to water and sediment concentrations. One - used with the historical PCB Aroclor database - is referred to as the Bivariate Statistical Model. The other - derived using historical and current data - is referred to as the Probabilistic Bioaccumulation Food Chain Model. In each case, the model relates PCB exposure concentrations in water and sediments to body burdens. The major difference between the two approaches is that the Bivariate Statistical Model uses available time series data to develop statistical relationships between concentrations in water and sediments and those in fish while the Probabilistic Bioaccumulation Food Chain Model relies upon feeding relationships to link body burdens to water and/or sediments.

The two approaches complement one another. Each utilizes derived Bioaccumulation Factors (BAFs). The agreement between these and the resultant estimates of body burdens provide a check on the two approaches. It is anticipated that there will be some modeling applications for which the Bivariate Statistical Model is the better tool and other applications where the Bioaccumulation Model will provide the desired information. The Bivariate Model provides mean body burden estimates while the Probabilistic Model explicitly incorporates feeding preference data and uncertainty and variability information around the mean estimate. By incorporating observed variability in the underlying data, the Probabilistic Model provides a context for the results of the Bivariate Model. While the Bivariate Model provides mean estimates, the Probabilistic Model provides population statistics, such as what percent of a fish species population is expected to experience concentrations at or below a specified level.

In addition, a third approach is being explored which is not described in this report but will be part of the next task. This approach involves a modification of the Gobas (1993) food web model. This model relies on the theory of fugacity, or chemical potential, and is focused specifically on food digestion and absorption in the gastrointestinal tract. The model incorporates both sediment and water sources, but, similar to the probabilistic model presented here, relies on prey consumption and food web dynamics to describe the uptake of PCBs. The Gobas model also incorporates uncertainty and variability information.

Selection of fish species for modeling body burdens was based on several criteria including: 1) importance for fishing, 2) abundance, 3) importance in diet of other fish, 4) representative of particular habitats or trophic levels, and 5) representative of other fish species. Upon discussion with NYSDEC, USEPA, and NOAA the following species were selected for bioaccumulation modeling:

Fish Species	Characteristics
Spottail Shiner	Forage Fish, Feeds on invertebrates in water column and sediments
Pumpkinseed	Forage Fish, Feeds on invertebrates in water column (on aquatic plants) and to a limited degree sediments; popular recreational fish but seldom eaten
Brown Bullhead	Lives in contact with sediment and feeds on a variety of animal life on or in the sediments; can be fished recreationally and is eaten occasionally
Yellow Perch	Inhabits water column and feeds on invertebrates and small fish; popular recreational fish and is commonly eaten
Largemouth Bass	Larger individuals feed primarily on fish but will also eat other vertebrates and invertebrates; popular recreational fish and is commonly eaten
White Perch	Feeds on invertebrates and small fish; lives in the tidal portion of the Hudson; undergoes migrations within the river

Ecological profiles for the selected fish species are provided in Appendix A and are used to discern behavioral and trophic characteristics that could affect accumulation of PCBs.

The Bivariate Statistical Model uses pumpkinseed, brown bullhead, largemouth bass and white perch. Sufficient historical data were not available for the other species on this list; however, cyprinids were added to the statistical analysis.

In addition to the fish species listed above, the striped bass is included in the evaluation. However, no new models have been developed for this species. A major confounding factor is that the striped bass are a migratory species that are resident in the river for only a portion of the year. As such, it is inappropriate to assume that all PCB exposure occurs within the Hudson River, and under the current modeling framework, this is a key assumption. The modeling program relies upon the work of Thomann to derive estimates for striped bass. It would be desirable to have a model for the short nose sturgeon, an endangered fish species in the tidal portion of the Hudson. However, data are insufficient to develop a model for this species. It is anticipated that a species-to-species extrapolation will be employed to evaluate the short nose sturgeon, based on physiological, feeding and habitat selection characteristics.

8.2 Background

8.2.1 PCB Compounds

This report examines bioaccumulation of Aroclors for the historical datasets and selected congeners for the Phase 2 dataset. A challenge to developing a modeling framework for PCB bioaccumulation is that PCBs consist of 209 individual congeners, each of which exhibit varying degrees of bioaccumulation potential, depending on the degree and substitution of chlorination. The more highly-chlorinated congeners tend to accumulate in fish tissues. This effect may be a function not of increased uptake, but rather decreased elimination efficiency from the fish.

Until recently most environmental studies of PCB contamination measured only complex mixtures or total PCBs. Much of the historical PCB data are reported as Aroclors, mixtures comprised of various congeners, some of which are accumulated more effectively than others. While Aroclors accurately describe commercial PCB mixtures, they may be poor descriptors for PCB mixtures in fish and environmental media. This can pose limitations on model development, as discussed in subsequent sections.

Studies that have measured PCBs as individual congeners have provided insights into the bioaccumulation processes for water column- and sediment-based communities. Several researchers have noted that whether or not total PCB levels increase with position in the food chain, chlorine content of PCB body burdens tends to increase (Smith et al., 1985; Oliver and Niimi, 1988; Van der Oost et al., 1988; MacDonald et al., 1993). Congener patterns of caged fathead minnows and feral brown bullhead from the area around Thompson Island Pool in the Hudson River were generally similar, sharing 60 percent of their 20 most abundant peaks, but the bullhead had higher concentrations of hexa- and heptachlorobiphenyls (Jones et al., 1989). The fish contained 17 peaks that were not detectable in water samples. It has been noted that when young bluefish enter the Hudson River from offshore, heavier, more chlorinated congeners were accumulated to a greater level than lighter, less chlorinated congeners (LeBlanc and Brownawell, 1994).

A variety of factors control accumulation of PCB congeners (Shaw and Connell, 1984; Jones et al., 1989; Kadlec and Bush, 1994; Ankley et al., 1992; LeBlanc and Brownawell, 1994):

1. Individual PCB congener characteristics, including solubility and partition coefficients, degree of chlorination, and stereochemistry. Shaw and Connell (1984) found that more planar molecules are more strongly absorbed than those with more regular shapes.
2. Characteristics of the fish, including lipid content of gills, blood, and tissue, cardiac output, ventilation volume, gill surface area, epithelium layer of gill, aqueous stagnant layer of gill, ability to biotransform PCBs, excretion rates.
3. Environmental factors, including temperature, pH, light, current, suspended particles, dissolved organic compounds.

8.2.2 PCB Accumulation Routes

Fish and other aquatic animals are exposed to PCBs through direct contact with water (bioconcentration), and sediment, as well as through dietary sources (bioaccumulation). Due to their hydrophobicity, PCBs tend to accumulate in the lipid portion of organisms. PCBs have also been found to accumulate in predatory fish tissues at higher concentrations than the concentrations in the surrounding water would predict (Thomann and Connolly, 1984), a process known as biomagnification. Depending upon the position of an aquatic organism within the aquatic food web, exposure may be intensified through food sources as organisms consume other organisms that have bioaccumulated PCBs in the lipid portion of their tissues. Because of the important role of food as an exposure pathway, the feeding ecology of a fish species is a key aspect in distinguishing between the relative contribution of the water column and sediments to body burdens of PCBs.

Direct Uptake from Water

For fish, direct uptake of PCBs from water occurs primarily across the gills. No significant evidence exists for absorption through the epidermis (Shaw and Connell, 1984).

The significance of direct uptake from water of PCBs has been debated. Based upon laboratory studies, Shaw and Connell (1984) argued that uptake via the gills was the major route of accumulation of PCBs. Some field studies have indicated that water column uptake could account for PCB concentrations observed in biota, if PCB concentrations were normalized for lipid content of the organism (*e.g.*, Clayton et al., 1977).

Other researchers have continued to examine the potential for bioconcentration through the gills to account for PCB concentrations. Caged rainbow trout that were fed clean, commercial food appeared to accumulate PCBs directly from contaminated waters of the St. Lawrence River (Kadlec, 1994; Kadlec and Bush, 1994). Barron (1990) noted that simple evaluations of uptake directly from the water column have assumed that bioconcentration is controlled by the hydrophobicity of the compound, as measured by its octanol-water partition coefficient. He argued that bioconcentration appears to be independent of octanol-water partition coefficients when the coefficient is small or when the molecule to be accumulated is large. He summarized other factors that affect bioconcentration: molecular shape, degree to which the compound is bound to dissolved organic matter, lipid content of the gills, size of the organism, blood flow, variations in enzyme content and activity, and exposure temperature and ionic content.

Uptake via Food

Field studies and modeling efforts have indicated that biomagnification through the food chain is an important component for bioaccumulation. Sloan et al., (1984), for example, suggested that the presence of higher chlorinated Aroclor mixtures in fish of the Lower Hudson River might reflect a food chain component to bioaccumulation. Using existing field data, Thomann (1981, 1989) derived steady-state food chain models, considering uptake of contaminants from both water and food sources through several trophic levels. The models indicated that food assimilation, excretion, and net weight gain were important characteristics that determined bioaccumulation levels. They also demonstrated that for top predators, such as Hudson River striped bass, almost all the observed PCB body burden could be attributed to a food source. In Lake Michigan lake trout, only 2 to 3 percent of the PCB accumulation could be predicted from water column concentrations using an age-dependent model (Thomann and Connolly, 1984), while transfer through the food chain accounted for up to 99 percent of the body burden of PCBs in Lake Michigan lake trout.

Many researchers have tested, refined, or elaborated upon Thomann's food chain models. One test of the approach examined PCB accumulation in young-of-the-year bluefish which enter the Hudson River Estuary from relatively uncontaminated offshore waters and grow quickly (LeBlanc and Brownawell, 1994). Connolly et al., (1985) considered growth rates, respiration rates, food assimilation efficiency, predator-prey relationships, PCB assimilation efficiency, and bioconcentration factors for PCBs when they applied a model to existing data from the Hudson River system. They predicted PCB levels in Hudson River striped bass, assuming various reductions in concentrations of PCBs in the water column. They also began efforts to incorporate lipid- and non-lipid components of the striped bass into the model. Pizza and O'Connor (1983) conducted laboratory experiments to determine rates of PCB accumulation from the gut and elimination from the body in young-of-the-year striped bass from the Hudson River. An EPA model, Food and Gill Exchange of Toxic Substances, or FGETS, has been used to predict average concentrations of contaminants in the food web over time (*e.g.*, Woolfolk et al., 1994). This model incorporates bioconcentration of contaminants from the water column and biomagnification in the food chain.

Gobas et al., (1993) examined the roles of food digestion, food absorption, and rates of gill elimination and metabolic transformation upon bioaccumulation. This model has recently been updated to include exposure from both water and sediment sources, and a Monte Carlo-based uncertainty analysis. A further aspect to the work presented here will be to develop the Gobas model for use on the Hudson River. This will provide a check on the models presented here and may provide further insight into the role of water versus sediment in forage fish and piscivorous fish exposures.

Uptake from Sediments

Equilibrium partitioning has been suggested to be the major factor controlling bioaccumulation in sediment-based benthic communities. Bierman (1990) used field data from the Great Lakes to determine that for animals at the lower and middle parts of the food chain, including oligochaetes, chironomids, amphipods, sculpin, small smelt, and large smelt, predicted bioconcentration factors based upon equilibrium partitioning coefficients accounted for concentrations of hydrophobic organic compounds. Comparing laboratory and field data, Ankley et al., (1992) confirmed that for oligochaetes, concentrations of PCBs in the sediments could be used to predict concentrations of PCBs in organisms, but that for other species, food or possibly ingestion of contaminated particles could affect concentrations. Ingestion of contaminated food also seemed to be a factor in accumulation of PCBs in a freshwater lake (Van der Oost et al., 1988).

A steady-state food chain model with a benthic invertebrate component was developed to account for both water column and sediment sources of contaminants (Thomann et al., 1992). This model considered four exposure routes for ingestion

of particulate contaminants: sediment organic carbon, overlying plankton, interstitial water, and overlying water. Applying the model to an amphipod-sculpin food web in Lake Ontario (Oliver and Niimi, 1988), Thomann and his co-workers (1992) found that accumulation was based primarily upon a benthic food web rather than upon direct uptake from the water column. They noted however, that including the overlying water and phytoplankton as a food source were necessary to explain the field data. Considering only interstitial water and sediment particles as contaminant sources was not satisfactory.

8.3 Theory for Models of PCB Bioaccumulation

The Bivariate Statistical and Probabilistic Food Chain Models share a common theoretical basis including:

1. PCB body burdens in fish are related ultimately to exposure concentrations in water and/or sediments;
2. PCBs in the water column and sediments are not necessarily in equilibrium with each other;
3. Within the water and sediment compartments, an equilibrium or *quasi* - steady-state condition exists at temporal scales on the order of a year and spatial scales on the order of a river segment;
4. Fish body burdens are in *quasi*-steady-state with the water and/or sediment at time scales on the order of one or more years.

PCB concentrations measured in biota are assumed to be in steady state with PCBs in the environment for the development of bioaccumulation factors (BAFs), and thus can be related by linear coefficients or bioaccumulation factors similar to partitioning coefficients. A steady-state condition is usually considered to hold within a given year; thus the BAF approach represents temporal changes only annually. The simplest approach considers that biota and *all* environmental compartments are in equilibrium with one another, in which case the concentration in any medium can be predicted from the concentration in any other medium. The BAF method is readily modified to address situations in which a disequilibrium exists at steady state between different environmental compartments.

Consider first a completely equilibrated system: Fish may accumulate PCBs through partitioning from the water column, through ingestion of sediment, or through the food chain, while organisms at lower trophic levels may also accumulate PCBs from both water column and sediments. Describing exact accumulation pathways is the task of food web models, but concentrations in any medium or "compartment" in a fully equilibrated system can be predicted from those in any other compartment. As PCBs partition strongly to organic matter and have low solubility, the major environmental reservoir is typically the sediment.

"Partitioning" from sediment to biota is conceptually similar to equilibrium partitioning from sediment and pore water as well as from sediment to the water column. Thus, for an equilibrated system, dissolved concentrations in sediment pore water might provide a good index of the bioavailable component. Typically, analytically resolving truly dissolved and DOC-complexed fractions is a very difficult task for pore water samples, but, for lipophilic compounds in sediments with typical organic carbon contents, partition coefficients are such that the mass present in dissolved and DOC-complexed forms is relatively insignificant compared to the total particulate-sorbed mass. This implies that the dissolved portion can be quite well predicted from the sediment-water partition coefficient, regardless of DOC levels. On the other hand, pore water concentrations vary significantly in response to sediment organic carbon fraction (*foc*). Therefore, sediment concentration *normalized to foc* is the best readily available predictor of dissolved concentrations in an equilibrated system (Di Toro et al., 1991). This approach is being used by EPA's Office of Water for establishing sediment quality criteria (USEPA, 1991).

Of course, PCBs may enter the food chain both through the dissolved phase and ingestion of particulate matter. As Di Toro et al., state, "biological effects (to invertebrates) appear to correlate to the interstitial water concentration. This has been interpreted to mean that exposure is primarily via pore water. However, the data correlate equally well with the organic carbon-normalized sediment concentration. This suggests that the sediment organic carbon is the route of exposure. In fact, neither of these conclusions necessarily follow from these data."

The reason for this surprising conclusion is contained in fugacity, or chemical potential theory, which holds that the biological activity of a contaminant is controlled by its chemical potential (Mackay, 1979). As discussed by Di Toro et al., if pore water and organic carbon phases of the contaminant are in equilibrium then the chemical potentials exhibited by the two phases are equal. "Hence, so long as the sediment is in equilibrium with the pore water, the route of exposure is immaterial. Equilibrium experiments cannot distinguish between different routes of exposure." Thus, in the simplified equilibrium case, it is necessary to estimate the chemical potential in only one phase. The question then becomes determining which phase is easiest to measure. Where DOC complexing occurs, sediment concentration normalized to *foc* is clearly the most directly measurable index of chemical potential.

Fish may accumulate PCBs via pathways which arise in the water column as well as from the sediment. The simple equilibrium BAF approach works if sediment and water-column concentrations are in equilibrium with one another, or if all PCB accumulation in fish derives from pathways commencing in the local sediment. On the other hand, if fish accumulate PCBs from both water-column and sediment pathways, *and* water-column concentrations are not in equilibrium with pore water in the same locale, the full-equilibrium assumptions are not valid. In the Hudson and other flowing rivers, it is likely that the upper sediment layer and the water

column are generally *not* in equilibrium with one another for hydrophobic toxicants. Further, the upper, bioactive sediment zone is typically not in equilibrium with deeper, buried sediments. However, the sediment-sorbed concentrations and pore-water concentrations within the bioactive zone should be very close to equilibrium, while, in the water column, the dissolved and sorbed fractions should also be close to equilibrium, except during transient events.

The equilibrium partitioning/fugacity arguments set forth by Di Toro et al., (1991) state that the best readily measurable index of chemical potential should be the sediment sorbed fraction normalized to *foc*. This argument applies to both sediments and water column. Both should be compared to the lipid-normalized burden in the organism (Chiou, 1985), as BAF estimates are best expressed on a lipid-normalized basis (USEPA, 1994). BAF factors are expected to vary from species to species with trophic level and foraging preferences. Variability may also reflect differing lipid compositions, with correspondingly different rates of uptake of lipophilic compounds, between fish species (Ewald and Larsson, 1994).

Preliminary analysis suggested that both water and sediment pathways may be important for the accumulation of PCBs in Hudson River fish, and that water column and sediment concentrations are not in equilibrium with one another. TAMS/Gradient (1991) Phase 1 RI/FS analyses revealed that summer average water-column concentrations appear to provide a good predictor of average PCB burden in fish species, confirming earlier observations of Brown et al., (1985). This could reflect a dominant role for water-column pathways, or simply an equilibrium between water-column and pore-water PCB concentrations. A role for sediment pathways is suggested by the observation that concentrations in fish in the Thompson Island Pool appear to be elevated above those collected downstream at River Mile 175 by a factor greater than the observed change in water-column concentration. Water-column PCB concentrations in the Upper Hudson below Thompson Island Dam do not appear to be in equilibrium with the upper level of the sediment; for instance, TAMS/Gradient 1993 flow-averaged sampling indicated that total PCB concentrations decline by about 40 percent between Thompson Island Dam and River Mile 156.6 (Waterford), largely representing dilution. The decline in surface sediment concentrations appears to be much more substantial: The GE Sediment Sampling and Analysis Program (O'Brien & Gere, 1993a) revealed a decline in average total PCB concentrations in the top 5 cm of sediment of 90 percent between Thompson Island Pool (River Mile 188.3 to 193) and the reach from River Mile 155 and River Mile 170. In summary, below Thompson Island Dam the water column is not in equilibrium with *local* sediments. Thus, models for bioaccumulation need to consider both water and sediment pathways, rather than relying on a BAF based on concentrations in a single medium.

8.4 Bivariate Statistical Model for Fish Body Burdens

8.4.1 Rationale and Limitations for Bivariate Statistical Model

The Bivariate Statistical Model relies on the available time series of environmental and fish data in the Upper Hudson to relate observed PCB concentrations in fish to PCB levels in the water and sediment. If water and sediment concentrations are not in equilibrium, a single BAF is not adequate; instead bioaccumulation is controlled by the simultaneous effects of both water and sediment concentrations. Thus, a statistical model with two independent variables (water and sediment concentrations) is appropriate.

The development of statistical relationships is enhanced by the availability of extensive historical monitoring data that enable comparison of PCB levels in fish and the environment over time. The nature of these data, which consist primarily of Aroclor-equivalent quantitations in the fish and total PCB estimates by packed-column gas chromatography in the water column, however, constrains the statistical approach. Although more recent studies by TAMS/Gradient, NOAA, and GE provide congener-specific PCB measurements in all media, these data are limited in that they (1) are available only for the 1990s, (2) represent only a small number of individual samples for a given fish species, and (3) do not provide a time-series perspective on the relationship between fish body burdens and environmental concentrations.

Statistical relationships do not, of course, prove physical causality. Statistical models that capture historic conditions are not guaranteed to predict accurately future conditions, particularly if the characteristics of the PCB source change over time. The Bivariate Statistical Model, however, is an important first step for the development of more complex, food web models, for which the database is limited. By reflecting historical trends, the Bivariate Statistical Model provides important constraints on the form and parameterization of the food web bioaccumulation model. The mean estimates provided by the Bivariate Model are complemented by the explicit incorporation of the uncertainty around the means, as provided by the Probabilistic Model.

8.4.2 Theory for Bivariate Statistical Models of PCB Bioaccumulation

The general theoretical framework for deriving Bivariate Statistical Models was introduced in Section 8.3. The fact that the water and sediment compartments are not in equilibrium with each other, but are approximately internally equilibrated, suggests that bivariate BAFs that relate body burden to *both* sediment and water-column chemical potential could account for bioaccumulation pathways from both water and sediment. These bivariate BAFs could then be used to predict fish body burdens for various combinations of water and sediment exposure levels subject to the limitations described above. Correlating fish body

burdens to both water and sediment removes the difficulty of disequilibrium between the sediment and water compartments.

The Bivariate Statistical Model is essentially a 'black box' approach wherein the details of exposure pathways and physiological processes are not specified but the net effect is captured. The actual PCB concentration found in a given fish depends on the cumulative effects of dietary/food chain accumulation, plus direct accumulation from the water (and perhaps sediment), all balanced by species-specific rates of depuration or metabolism. Net accumulation in a fish species thus depend on all lower trophic levels. There are, however, only two main external forcing functions, water and sediment PCB concentrations, which enable a 'black box' model to be developed through statistical analyses with water and sediment concentrations as input and fish burden as output. Detail on specific food chain relationships is provided in Section 8 and Appendix A.

For steady-state concentrations in the environment, the net result of the unspecified processes contained within the 'black box' is functionally equivalent to a steady-state food web model. For instance, the simplified steady-state food web model of Thomann et al., (1992) for Lake Ontario, which avoids the need for a detailed study of population dynamics through steady-state assumptions, is externally forced by water and sediment concentrations alone. It is thus equivalent to a bivariate BAF relating fish body burden to water and sediment concentrations, where the food web interactions determine the values of the two BAF factors. Therefore, a bivariate regression relating average PCB body burden in a given species (by location and year) to concentrations in local water and sediment provides a useful tool for assessing bioaccumulation of PCBs by fish, for aiding in the development of the Food Chain Model described in Section 8.5, and for evaluating the output of that model.

As discussed in Section 8.3, fugacity theory indicates that chemical potential is best estimated by the sorbed fraction in both sediments and water column, normalized to *foc*. This suggests a regression analysis to predict fish PCB burdens from environmental concentrations through species-specific relationships should take the following form:

$$\frac{Cf_i}{fl_i} = \left[Bw_i \cdot \frac{Cs_w}{foc_w} \right] + \left[Bs_i \cdot \frac{Cs_s}{foc_s} \right] \quad (8-1)$$

in which, for species *i*:

- Cf = PCB concentration in fish (wet-weight basis)
- fl = Lipid fraction in fish
- Bw = Partial BAF relating fish concentration to water-column concentration

Cs_w	=	PCB concentrations on suspended solids
foc_w	=	Organic carbon fraction of suspended solids
B_s	=	Partial BAF relating fish concentration to upper-zone sediment concentration
Cs_s	=	PCB concentration in upper zone sediments (dry-weight basis)
foc_s	=	Organic carbon fraction of the sediments.

While this formulation is theoretically optimal, foc_w is not available in the historic database for the Hudson River; as a result, B_w must be expressed on a whole-water basis as a matter of practical necessity.

8.5 Probabilistic Bioaccumulation Food Chain Model

8.5.1 Rationale and Limitations

The Probabilistic Food Chain Models are developed to predict distributions of PCB body burdens within the selected fish species. These models compliment the Bivariate Statistical Models that predict single population statistics such as the average values of PCBs. The Probabilistic Models have been developed to provide:

1. information on the fractions of the fish populations that are at or above particular PCB levels; and
2. an empirical framework for constructing biologically-based food chain relationships that explicitly incorporate variability and uncertainty inherent in the underlying data.

PCB body burdens in Hudson River fish vary among individuals within a species for any given reach of the river. This intra-species variability in concentrations can be described as a distribution. The characteristics or shapes of these distributions can be important for evaluating human health and ecological risks. For example, two distributions may have the same average value but may differ in spread, one having values distributed closely around the average, the other including much higher as well as much lower values. The distribution with a greater fraction of high values may pose a greater risk than the tighter distribution. Probabilistic models that predict the characteristics of distributions provide risk assessors with the information needed for making these evaluations. Probabilistic models also provide a tool for quantifying the uncertainties associated with estimating body burdens of PCBs.

The distribution of concentrations of PCBs within a species reflects a number of factors that are also variable. These include the composition of PCBs, spatial and temporal exposure field of PCBs in water and sediments, the uptake and depuration

rates of PCBs within and among trophic levels, and the feeding behavior and history of the fish. Many of these factors are unknown or poorly known for the selected Hudson River species. The approach taken in building the Probabilistic Food Chain Models is to combine information from available measurements for the river with knowledge concerning the ecology of fish species and the trophic relationships among fish and invertebrates.

The models presume *quasi* steady-state conditions for which average annual exposure concentrations in water and surface sediments change slowly relative to the species uptake and depuration kinetics. The models are constructed by identifying the major pathways linking individual fish species with sediment and water components. These pathways include direct exposure as well as trophic relationships. Within the models, each major pathway is represented as a transfer or bioaccumulation factor. Using information on species' ecology, statistical distributions for PCB transfer or bioaccumulation factors are developed among media and biological components. These factors are derived from measurements of PCB concentrations in various compartments and do not require assumptions about kinetic processes, although it is assumed that fish will be in a quasi steady-state with the environment. The transfer and bioaccumulation factors reflect the sum of the underlying processes and are specific to Hudson River fish and environmental conditions. The derived factors are compared to those in the literature for reasonableness.

The models are designed to identify the relative contributions of PCBs in Hudson River sediments and water to body burdens of the six selected fish species. Because exposure to PCBs may occur via water column and sediments, it is important to distinguish between these two media. Food is expected to be the primary route of exposure for fish but direct uptake from water may also be important depending on the specific chemical. In developing the models, the role of direct water uptake versus food was examined.

Because of the important role of food as an exposure pathway, what and where a fish eats are viewed as key aspects of distinguishing between the relative contribution of the water column and sediments to a species' body burden of PCBs. Some species feed predominantly on benthic invertebrates, others on water column invertebrates, and still others on forage fish. Some species, such as the largemouth bass, feed on all three components to varying degrees.

8.5.2 Model Structure

The conceptual framework for the probabilistic PCB food chain models is illustrated in Figure 8-1. Variables are identified in Table 8-1. A separate model is developed for each fish species reflecting that species biology and available information on PCB BAFs. These models can be developed for individual congeners, homologue groups, Aroclors, or total PCBs. In this report, results for the calibration congeners, Aroclors 1016 and 1254 and total PCBs are presented. The calibration congeners were selected to represent a range of physical and chemical parameters that drive fate and transport and uptake in the Hudson River. However, the parameters of interest to risk assessors and site regulators are generally Aroclors and total PCBs. The models are designed to evaluate *quasi* steady-state conditions on an annual basis. The features of the models are:

1. Two groups of invertebrates are described: a) invertebrates that live within sediments and feed primarily on sedimentary material (primarily deposit feeders) and, b) invertebrates that feed primarily on organic particulate matter transported in the water column (zooplankton, many epiphytic invertebrates, and some filter feeding invertebrates).
2. Invertebrates in group "a" are presumed to reflect localized sediment concentrations and to be in steady state with the sediments as described by lipid and organic carbon normalized BAFs.
3. Invertebrates in group "b" are presumed to reflect PCB concentrations associated with particulate material in the water column on an organic carbon normalized basis. These invertebrates are presumed to be exposed to PCBs associated with organic particulate material in the form of detritus or algae. In the Hudson, it is presumed that both forms of organic material will be important in the diets of invertebrates. The invertebrates that feed in this manner are presumed to be in steady state with temporally averaged water column concentrations of PCBs on an organic solids basis as described by organic carbon normalized BAFs.
4. In most cases, the models are designed to estimate body burdens in adult fish. These larger fish are the ones important for human health risk assessment. In addition, because the primary population-level risk of PCBs to fish is reproductive impairment, body burdens in adults can be used in the ecological evaluation. Because young fish of some species (e.g., Pumpkinseed sunfish) are important as forage fish, body burdens are estimated for these juveniles. Fish fall into one of several types depending on their foraging strategies. The species-specific models incorporate such information and recognize the variability that exists among and within species.

5. The lipid normalized BAF factors between invertebrates and fish, and fish and fish are represented by distributions derived from Phase 1 and 2 studies carried out in the Hudson and from the literature. Values are derived for the calibration congeners, Aroclors, and total PCBs.
6. The food chain models are designed to take as input the water and sediment concentrations predicted by the fate and transport models described in earlier sections. The key input parameter for sediments is the PCB concentration normalized to sediment organic carbon. The key input parameter for the water column is the PCB concentration in the particulate organic carbon phase. These exposure concentrations can be provided as summer or annual averages. Since feeding occurs primarily in the warmer months, the probabilistic model has been developed using summer averages. It is anticipated that the fate and transport models will provide input parameters on a summer-averaged basis.

Based on the above, the following media and biological compartments are identified: 1) water, 2) sediment, 3) water invertebrates, 4) sediment invertebrates, 5) forage fish, and 6) the individual fish species. The relationships between fish species and compartments are shown in Table 8-2.

The food chain models are designed to be implemented in one of three forms, a) a Monte Carlo Spreadsheet Model, b) equations combining individual distributions into cumulative distributions, and c) a nomograph or look-up table.

For the Monte Carlo Spreadsheet Model, the relationships among compartments and the distributions for BAFs are incorporated into an Excel spreadsheet with a Crystal Ball™ software add-in. Excel is a standard spreadsheet and provides the basic computational framework. Crystal Ball software permits the input data to be represented as distributions rather than single point values; the software also enables Monte Carlo analyses to be performed. The species-specific Excel/Crystal Ball spreadsheet incorporates uncertainties in exposure concentrations, food chain transfers, foraging behavior, and lipid content. Monte Carlo operations yield cumulative distributions of body burdens on a lipid normalized and whole fish basis for each species. Key variables in the Probabilistic Model are represented by a distribution of values rather than a single point estimate (such as a mean or upper-bound value). Monte Carlo simulation is a means of sampling from these distributions within a computational framework. Generally, the greater the number of simulations, the lower the standard error associated with the mean. In developing the Probabilistic Model, Monte Carlo simulations were run a minimum of 10,000 trials.

The distributions are representative of variability in the data as described in subsequent sections. The distributions can also represent uncertainty, for example, by providing a range of feeding proportions rather than single values. However, in

the analyses presented here, the derived distributions are representative of data variability.

8.5.3 Spatial Scale for Model Application

The river segments used to assess exposure to fish are the same as those used in the HUDTOX fate and transport model. For most fish species, these model segments are expected to encompass the exposure zones for fish that may be caught in a particular segment of the river. The primary zone of exposure for most fish species is presumed to be the summer foraging areas. Fish are expected to obtain most of their PCB body burden via food. Profiles for the species (Appendix A) indicate most of the feeding occurs during the warmer periods of the year. On a relative basis, little feeding occurs in the winter. Therefore, the summer foraging areas are where most of the fish species' exposure occurs. Because most of the selected fish species exhibit limited spatial movements during the summer, foraging areas and exposure zones can be highly localized. A notable exception is the white perch, a semi-anadromous species that migrates over stretches of the river.

The HUDTOX model provides single mean values for sediment and water for each of the segments. In some segments, there may be little spatial variability around this mean. This is probably the case in the lower Hudson. However, for other segments - including Thompson Island Pool - there are strong spatial gradients in sediment concentrations (and perhaps water) that reflect differences in sediment type as well as locations of "hot spots". Thus actual exposures may vary greatly around the mean. Different fish species will also tend to forage over particular sediment types further complicating the ability to represent the exposure field. These factors probably contribute to the observed variability in fish body burdens in Thompson Island Pool and will be a source of uncertainty in predicting the distribution of fish body burdens when model estimates of water and sediment are available only for mean conditions.

8.5.4 Temporal Scales for Estimating Exposure to Fish

Exposure concentrations for water and sediments are estimated as summer averages (May through September). This averaging period is coincident with the time that fish are at their summer foraging areas.

8.5.5 Characterizing Model Compartments

Sediment to Benthic Invertebrate Compartment

This compartment of the model relates the concentrations of PCB in benthic invertebrates to sediment concentrations of PCB. It assumes that the PCB levels in the invertebrates are related directly to levels in the surrounding sediments. This relationship is represented by an empirically-derived biota sediment accumulation factor (BSAF) that reflects the combination of passive and/or active

bioaccumulation mechanisms occurring in the sediments. PCB uptake into benthic invertebrates appears to be the result of partitioning between the organic carbon of the sediments and the lipid of the invertebrate species (Bierman, 1990). This relationship is a simple ratio:

$$BSAF = \frac{C_{benthic}}{C_{sediment}} \quad (8-2)$$

where,

$BSAF$ = biota - sediment accumulation factor

$C_{benthic}$ = the concentration of PCB in an organism as ug/g lipid

$C_{sediment}$ = the concentration of PCB in sediments as ug/g organic carbon

Particulate Water Column:Water Column Invertebrate Compartment

The particulate water column to water column invertebrate exposure pathway is important because water column invertebrates represent the single largest dietary contribution to the forage fish and several larger fish species, including white and yellow perch. This exposure route also has direct implications for the exposure of higher order piscivores, such as largemouth bass, through the invertebrates to forage fish to piscivore pathway.

The particulate phase in the water column represents the primary dietary contribution to water column invertebrates (zooplankton and invertebrates that live on the surfaces of rocks or aquatic plants). Because these invertebrates comprise a significant portion of the diet of forage fish and some game fish, the food chain model is sensitive to the BAF values used to represent this compartment. Other studies have indicated the importance of this food chain transfer step (Oliver and Niimi, 1988; Skoglund, 1996).

Individual PCB congeners can be strongly associated with either the truly dissolved phase in the water column or the particulate phase. These differences average out to some extent when considering total PCBs. The Data Evaluation and Interpretation Report (TAMS/CADMUS/Gradient, 1996 - pending publication) provides estimated partition coefficients for a number of key congeners. These results are summarized in Table 8-3 for the calibration congeners. Clearly, the fraction of PCB concentrations associated with the particulate phase increases with increasing chlorination. For the lighter chlorinated congeners, bioaccumulation is driven primarily by direct uptake from the dissolved phase in the water. For the higher chlorinated congeners, consumption of particulate matter represents the route of greatest bioaccumulation.

Under the assumption that the majority of water column PCBs are associated with particulate organic carbon, we evaluated the relationship of water column invertebrates to the particulate phase in the water column as:

$$PWBAF = C_{invert}/C_{oc} \quad (8-3)$$

where,

$PWBAF$ = The bioaccumulation factor between water column invertebrates and particulate bound PCB

C_{invert} = mg PCB per Kg lipid in invertebrate tissue

C_{oc} = mg PCB per Kg organic carbon in suspended particulates.

Forage Fish Compartment

Several of the fish species selected for modeling consume other, smaller forage fish of which there are numerous species in the Hudson. Rather than quantify PCB concentrations in individual forage fish species, the model assumes that piscivorous fish will consume any species less than 10 cm. This assumption is supported by forage fish abundance data for the Hudson River from the literature as well as piscivorous fish gut analyses (MPI, 1984). A composite forage fish compartment has been developed that reflects the composition of forage fish in the Hudson and the feeding habits of these fish. The details of how the forage fish compartment was derived are presented in Appendix A. The analysis indicated that Hudson River forage fish are composed of species that feed to varying degrees on invertebrates in the water column and in the sediments. When the relative abundance and feeding behavior of the species are taken into account, the composite forage fish diet is comprised of approximately 67% water column invertebrates and 33% sediment invertebrates. All piscivorous fish that feed on Hudson River forage fish are assumed to be preying on species that - on average - feed on water column and sediment invertebrates in these percentages.

The forage fish bioaccumulation factor (FFBAF) is defined as:

$$FFBAF = \frac{C_{ff}}{C_{diet}} \quad (8-4)$$

where,

$FFBAF$ = forage fish bioaccumulation factor

C_{ff} = concentration in composite forage fish (μg per g lipid)

C_{diet} = weighted average of diet concentration (μg per g lipid)

Piscivorous Fish Compartments

Adult piscivorous fish eat a combination of forage fish and invertebrates. Since forage fish concentrations are derived primarily from water column invertebrate concentrations, it is assumed that direct ingestion of water column invertebrates by piscivorous fish is encompassed in this step. In the model, therefore, piscivorous fish PCB body burdens are quantitatively related (in varying degrees, depending on the fish species) to the benthic invertebrate and forage fish boxes.

The piscivorous fish under consideration include largemouth bass, white perch and yellow perch. These species also feed upon invertebrates, which can represent from 10% of the diet in adult largemouth bass to 85% of the diet in the case of yellow perch. The piscivorous fish bioaccumulation factor (BAF) is defined as:

$$BAF = \frac{C_{fish}}{C_{diet}} \quad (8-5)$$

where,

- BAF = piscivorous fish bioaccumulation factor relative to diet
- C_{fish} = concentration in piscivorous fish (μg per g lipid)
- C_{diet} = weighted average of diet concentration (μg per g lipid).

In the case of yellow perch, the weighted average in the diet is expressed as 15 percent forage fish, 20 percent benthic invertebrates and 65 percent water column invertebrates. The largemouth bass diet is 90 percent forage fish and 10 percent benthic invertebrates.

Demersal Fish

The final category of fish to be considered are the demersal or bottom-feeding fish. The best species to consider for this box is the brown bullhead, which feeds primarily from the bottom. Brown bullhead lipid-normalized concentrations were compared to benthic invertebrate lipid-normalized concentrations as well as sediment TOC-normalized concentrations.

The BSAF for brown bullhead is defined as:

$$BSAF = \frac{C_{BB}}{C_{sed}} \quad (8-6)$$

where,

$BSAF$ = brown bullhead bioaccumulation factor

C_{BB} = concentration in brown bullhead (μg per g lipid)

C_{sed} = concentration in the sediment (μg per g carbon).

The dietary bioaccumulation factor is defined as:

$$BAF = \frac{C_{fish}}{C_{invert}} \quad (8-7)$$

where,

BAF = brown bullhead bioaccumulation factor

C_{fish} = concentration in brown bullhead (μg per g lipid)

C_{invert} = concentration in benthic invertebrate (μg per g lipid).

9. CALIBRATION OF BIVARIATE STATISTICAL MODEL FOR FISH BODY BURDENS

As described in Section 8, two parallel tracks were pursued for modeling bioaccumulation of PCBs in fish in the Hudson River: a statistical model, based entirely on evaluation of observed data from the Hudson; and a food web model, which incorporates toxicokinetic, physiologic, and trophic level constructs. The two efforts are complementary: The statistical model calibration, presented in this section, aids in interpretation of historic data and provides a foundation for calibrating the food web model,

9.1 Data Used for Development of Bivariate BAF Models

Equation 8-1 presents an idealized formulation for developing bivariate BAF models. Actual implementation is constrained by data availability. Among other issues, quantitation methods used for fish are not directly equivalent to those used for water, and water column organic carbon fraction has not regularly been monitored. Establishing the spatial/temporal history of sediment concentrations also presents difficulties.

Statistical development of a bivariate BAF requires a sufficiently large range of data (over differing environmental conditions in space and/or time) to distinguish accumulation originating from water column and sediment pathways. While there is evidence for disequilibrium, sediment and water concentrations are still correlated with one another. As a result, the impacts of each individual source on fish become more difficult to distinguish, and a larger database is required to determine bivariate BAF factors than would be required for a single BAF. Data and methods used for development of the BAF models are described below.

9.1.1 Fish Data

The analysis is based on NYSDEC fish data from the Upper Hudson River below Fort Edward coupled with NYSDEC data from the uppermost part of the Lower Hudson River (above River Mile 142). Samples collected between River Mile 142 and 153 are from the freshwater portion of the Lower Hudson. The species collected in this area are, however, largely the same as those collected in the Upper Hudson, and PCBs in this reach are derived primarily from the Upper Hudson. It is therefore appropriate to include samples between River Mile 142 and 153, thus providing a larger database for analysis. Table 9-1 summarizes the present count of samples available in the database.

The longest-running and most extensive sample data in the Upper Hudson come from NYSDEC collections at River Mile 175 (between Schuylerville and Stillwater) and at River Mile 153 (just below Federal Dam, and thus technically in the Lower Hudson). A good representation over time is also available for River

Miles 189-190 (Thompson Island Pool), and smaller amounts of data are available at River Mile 160 (Waterford, above Federal Dam). The species for which the most data are available are pumpkinseed (*Lepomis gibbosus*), largemouth bass (*Micropterus salmoides*), and Brown bullhead (*Ictalurus nebulosus*). Lesser, but still extensive, data are available for cyprinids or carp (*Cyprino carpinus*) and yellow perch (*Perca flavescens*).

These species represent a range of trophic levels, habitat preference, and foraging behavior: Largemouth bass are piscivorous, with adults occupying the top of the aquatic food chain. Yellow perch represent an intermediate trophic level, foraging on invertebrates and small fish. Unlike largemouth bass, yellow perch are migratory. Pumpkinseed are at a lower trophic level: they feed primarily on invertebrates and are an important food source for larger fish. Cyprinids are also at a lower trophic level, feed primarily on invertebrates in the water column, and also consume detrital algae. Brown bullhead are omnivorous bottom feeders, with diet including offal, waste, small fish, mollusks, invertebrates, and plants. Feeding preferences also vary with the age and size of the individual. The profiles of selected species are addressed in greater detail in Appendix A. Thus, a range of trophic positions and forage preferences are available for analysis in the historic data.

Raw data for the NYSDEC Hudson River fish analyses through 1988 were summarized in the Phase 1 report. Through the 1992 sampling, there are a total of 10,599 fish analyses available in the TAMS/Gradient database, of which 3,432 were collected between River Miles 142 and 194. Table 9-2 summarizes available lipid-normalized PCB data for the most frequently sampled species in the database. Tables 9-3 and 9-4 summarize data by year and location for pumpkinseed, largemouth bass, brown bullhead, cyprinids and yellow perch. For these tables, Aroclor concentrations have been corrected to a basis consistent with the quantitation method in use from 1983 on, as described in Section 9.1.2.

The bivariate statistical model development used all data for these species collected between River Miles 142 and 194. Most of these samples were collected in late spring (April - June), but some samples were collected in different seasons. Sampling time for individual species as well as target size and age groups have also varied somewhat from year to year. These differences likely contribute to variability in observed PCB body burden, but are not addressed in the statistical analyses, except for correction to concentration on a lipid basis. The more complex probabilistic bioaccumulation model (Section 10) provides a more sophisticated treatment of these and other factors which affect observed PCB body burden in Hudson River fish.

9.1.2 Standardization of PCB Results for NYSDEC Fish Analyses

Valid interpretation of historical trends in PCB concentrations cannot be made without consideration of the changes in analytical methods which have occurred over time. That is, a comparison is valid only when there is consistency in what is being measured. The most dramatic change in analytical methods is that between the Phase 2 TAMS/Gradient data, using state-of-the-art, capillary-column, PCB congener analyses, and older analyses based on packed-column quantitation of Aroclor equivalents. Because an Aroclor is a complex mixture of many individual congeners, interpretation of the historic Aroclor data raises difficult technical issues. In addition, Aroclor quantitation methods have changed over time, and these changes have significant implications for the interpretation of historical trends in the data and the development of valid statistical relationships.

The NYSDEC fish analyses report packed-column Aroclor quantitations and percent lipid, so lipid-normalized Aroclor values may be calculated. Congener-specific data are generally not available. Quantitations have consistently used Aroclor 1016 and Aroclor 1254 standards; an Aroclor 1221 standard was used through 1990, but not thereafter. Reported detection limits range from 0.01 to 1.0 ppm wet weight for each Aroclor, with detection limits for most samples at 0.1 ppm. An Aroclor 1242 standard was not used, despite the fact that most GE releases to the river were Aroclor 1242. Aroclor 1242 is, however, similar in composition to Aroclor 1016, although relative weight percents of individual congeners differ. Total PCBs have generally been calculated by NYSDEC as the sum of Aroclor 1016 plus Aroclor 1254, because (1) 68 percent of the total Aroclor 1221 results, and 55 percent of those between River Mile 142 and 196 are reported as non-detects (versus less than 1 percent non-detects for Aroclor 1016 and Aroclor 1254 in this section of the river); (2) Aroclor 1221 quantitations are not available for later data; and (3) when Aroclor 1221 is detected, substantial double-counting may occur between quantitations to Aroclor 1016 and Aroclor 1221 standards.

The NYSDEC quantitations to Aroclor standards were based on only a few packed-column peaks, and are sensitive to the quantitation method used, which has changed over time. Further, the mix of PCB congeners present in the environment is not exactly equivalent to any fresh Aroclor or mixture of Aroclors: In particular, there are dechlorination product congeners present in the system, and natural partitioning or fractionation effects have also altered the mixture, with the more strongly-sorbing congeners tending to remain in the particulate phase, while other congeners move more readily into the water column and air. In biota, congener-specific rates of accumulation and depuration further alter the mixture.

An interpretation of what was actually measured in historical packed-column analyses can be made by converting the TAMS/Gradient Phase 2 fish congener data to equivalent Aroclor measurements *as if* analyzed by NYSDEC methods. In this

approach the congener concentrations are analyzed to deduce the packed column peak areas which would have been measured by NYSDEC methods, followed by estimation of the corresponding NYSDEC estimate of Aroclor concentrations.

According to the description of the NYSDEC method given by Sloan et al., (1984):

Quantitation was done by comparing several peak heights or areas to those produced by the respective Aroclors. The principal peaks used for quantitation include a single one for Aroclor 1221 representing a monochlorobiphenyl; two for Aroclor 1016 reflecting mixtures of trichlorobiphenyl; and three peaks for Aroclor 1254 primarily composed of tetra-, penta- and hexachlorobiphenyl congeners.

While the NYSDEC method employs several peaks for Aroclor quantitation, these are evaluated via a single composite response factor. Given selection of m packed-column peaks for quantitation, the reported Aroclor value is obtained as

$$[Aroclor] = \left(\sum_{j=1}^m area_j \right) \cdot RF_s \quad (9-1)$$

where,

$[Aroclor]$ = the reported concentration of the PCB Aroclor,
 $area_j$ = the area associated with packed-column peak j , and
 RF_s = a composite or net response factor defined as the concentration of standard Aroclor injected divided by the sum of the peak areas of the selected packed-column peaks.

The area within the selected packed-column peak is related to the sum of the concentrations of individual PCB congeners associated with those peaks by congener peak response factors:

$$\sum_{j=1}^m area_j = \sum_{i=1}^n \frac{[congener_i]}{RF_{ci}} \quad (9-2)$$

where,

n = number of congeners associated with selected packed column peaks,

[congener_i] = concentration of an individual PCB congener *i* associated with the selected packed column peaks, and

RF_{ci} = the response factor for congener *i*, defined as the concentration of congener *i* in the Aroclor standard divided by the peak area contributed by this congener.

Where the congener response factors within the peaks are relatively consistent, this may also be approximated as

$$\sum_{j=1}^m \text{area}_j \approx \frac{\sum_{i=1}^n [\text{congener}_i]}{\text{RF}_p} \quad (9-3)$$

where

RF_p = area-weighted mean response factor for the selected packed column peaks or their constituent congeners in a capillary column analysis. RF_p is defined as the concentration of the Aroclor standard times the weight percent of PCB congeners contained in the selected peaks divided by the peak area, or:

$$\text{RF}_p = [\text{Aroclor}_{\text{std}}] \cdot \frac{\sum_{j=1}^m \text{wt \% peak}_j}{\sum_{j=1}^m \text{area}_j} = [\text{Aroclor}_{\text{std}}] \cdot \frac{\sum_{i=1}^n \text{wt \% congener}_i}{\sum_{k=1}^n \text{area}_k}$$

Substituting Equation (9-3) into Equation (9-1) yields

$$[\text{Aroclor}] \approx \sum_{i=1}^n [\text{congener}_i] \cdot \frac{\text{RF}_s}{\text{RF}_p} \quad (9-4)$$

Because the ratio of the response factors on the right-hand side of this equation is equivalent to the inverse of the weight percent of total PCBs contained in the selected packed column peaks, this simplifies to:

$$[\text{Aroclor}] \approx \frac{\sum_{i=1}^n [\text{congener}_i]}{\sum_{j=1}^m \text{wt \% peak}_j} \quad (9-5)$$

where the denominator represents the total weight percent of the Aroclor contained in the congeners making up the packed column peaks used for quantitation. The relationship is only approximate, because the response factors of individual congeners are not equal. Analyses of response factors in congener calibration indicates, however, that there is a relatively small range of response factors among the congeners which are included in peaks used by NYSDEC for quantitation of each Aroclor and which are found at relatively significant concentrations in the Hudson River. Thus, the simple approximation of (9-5) is judged to provide an adequate basis for comparison.

The NYSDEC fish Aroclor quantitations used three different sets of packed-column peaks for each Aroclor, with changes in 1979 and 1983 (John F. Brown, Jr., personal communication to T.D. Gauthier, 1994). Beginning in 1983, a consistent method has been employed. The peaks and associated congeners for quantitation of Aroclor 1016 and Aroclor 1254 are shown in Table 9-5.

Translating between congener data and NYSDEC Aroclor quantitations also requires the total weight percent of the quantitated peaks in the Aroclor standard, which is obtained by summing the weight percents of relevant congeners obtained in the April 1994 analyses of Aroclor standards conducted for the TAMS/Gradient team (shown in Table 9-6).

For each TAMS/Gradient Phase 2 fish sample, Aroclor quantitation equivalents were estimated by the three NYSDEC methods and their total compared to the sum of congeners. Results clearly indicate that the NYSDEC sum by the 1977 method consistently *overestimates* the wet-weight total PCB concentration in fish (Figures 9-1 to 9-3). The 1979 and 1983 methods consistently *underestimate* total PCBs. The average percent difference between NYSDEC-method estimates and the sum of congeners estimates is +25.5 percent for the 1977 method, and -13.1 percent and -14.6 percent for the 1979 and 1983 methods, respectively.

These observations have important implications for analysis of the older fish data. Specifically, the Phase 1 report noted (see Figure B.3-14) that an apparent order of magnitude decrease in Aroclor 1016 in fish occurred between 1978 and 1980 at all stations. It now appears that a significant portion of this decline (*i.e.*, a decline of about 40 percent) may be due solely to the change in quantitation peaks that occurred in 1979. This "artificial" decline is imposed on a genuine, but smaller than previously estimated, decline in actual PCB concentrations in fish over this time period.

Why does the change in quantitation methods produce these results? The TAMS/Gradient Phase 2 fish data can be used to compare the consistency of NYSDEC Aroclor quantitations over time, as shown in Figures 9-4 through 9-7. In these figures, the congener concentrations in each Phase 2 sample were used to estimate Aroclor quantitations "as if" analyzed by each of the historical NYSDEC

packed-column quantitation schemes. For Aroclor 1016, the 1977 method produces substantially higher estimates than the 1983 method. The 1979 and 1983 Aroclor 1016 methods provide nearly consistent results. In contrast, there is little difference between the Aroclor 1254 results calculated by the different methods. The 1977 methodology for Aroclor 1016, which used packed-column peak 47, includes a number of congeners (BZ #47, BZ #49, and BZ #52) that consistently contribute a significantly higher percentage to fish concentration than to the Aroclor standard. In addition, BZ #52 is an important contributor to Aroclor 1254 (5.2 percent by weight), and its use as a quantitation peak for Aroclor 1016 results in double-counting with Aroclor 1254. Using these congeners in the packed-column quantitation scheme overestimates the total amount of "Aroclor" in a fish sample. In contrast, the congeners used in the 1983 method consistently have a greater percent contribution in the Aroclor 1016 standard than in the fish samples, resulting in a smaller Aroclor 1016 estimate than is needed to reconstruct a total PCB estimate when summed with Aroclor 1254.

Results indicate that the NYSDEC fish database (without correction) should be internally consistent for Aroclor 1254, but will be approximately consistent for Aroclor 1016 only from 1979 on. To use the entire dataset, corrections must be introduced to account for the changes in quantitation schemes (including minor corrections for Aroclor 1254). The present analysis is based on NYSDEC Aroclor quantitations by, or corrected to, the 1983 scheme. Because the relationships are nearly linear, the correction is accomplished through regression relationships. The resulting correction schemes are summarized in Table 9-7. Application of the corrections place the entire series of historical data on a consistent basis, appropriate for statistical analysis.

9.1.3 Water Column Data

For most of the period of fish sampling, the only data available on water-column concentrations are the USGS monitoring. These data commence in 1977 for most locations in the Upper Hudson, with 6 to 58 samples per station per year. Sampling locations and methodology were described in detail in TAMS/Gradient (1991). For this analysis, USGS data coincident with the fish data were utilized from 1977 through the end of calendar year 1992.

Most of the historical USGS results are available as total PCB (whole water) quantitations only. USGS also quantitated Aroclors from 1986 on. The method used, however, consisted of obtaining a visual match of the sample chromatogram to either a single Aroclor standard or a mixture of Aroclor standards, followed by quantitation based on total peak area. The USGS method thus does not provide a direct link to specific congeners, unlike the fish analysis, and individual Aroclor quantitations are subjective. Therefore, only the total PCB estimate reported by USGS was used for this analysis. When a reported total was missing from the database, a total was calculated as the sum of detected Aroclor concentrations.

Few USGS samples distinguish dissolved and particulate PCB fractions, and almost no organic carbon data were collected. Therefore, the idealized formulation given in Equation 8-1, involving the particulate fraction corrected to an organic carbon basis, cannot be employed. Instead, all regressions were based on total, unfiltered PCBs. Predictive equations for fish concentrations of Aroclors and total PCBs can be developed based on total water concentration; the resulting coefficients, however, will only be true BAFs for total PCBs.

As noted in the Phase 1 report (TAMS/Gradient, 1991) and by Brown et al., (1985), a good predictor of yearly average fish PCB burden appears to be the summer average water-column concentration. Therefore, analyses use summer averages of water-column data, based on observations from June through September (Table 9-8). USGS reported a detection limit of $0.1 \mu\text{g/L}$ for samples collected prior to November 1986, and $0.01 \mu\text{g/L}$ thereafter. Total PCB non-detects were set to one-half the detection limit in the calculation of averages. Particularly for the period prior to October 1986, many observations are at or near the detection limit, and sample size is low in some years at some stations. Thus, the relative accuracy of the water column-data is low, which decreases predictive ability.

9.1.4 Sediment Data

Sediment data are the most problematic for establishing a bivariate BAF, because no detailed time series/cross-sectional coverage exists. Having yearly averages of surface and subsurface sediment concentrations at the locations where fish samples were collected would be ideal, but these data do not exist. Additionally, sediment concentrations in the Hudson are known to exhibit a high degree of heterogeneity, so that means from small samples are likely to be unrepresentative. The most intensive sediment work is the 1984 sediment survey, but this covers only the Thompson Island Pool. The 1977/78 sediment survey covers the whole contaminated portion of the upper river; the quantitation methods, however, differ from those used in other studies, and, because of subjective interpretation procedures used in the Aroclor quantitation scheme, are not readily comparable to other data. Finally, recent studies by GE (O'Brien & Gere, 1993a) and the TAMS/Gradient team provide congener-specific coverage of recent sediment conditions.

The sediment component in a bivariate statistical model of bioaccumulation includes a variety of exposure pathways, which are not necessarily well-represented by a single concentration value. During summer low flow conditions, concentrations in sediment at the sediment-water interface are likely near equilibrium with the water column; sediment a few cm beneath the surface, however, may not be in equilibrium with the water column. If quasi-equilibrium exists, concentrations at the sediment water interface may not provide much additional information on exposure beyond that available from water column

concentrations. On the other hand, PCBs from sediment stores which are not in equilibrium with the water column may also contribute to exposure pathways. For instance, benthic organisms may serve as a "pump" to bring PCBs from somewhat deeper sediments into the water column food chain, and localized hotspots or seeps of sediment pore water may provide exposure concentrations significantly higher than the average of surface sediment concentrations.

Two indirect approaches were investigated to compensate for the lack of detailed time-series data for sediments, one assuming changes with time in sediment exposure concentration based on interpretation of dated sediment cores and the other assuming relatively constant *average* sediment concentration at a given location over time:

Approach 1: The first approach utilizes time-varying concentrations in newly deposited sediment and is based on use of dated high-resolution sediment cores in the TAMS/Gradient database. In cores reflecting steady deposition, a dated core layer provides an indication of the PCB content of sediment deposited from the water column at the core location in a given year. The congener data from the core analyses can be normalized to organic carbon (OC), and/or converted to Aroclor quantitations on an "as if" basis comparable to fish quantitation methods. It is not clear, however, to what extent the concentrations measured in the cores reflect the exposure concentration of PCBs entering the food chain from the sediment pathway. In-channel depositional areas suitable for the production of a dateable depositional record are limited, and may better reflect a Spring total water-column concentration than a sediment exposure concentration. PCB levels from the dated cores were used in two ways in the regressions. First, models were investigated based on year-by-year interpretations of dates and associated concentrations in the cores. As these data appear to show significant random noise, and date attributions are uncertain, models were also evaluated using statistically smoothed versions of the core profiles. A more detailed analysis of the high-resolution core data is presented in TAMS/CADMUS/Gradient (1996 - pending publication).

Approach 2: The second approach assumes that the sediment exposure concentration of relevance to modeling biotic accumulation pathways is not the concentration in newly deposited sediment, but the average near surface concentration or store of PCB mass. Note that what is sought for the statistical model is the sediment exposure concentration which contributes to total exposure separate from, or not in equilibrium with the water column PCB concentration. The total store of near surface PCBs is relatively constant over time at a given location: Most of the Upper Hudson is near a dynamic equilibrium in the sediment bed, *i.e.*, neither much deep burial or massive channel scour seems to occur in most years. Evidence from the Thompson Island Pool coupled with geochemical evidence on degradation potential (TAMS/CADMUS/Gradient, 1996 - pending publication) suggests that the inventory of in-place PCBs changes only slowly with time. Further, during the period analyzed (1977-1992), no significant flood-scour events

have occurred on the Upper Hudson comparable to the approximately 75- to 100-year event of 1976, which caused a major redistribution of contaminated sediments. Therefore, Approach 2 assumes that the bioavailable stores of PCBs in sediment at a given location have been approximately constant since the late-1970s. Under this assumption, a model can hold sediment concentration constant through time at a given location. The GE sediment sampling program data (O'Brien & Gere, 1993a) provide an internally consistent picture of PCBs throughout the Upper Hudson and can be normalized to organic carbon content for use in Approach 2.

9.1.5 Functional Grouping of Sample Locations for Analysis

Four functional groupings of available data by location were formed for the purposes of analysis. These represent the major fish sampling locations and associated environmental data. The groups are identified below, along with data assumptions:

Group 1: River Mile 189 to 193, representing the Thompson Island Pool. USGS has not monitored water column concentrations at the Thompson Island Dam (downstream end of this reach), and only data are available from the USGS monitoring station at the next dam at Fort Miller. On the other hand, analyses discussed in the Data Evaluation and Interpretation Report (TAMS/CADMUS/Gradient, 1996 - pending publication) suggest that water-column concentrations in the upper Hudson River are approximately constant, on average, between the Thompson Island Dam and the confluence with the Hoosic River during low-flow conditions, as there is little tributary inflow in this reach. Therefore, summer average water-column concentration is represented by the USGS monitoring at Stillwater (taken just above the Hoosic confluence at River Mile 168). (USGS Fort Edward at Rogers Island water-column data are *not* representative of water-column concentrations downstream in the Thompson Island Pool, due to loading of PCBs from sediments within the pool, and the Rogers Island water-column data are not strongly correlated with fish concentrations between River Miles 189 and 193.) Dated core data (for sediment Approach 1) were taken from TAMS/Gradient Core 19. Core 23 (also dated) was omitted as unrepresentative: it is in the Moses Kill Delta and PCB concentrations appear to be much lower than in other Thompson Island Pool cores. GE near surface sediment data (Approach 2) for River Mile 188.5 to 193.5 (their Reach 8) provided average PCB concentrations of 42.55 ppm, or 2358.75 mg PCB/kg-OC.

Group 2: River Mile 175, the NYSDEC fish collection station between Schuylerville and Stillwater. Water-column concentrations are represented by the USGS Stillwater data at River Mile 168. Thus, Group 2 is assigned the same water-column concentration as Group 1, but differs in sediment concentrations. Sediment concentrations (Approach 1) used high-resolution data from TAMS/Gradient Cores 21 and 22, both from River Mile 177.4, with interpolation

across the two profiles. GE total PCB sediment averages (Approach 2) for River Mile 173.5 to 177.5 (Reaches 5GH and 5IJ) were 16.52 ppm, or 1257.04 mg PCB/kg-OC.

Group 3: River Mile 160, above Federal Dam (recent NYSDEC collection only). Water-column concentrations are represented by the USGS Waterford USGS station at River Mile 156.5. No dateable cores were retrieved in this reach, so this station was omitted from regressions using Approach 1. For Approach 2, GE sediment concentration averages for River Miles 159.7 to 163.6 (Reaches 2AB and 2CD) were 6.48 ppm, or 669.69 mg PCB/kg-OC.

Group 4: River Mile 142 to 155, representing collections in the upper part of the Lower Hudson, below Federal Dam. These stations are influenced by the Mohawk River, especially below River Mile 154.5. Water-column concentrations were represented by the Waterford station *diluted* by the increased flow from the Mohawk River. Based on Phase 2 investigations, PCB contributions in the Mohawk River are assumed negligible compared to loads from the Upper Hudson. Dated core data from TAMS/Gradient Core 11 at River Mile 143.5 (Albany Turning Basin) were used for Approach 1. GE sediment averages (Approach 2) for River Miles 154.3-155.7 (Reaches 1E and 1F) were 1.125 ppm, or 77.20 mg PCB/kg-OC.

9.2 Results of Bivariate BAF Analysis

Regression models were created for the four individual sample groups described above and across all groups based on (1) correlation to water-column concentration only, (2) water column concentration with sediment Approach 1, and (3) water-column concentration with sediment Approach 2. Results were generally consistent among groups, implying that cross-sectional models across groups are appropriate; therefore, the cross-sectional model results are presented.

For a given location and year, the PCB analyses of individual samples for a given species exhibit a high degree of variability, reflecting individual characteristics and intra-year environmental effects that cannot be addressed in the simple regression approach described here. In contrast, the central tendency or mean of species-location-year observations shows much less variability. Analysis of means used a weighted regression, with weights determined as the square root of the sample size. As expected, models on means have much stronger predictive ability than models on individual observations. As the intention of the bivariate BAF analysis is to provide initial information on the central tendency of fish body burden response, models on the means are reported here. Tables 9-9 and 9-10 display the results of the analysis.

In developing final models, the following key points emerged:

- Summer average water-column concentration alone is a good predictor for average Aroclor 1016 burden (as quantitated by NYSDEC) in most species of fish. Water-column concentration is not as good a predictor for Aroclor 1254 burden. When combined with the relationship to water-column concentration, a time trend versus year was usually significant for Aroclor 1254, but not Aroclor 1016, in the regressions. This suggests that other time-variable factors beside water-column concentration are significant for Aroclor 1254.
- Incorporation of estimates of time-dependent changes in depositional sediment PCB concentration did not improve model predictive ability. The high-resolution core data (sediment Approach 1) were almost never strong predictors of fish PCB burden, either alone or in combination with water column concentrations. The relationship to the core data was often not statistically significant when water was included. Some statistically significant relationships to the core data were negative, *e.g.*, between fish body burden Aroclor 1254 and Aroclor 1254 (normalized to OC) in the sediment. These data do not appear to be useful for estimating sediment-pathway PCB exposure.
- Assuming constant sediment exposure concentrations by location (sediment Approach 2) provides much stronger predictive ability. Water and OC-normalized sediment concentration together provided a satisfactory set of explanatory variables for Aroclor 1016. In stepwise multiple regression tests, other variables were statistically significant only occasionally and water was always the single most significant variable. For Aroclor 1254, a negative trend with time (in addition to water and sediment concentrations) was still found statistically significant for largemouth bass, but was only marginally significant at the 5 percent level and contributed a minor portion of total explanatory power. Regressing on water and sediment alone provided only a small increase in standard error of the estimates obtained with the time variable included (maximum 7 percent increase for the largemouth bass model). The statistical correlation to time may reflect a real trend, such as a slow decline in bioavailable sediment concentration; however, the apparent trend may also be an artifact of the data because (1) water concentrations have tended to decline over time toward USGS detection limits, resulting in less "power" in recent observations; (2) assumed constant sediment values are likely not entirely accurate; (3) largemouth bass, which are at the top of the food web, may integrate exposures over several years; and (4) the spatial distribution and collection time of fish samples has varied from year to year.

9.3 Discussion of Bivariate BAF Results

For comparison to published results, Tables 9-9 and 9-10 contain estimates of a univariate \log_{10} BAF for total PCBs in units of liters of water per kg of fish lipid. This univariate BAF is based on the fitted regression coefficients on water column concentration, B_w . Because the water column concentrations are reported as ppb ($\mu\text{g/L}$) and fish concentrations as ppm (mg/kg-lipid), the univariate BAF is estimated from the regression coefficient as:

$$\log_{10}(\text{BAF}) = \log_{10}(B_w \times 10^3) \quad (9-6)$$

where,

$$\text{BAF} = \frac{(\text{kg-PCB}) \cdot (\text{kg-lipid})}{(\text{kg-PCB}) (\text{L-water})}$$

The calculated log BAFs for total PCBs presented in Table 9-10 (as measured by the sum of NYSDEC Aroclor 1016 and Aroclor 1254 quantitations) range from 6.14 for pumpkinseed to 6.79 for goldfish when expressed on a L/kg basis. These univariate BAFs, relating lipid-normalized body burden in fish to total PCB concentrations in water, are sometimes denoted as BAF_l^t (USEPA, 1994). BAFs are also frequently reported on the basis of the freely-dissolved fraction of a chemical in the water column, BAF_l^{fd} . The two forms of the univariate BAF can be related as

$$\text{BAF}_l^{\text{fd}} = \frac{\text{BAF}_l^t}{f_d} \quad (9-7)$$

where f_d is the freely dissolved fraction of the chemical. Estimates of the average dissolved fraction of key PCB congeners in the Hudson are presented in the Data Evaluation and Interpretation Report (TAMS/CADMUS/Gradient, 1996 - pending publication). Under average conditions in the Upper Hudson, the dissolved fraction appears to be about 50 percent for congeners in the range of BZ#25 through BZ#53 used to quantitate Aroclor 1016, and about 33 percent or less for the congeners used to quantitate Aroclor 1254. Using Equation (9-7), base-10 logarithms of BAF_l^{fd} s would thus be equal to the calculated BAF_l^t s plus about 0.3 to 0.52 units.

USEPA (1994) summarizes estimated BAF_l^{fd} s for PCB congeners by trophic level based on the food web/fugacity model of Gobas (1993) for conditions in Lake Ontario. Results calculated here compare favorably to results presented by USEPA (1994) for BZ #28 and BZ #31. These congeners are both included in the quantitation scheme used by NYSDEC for Aroclor 1016, and constitute about 14 percent of the total weight of raw Aroclor 1242. For BZ#28 and BZ#31, the

Gobas model predicts a BAF_1^{fd} of 6.51 for alewives. Similar to pumpkinseed, this species feeds on invertebrates that accumulate PCBs from the water column (assumed alewife diet of 60 percent zooplankton and 40 percent *Diporeia* sp.) The Gobas model estimate compares well to the estimate of 6.14 ± 0.3 presented here for pumpkinseed BAF_1^{fd} . Similarly, the Gobas model result for BZ#28 and BZ#31 in piscivorous fish is 6.68, which compares well with the Hudson River largemouth bass estimate of $BAF_1^{fd} = 6.51 \pm 0.3$.

Figures 9-8 through 9-13 display the ability of the final regression equations to predict observed mean concentrations over all stations for Aroclor 1016 and Aroclor 1254 lipid-normalized averages in pumpkinseed, largemouth bass, and brown bullhead, the three species for which the most data are available. Each yearly observation is keyed to location. It should be recalled that the regression was weighted to the square root of sample size; thus, some points that lie away from the match line represent small samples which had little weight in the regression. As indicated by the R^2 values presented in Table 9-10, the fit is generally better for Aroclor 1016 than for Aroclor 1254. The difference in goodness-of-fit in part reflects limited knowledge of the time course of PCB concentrations in the sediments and changing congener composition in the sediments between stations, but may also represent greater sample-to-sample variability in the accumulation of more highly chlorinated congeners. On the plot for Aroclor 1254 in largemouth bass (Figure 9-12), the models appear generally to underestimate burdens at River Mile 175, but overestimate those downstream at River Miles 142-155. This may reflect inaccurate sediment averages at one or both stations. Also, water-column concentrations near the detection limit may be overestimated downstream resulting in a slight bias in the regression relationship.

The most complete fish time-series data in the Upper Hudson are those collected at River Mile 175. Figures 9-14 through 9-19 compare predictions to observations across time at this station for pumpkinseed, largemouth bass, and brown bullhead. The Aroclor 1016 results generally track well, while the Aroclor 1254 results show greater variability. Some discrepancies are attributable to small sample size: most sample sizes were between 20 and 30 individuals or composites, but some were as small as a single individual. Also, systematic changes in collection probably affected results. For instance, from 1979 to 1989 largemouth bass and brown bullhead were collected at River Mile 175 in June, while pumpkinseed were collected in September. In 1991 and 1992, collections of all three species shifted to May, with a few December samples. Shifting to earlier in the year likely affects the observed PCB burden. Finally, the size and weight of fish collected varies from sample to sample. For instance, Pumpkinseed collected at River Mile 175 between 1981 and 1988 were primarily yearlings, with mean weights in the range of 16 to 50 g, whereas those collected in 1991 and 1992 had mean weights of about 250 g. Size has important implications for feeding preferences and is also correlated with age, which was not measured.

Nonetheless, no clear relationship could be established between PCB burden and either weight or length. The relationships presented here represent broad averages across a variety of factors, including season and size, in keeping with the goal of establishing a scoping tool preparatory to the physically-based food web analysis.

All regression equations in Table 9-10 are calculated with the same independent variables and therefore provide a consistent basis for examining estimated relative contributions of sediment and water. The regression partial sums of squares associated with the two independent variables (water-column concentration and sediment concentration normalized to organic carbon) can be used to calculate the proportion of total explained variability attributed to water and sediment sources (Table 9-11), with the caveat that the sediment exposure pathway in the statistical model represents only those sediment exposure pathways not explained by water column concentrations. For Aroclor 1016, between 61 and 99.7 percent of the explained variability is estimated to be due to water-column inputs. The estimated water-column contribution for Aroclor 1016 is high even for bottom-feeding brown bullhead. As quantified by NYSDEC, Aroclor 1016 results represent primarily trichlorinated congeners below BZ #45, which are generally expected to be strongly driven by the water column, as opposed to sediment pathways.

A different picture emerges for more highly chlorinated congeners represented in Aroclor 1254 quantitations, with considerable range in the importance of the sediment pathway, which appears to reflect the trophic level and forage preference of the species. The water-column pathway remains dominant for some species, including pumpkinseed and cyprinids, which forage primarily in the water column, and yellow perch, which are migratory. In contrast, brown bullhead, which forage primarily in the sediment, have an estimated 86 percent contribution from the sediment pathway. At the highest trophic level, largemouth bass, which are primarily piscivorous, are estimated to obtain about 42 percent of their measured Aroclor 1254 burden from the water column and about 58 percent from sediment pathways. These intermediate numbers suggest that the bass integrate, or average out, food web contributions from both water-column and sediment/detrital feeders.

9.4 Summary

Bivariate BAF models, relating lipid-based PCB burden in fish to PCB concentrations in both the water column and sediment, provide good explanatory power in predicting annual mean total PCB and Aroclor body burden in five fish species throughout the Upper Hudson River, based on analysis of NYSDEC monitoring data for 1975 through 1992. Water-column and sediment PCB concentrations are clearly not in complete equilibrium in most of the Upper Hudson,

and inclusion of sediment concentration as an independent variable results in a significant increase in explanatory power.

The analysis indicates that a steady-state food web model, functionally equivalent to the bivariate BAF in terms of input and output, is feasible. It should, however, be emphasized that the specific values of coefficients developed in the analysis of the NYSDEC data are highly dependent on the nature of Aroclor quantitations in fish and the water column, which do not represent the complete congener pattern of true Aroclors and additionally were not obtained by consistent methods. Finally, scoping models are adequate to estimate annual means, but do not reflect individual and within-year variability expected to result from age and variations in foraging with size, nor seasonal patterns related to temperature and the spawning cycle. These issues are addressed through the development of the Probabilistic Bioaccumulation Food Chain Model in Section 10.

10. CALIBRATION OF PROBABILISTIC BIOACCUMULATION FOOD CHAIN MODEL

The components of the food chain model and general model structure are described in Section 8.5. The model takes as exposure concentrations the summer-averaged water concentration for PCBs normalized to particulate organic carbon and the annual average sediment concentration for PCBs normalized to fraction of organic carbon. As discussed in Section 8.5, these exposure concentrations are converted to body burdens of PCBs through a number of bioaccumulation factors (BAFs) that link media and food chain components. These BAF values and the uncertainty or variability around them are derived from the available data for the Hudson and from data for other systems. This section of the report describes how these BAFs were derived for each food chain component, examines the goodness-of-fit between modeled body burden data and observations in the river, and provides an illustration of how the model is anticipated to be used in a predictive mode for one of the selected fish species - the yellow perch.

Analyses presented here are based on Release 3.1 of the TAMS/Gradient database, except for the yellow perch example, which is based on unvalidated data from Release 2.3. Results presented here are draft and subject to change based on ongoing data validation. Results are presented primarily for illustrative purposes and to demonstrate the methodology, rationale, and limitations.

Each compartment in the model is described separately for each of the calibration congeners, Aroclors 1016 and 1254, and total PCBs. The relationship between each of the compartments is described by a distribution of accumulation factors based on field data. These BAFs relate the body burden of one compartment to the expected dietary exposure of that compartment. The dietary exposure is assumed to implicitly incorporate actual exposures from all sources (*i.e.*, direct water uptake). Distributions presented in this report are derived for the calibration congeners, Aroclors 1016 and 1254, and for total PCBs to describe the range of expected bioaccumulation factors between two compartments.

10.1 Overview of Data Used to Derive BAFs

Table 10-1 shows the ecological sampling locations by river mile and the corresponding water column stations.

10.1.1 Benthic Invertebrates

The TAMS/Gradient team collected 20 (including background) collocated benthic invertebrate and sediment samples during the Phase 2 field collection program. Five sediment samples and three to five benthic invertebrate samples were taken at each location. Benthic invertebrates were identified to the taxonomic group level for PCB analyses. PCB results were provided for individual congeners,

homologue sums, total PCBs, and Aroclor equivalents. In addition, percent lipid data are also provided. These data were used to characterize the relationship between sediment PCB concentrations and resulting benthic invertebrate body burdens.

10.1.2 Water Column Invertebrates

Phase 2 activities did not include data collection related to water column invertebrates. The data on water column invertebrates is obtained from the NYSDOH studies done as part of the Hudson River PCB Reclamation Demonstration Project (Simpson et al., 1986). NYSDOH conducted long- and short-term biomonitoring studies from 1976 to 1985 using caddisfly larvae, multiplate samples, and chironomid larvae. NYSDOH placed artificial substrate samplers (multiplates) along 17 sites for five weeks in the Hudson river from Hudson Falls to Nyack, New York (Novak et al., 1988). Samplers remained in place for five weeks during July through September collecting a composite of sediment, algae, plankton and various macroinvertebrates. After collection, the samplers were analyzed for Aroclors 1016 and 1254. Total PCB values are obtained by summing the individual values for Aroclors 1016 and 1254. Percent lipid values are also provided. These data, combined with information from the Phase 2 dataset, provide an indication of the relationship between water column invertebrates and water column sources.

The short-term biomonitoring study conducted by NYSDOH involved the chironomid larvae, *Chironomus tentans*. Twenty-five laboratory-raised chironomid larvae in nylon mesh packets were placed, in groups of ten, in steel mesh baskets at four Hudson River locations (one at Bakers Falls, two at Thompson Island Pool, and one at Fish Creek). One set of packets was exposed to the sediment at a collection site on the eastern shore of Thompson Island Pool. The remainder were placed in the water column. These short-term data are available for selected congeners and provide some information related to the time-frame and magnitude of the short-term relationship between water column invertebrates and water column sources.

10.1.3 Fish

The TAMS/Gradient team collected fish data from the same 20 benthic invertebrate and sediment locations. Between three to five of the selected fish species were collected at each location (i.e., not all species were collected from all locations, for further detail, refer to the TAMS/Gradient SAP/QAPP, 1992). Data are provided for individual congeners, homologue sums, total PCBs, and Aroclor equivalents. Percent lipid, length and weights of individual fish as well as composited samples are also provided.

NYSDEC has been collecting fish data for over 30 species in the Upper Hudson since 1975. From 1975 to 1988, fish data were collected every year. In 1988, fish sampling frequency changed from yearly to every other year. The bulk

of the sampling (75 percent) has been conducted for striped bass, largemouth bass, brown bullhead, pumpkinseed, American shad, and American eel.

For the NYSDEC samples, chemical analyses for Aroclors 1016, 1254 and in some years, 1221 and 1242, are provided in the database as well as weight, length, percent lipid, and, for some years, sex and age. Generally, 30 fish were collected for each species at several locations.

10.1.4 Literature Values

There are studies from the literature which provide additional information on the relationship between sediment, benthic invertebrates, water and water column invertebrates. (e.g. Whittle et al., 1983; Bierman, 1990; Bierman, 1994; Wood et al., 1987; Larsson, 1984; Lake et al., 1990; Oliver, 1987; Oliver & Niimi, 1988; Thomann, 1981; van der Oost et al., 1988; Thomann, 1989; Thomann & Connolly, 1984; Bush et al., 1994; Thomann et al., 1992; Harkey et al., 1994; Endicott et al., 1994; and others). These studies are primarily useful for comparative purposes, as they refer to systems which may experience conditions unlike those in the Hudson River.

10.2 Benthic Invertebrate:Sediment Accumulation Factors (BSAF)

Distributions of BSAFs between sediment concentrations and benthic invertebrate concentrations were derived by:

1. Evaluating the sediment data to determine which river miles display significant heterogeneity and variability in concentrations;
2. Calculating the BSAF by dividing a measured individual benthic invertebrate concentration by the geometric mean sediment concentration at a sampling location; and,
3. Conducting a statistical analysis to identify outliers and extreme values and presenting goodness-of-fit results for the final distribution representative of the relationship between benthic invertebrates and sediment.

10.2.1 Sediment Concentrations

An assessment of the range of sediment concentrations by river mile and congener provides information on the variability inherent in these data (TAMS/CADMUS/Gradient, 1996 - pending publication). Figures 10-1 through 10-8 provide box-plots of sediment concentrations by river mile. The box contains the middle 50 percent of values, called the interquartile range, and the lines extending from the ends of the box show the extreme values not considered outliers. Outliers are identified by an "o" and extreme outliers identified by an asterisk. An outlier is defined as a value that falls 1.5 times outside the interquartile range, and an

extreme value is more than 3 times outside the interquartile range. These values were not eliminated from the analyses, but rather provide important information on the variability of concentrations at a given river mile. Plots are provided for BZ#4, BZ#28, BZ#52, BZ#101 with BZ#90, BZ#138, Aroclor 1016, Aroclor 1254 and total PCBs for each river mile expressed as ug/g on a TOC-normalized basis.

Figures 10-1 through 10-8 provide information on the distribution of sediment concentrations at each river mile. The lower river, (miles 25.8 through 143.5) show significantly lower and less variable PCB concentrations than the upper river. Note that the Aroclor 1016 concentrations (Figure 10-6) are similar to the Total PCB concentrations (Figure 10-8), indicating the dominance of the lower chlorinated congeners in the upper river. BZ#4 (Figure 10-1) shows the highest concentrations of the individual congeners plotted.

10.2.2 Approach

BSAFs for benthic invertebrates were calculated from the Phase 2 dataset using collocated sediment and benthic samples. The sampling rationale will be presented as part of the ecological risk assessment (work in progress). PCB concentration and lipid data were available for Amphipods, Bivalves, Chironomid, Gastropods, Isopods, Odonata, Oligochaetes, Unsorted Total (everything in a sample), Sorted Total (unidentified remaining after sorting), and Epibenthic species.

The ideal data pairs to calculate BSAFs are individually collected samples of sediment and benthic invertebrates. In the absence of this ideal condition, we used individual benthic invertebrate samples and the geometric mean sediment concentration for a given co-located sampling location.

However, in the areas which display highly variable PCB concentrations in sediments, it is unlikely that the geometric mean adequately represents the exposure levels for benthic invertebrates, particularly for the lower chlorinated congeners or mixtures such as Aroclor 1016. The heterogeneity in sediment concentrations over small spatial scales contributes to higher variability in the BSAFs calculated from data collected in these areas. Thompson Island Pool is an area in which such variability in calculated BSAFs occurs. Matching individual invertebrate concentrations to the geometric mean sediment exposure in this area results in more variable ratios. Also, the ratios for Thompson Island Pool are higher in magnitude than for the upper river generally and significantly higher than the lower river.

Species identified as epibenthic showed BSAF that were not significantly different from any other species. In addition, the sampling program did not specifically sample for epibenthic species (Chernoff, 1995, personal communication) and were only identified as such during subsequent analyses. The BSAF calculated for each river mile were combined to represent the range of accumulation factors in river generally. The implications for the food chain model are that this distribution of BSAFs represent the range among the prey species of fish feeding off the bottom. This is a reasonable approximation if the fish feed on benthic invertebrates indiscriminately so that the probability of preying on a particular species is proportional to that species' abundance.

For those sampling locations at which there were enough data to run normality tests, it was determined that the benthic invertebrate data follow a lognormal distribution. This was verified by log-transforming benthic invertebrate PCB concentrations and running standard normality tests. Given lognormally distributed invertebrate concentrations, the appropriate statistic for use in the BSAF calculations is a geometric mean sediment concentration. The variability in the sediment and benthic invertebrate concentrations has a significant impact on calculated BSAF, because widely divergent individual benthic invertebrate concentrations are normalized to one sediment concentration considered to be indicative of exposures over time.

Bar charts were developed to show calculated BSAF by river mile and invertebrate species, and scatter plots were developed to show species BSAF by sediment concentrations. Finally, charts showing the goodness-of-fit between modeled output and observed concentrations are presented. A set of charts was prepared for the calibration congeners, Aroclors 1016 and 1254, and total PCBs.

The BSAF by river mile charts were developed using the data for the combined benthic species (no epibenthic species). The charts for BSAF by river mile and the BSAF by species show the mean BSAF within an error bar indicating plus and minus one standard error of the mean. These plots provide information on the variability of BSAF by river mile, and the species that contribute most to the observed variability. Identifying the species showing the greatest variability may indicate that the primary exposure is not sediment, but rather overlying water. This hypothesis will be examined in greater detail in the next phase of work. The scatter plots show BSAF for each of the species by the TOC-normalized geometric mean sediment concentrations. These plots show whether there is a relationship between sediment concentration and BSAF.

10.2.3 Calculations of BSAF Values for Benthic Invertebrates

BSAF for Congener BZ#4: Biota to Sediment Calculations

Figure 10-9 shows the BSAFs for BZ#4 (all species combined) by river mile. River miles 189 and 189.5, within the Thompson Island Dam area, have higher mean BSAF than the other river miles (over 10 and 4, respectively), and greater uncertainty in the estimate (wider error bars). Mean BSAF range from 0 to 1 for the remaining river miles, with narrower error bars.

Figure 10-10 shows the BSAF for BZ#4 (all river miles combined) by species. The BSAF for most species are less than 1.0; the narrow error bars indicate relatively little uncertainty in the mean BSAF. Three species have distinctly higher mean BSAF, accompanied by wider error bars. The BSAF for Chironomids, about 9, is the highest ratio, with the widest error bars, due at least partially to the small sample size (3). The chironomid samples are primarily from the Thompson Island Pool area, and show very high concentrations relative to both other invertebrates as well as the mean sediment concentration. The BSAF for the Isopods and the aggregate Sorted Total, about 4, are two to three times higher than the majority of the remaining species, with greater uncertainty in the estimates as represented by wider error bars.

Figure 10-11 provides the scatter plot of the BSAF for BZ#4 for each species by the sediment concentrations. Most points on the plot show BSAF from 0 to less than 10, regardless of sediment concentrations. The Chironomids have a high BSAF at a relatively low sediment concentration and the Isopods and the Sorted Total have high BSAF at the highest sediment concentration.

The variability in the BSAF for BZ#4 may be affected by its relatively high solubility. For BZ#4, the direct exposure of benthic invertebrates to pore water could be significant. The predicted phase distribution of BZ#4 in pore water relative to total sediment concentrations varies from 8 to 45 percent, depending on the method used (TAMS/CADMUS/Gradient, 1996 - pending publication). A fraction of this is DOC-bound. The bioavailability of the DOC-bound fraction is considered low (DiToro et al., 1991). The estimated concentration factor (ng g^{-1} dry weight) (Novak et al., 1990) for BZ#4 in chironomid is 5,830, and it required only 0.2 days to reach 90 percent equilibrium. This indicates that chironomid respond quickly to changes in water concentrations and may be showing more of a response to water concentrations than to direct sediment exposure.

BSAF for Congener BZ#4: Biota to Sediment Goodness-of-Fit

The model was run by applying the distribution derived above to each geometric mean sediment concentration by river mile. The 10th, 25th, 50th, 75th, 90th percentiles were calculated as well as a maximum. These percentiles were compared to the output from the frequency analysis on the benthic invertebrate data done using the SPSS™ software package. There were not enough invertebrate data to characterize the measured frequency distribution (high numbers of non-detects which skewed the distribution), so the goodness-of-fit was done by comparing individual benthic invertebrate concentrations to modeled output (Figure 10-12). The line identified as "measured" represents individual data points. The model 50th percentile output follows the data most closely, although individual elevated observations were captured by the maximum from the model.

BSAF for BZ#28: Biota to Sediment Calculations

Figure 10-13 shows the BSAF for BZ#28 (all species combined) by river mile. Most of the means are from approximately 0.5 to 1.5, with narrow error bars. The BSAF for river miles 189 and 189.5 show wider error bars, indicating greater uncertainty in the estimates of the mean. The widest error bar is around the river mile 100 mean estimate.

Figure 10-14 shows the BSAF for BZ#28 (all river miles combined) by species. The BSAF for Chironomids is about three times greater, and has wider error bars, than the BSAF of the other species. The BSAF for the Gastropods, about 1, has wider error bars than the other species. The samples sizes of the Chironomids and Gastropods are small (3 and 4, respectively).

Figure 10-15 provides the scatter plot of the BSAF BZ#28 for each species by the sediment concentrations. Most of the BSAF are between 0 and 1.5, for all sediment concentrations. Higher BSAF for Chironomids (about 6 and 3) are shown for sediment concentrations of approximately 21 ug/g. At this sediment concentration, a high BSAF, about 3.5, is also shown for the Unsorted Total. A high BSAF, roughly 2.5, is shown for Gastropods at 18 ug/g. At lower sediment concentrations, high BSAF are shown for the Unsorted Total (about 4 at 1 ug/g), for the Sorted Total and Isopods (about 3 and 2.5, respectively, at 8 ug/g). No trend by sediment concentration is observed.

The pore water contribution to BZ#28 is small, less than 10 percent (TAMS/CADMUS/Gradient, 1996 - pending publication). However, the concentrations may be high enough to contribute significantly to the benthic invertebrate body burdens. It may also be that chironomid and other benthic invertebrates may be responding to temporal water column PCB concentration changes.

BSAF for BZ#28: Biota to Sediment Goodness-of-Fit

The model was run by applying the distribution derived above to each geometric mean sediment concentration by river mile. The 10th, 25th, 50th, 75th, 90th percentiles were calculated as well as a maximum. A frequency distribution was estimated from the observed data for each sampling location in order to compare observed results to the modeled output. Both the observed and modeled percentiles were log-transformed and the observed benthic invertebrate concentrations plotted against the percentiles predicted from the model. Figure 10-16 shows the results of this analysis. The center line is the estimated regression line, and 95 percent confidence interval. The observed and modeled 50th and 90th percentiles compared favorably, although the shape of the observed distribution differed slightly from the modeled output.

BSAF for BZ#52: Biota to Sediment Calculations

Figure 10-17 shows the BSAF BZ#52 (all species combined) by river mile. Higher and more uncertain BSAF are shown for river mile 189. River mile 100 shows high uncertainty around the estimate of the mean BSAF. The other river miles have BSAF between 1 and 2, with less uncertainty in the mean estimate as evidenced by smaller error bars.

Figure 10-18 shows the BSAF BZ#52 (all river miles combined) by species. BSAF for most of the species are between 2 and 4, with fairly wide error bars, indicating relative uncertainty in the mean estimate. Three species have lower BSAF, between 0.5 and 1.5, with narrow error bars: amphipods, bivalves, and odonata. Chironomid, isopods and gastropods shows the highest BSAF and the greatest uncertainty around the BSAF estimate.

Figure 10-19 provides the scatter plot of the BSAF BZ#52 for each species by the sediment concentrations. Most of the BSAF are less than 5. There are three high BSAFs: for the Unsorted Total, about 15, at the lowest concentration, and for the sorted Total and Isopods, about 16 and 14, respectively, at approximately 9 ug/g.

BSAF for BZ#52: Biota to Sediment Goodness-of-Fit

The model was run by applying the distribution derived above to each geometric mean sediment concentration by river mile. The 10th, 25th, 50th, 75th, 90th percentiles were calculated as well as a maximum. These percentiles were compared to the output from the frequency analysis on the benthic invertebrate data done using the SPSS™ software package. After log-transforming the results, the observed benthic invertebrate concentrations were plotted against the percentiles predicted from the model. Figure 10-20 shows these results. The modeled and observed percentiles compare favorably.

BSAF for BZ#101 (with BZ#90): Biota to Sediment Calculations

Figure 10-21 shows the BSAF BZ#101 with BZ#90 (all species combined) by river mile. River mile 100 has the highest BSAF, about 4, with very wide error bars, indicating significant uncertainty in the mean estimate. River miles 189 and 189.5 also have slightly higher BSAF than the remaining river miles.

Figure 10-22 shows the BSAF BZ#101 with BZ#90 (all river miles combined) by species. Chironomids and Gastropods have the highest BSAF (about 4), with the widest error bars. The other river miles have BSAF between 0.5 and 2.5, with narrower error bars.

Figure 10-23 provides the scatter plot of the BSAF BZ#101 with BZ#90 for each species by the sediment concentrations. There is a wide range in BSAF from just above 0 to 6.5 for all sediment concentrations. There are two distinct points: BSAF near 10 for the Unsorted Total at the lowest concentration, and at 2 ug/g for the Sorted Total.

BSAF for BZ#101 (with BZ#90): Biota to Sediment Goodness-of-Fit

The model was run by applying the distribution derived above to each geometric mean sediment concentration by river mile. The 10th, 25th, 50th, 75th, 90th percentiles were calculated as well as a maximum. These percentiles were compared to the output from the frequency analysis on the benthic invertebrate data done using the SPSSTM software package. After log-transforming the results, the observed benthic invertebrate concentrations were plotted against the percentiles predicted from the model. Figure 10-24 shows the results of this analysis. The modeled and observed percentiles compare favorably.

BSAF for BZ#138: Biota to Sediment Calculations

Figure 10-25 shows the BSAF for BZ#138 (all species combined) by river mile. River mile 189 has the highest mean BSAF, about 4, with the widest error bars. River miles 25.8, 100, and 189.5 all show BSAF slightly above 2, while the remaining river miles show BSAF around 1.

Figure 10-26 shows the BSAF BZ#138 (all river miles combined) by species. Chironomid, gastropods and isopods show the highest BSAF, with wide error bars for chironomid and isopods. BSAF for the remaining species range from about 1 to 2, with narrower error bars.

Figure 10-27 provides the scatter plot of the BSAF BZ#138 for each species by the sediment concentrations. With one exception, the BSAF for all sediment concentrations cluster from 0 to about 6. The BSAFs for Isopods at about 1.4 ug/g is twice as great, approximately 12.

BSAF for BZ#138: Biota to Sediment Goodness-of-Fit

The model was run by applying the distribution derived above to each geometric mean sediment concentration by river mile. The 10th, 25th, 50th, 75th, 90th percentiles were calculated as well as a maximum. These percentiles were compared to the output from the frequency analysis on the benthic invertebrate data done using the SPSS™ software package. After log-transforming the results, the observed benthic invertebrate concentrations were plotted against the percentiles predicted from the model. Figure 10-28 shows the results of this analysis. The modeled and observed percentiles compare favorably.

BSAF for Aroclor 1016: Biota to Sediment Calculations

Figure 10-29 shows the BSAF for Aroclor 1016 by river mile (across all species). The BSAF are all less than 1 with narrow error bars for all river miles except 100, 189, and 189.5. The BSAF for river mile 189 shows the greatest variability.

Figure 10-30 shows the BSAF by species (across all river miles). The BSAF for chironomid and isopods are higher (approximately 4) with wider error bars than for the remaining species. Gastropods, which have shown variable BSAF for individual congeners, show no significant difference from other species for Aroclor 1016.

Figure 10-31 provides the scatter plot of the BSAF for Aroclor 1016 for each species by the sediment concentrations. The sorted total and isopods show high BSAF (16 - 18) at 350 ug/g geometric mean sediment concentration. The highest sediment concentrations show tightly clustered and fairly low BSAF.

BSAF for Aroclor 1016: Biota to Sediment Goodness-of-Fit

The model was run by applying the distribution derived above to each geometric mean sediment concentration by river mile. The 10th, 25th, 50th, 75th, 90th percentiles were calculated as well as a maximum. These percentiles were compared to the output from the frequency analysis on the benthic invertebrate data done using the SPSS™ software package. After log-transforming the results, the observed benthic invertebrate concentrations were plotted against the percentiles predicted from the model. Figure 10-32 shows the results of this analysis. The modeled and observed percentiles compare favorably.

BSAF for Aroclor 1254: Biota to Sediment Calculations

Figure 10-33 shows the BSAF for Aroclor 1254 (all species combined) by river mile. As has been observed in previous figures, the BSAF for river miles 100, 189 and 189.5 are highest and show the greatest variability. The BSAF for the remaining river miles are approximately 1 with fairly narrow error bars.

Figure 10-34 shows the BSAF for Aroclor 1254 by species (across all river miles). Unlike for Aroclor 1016, Aroclor 1254 BSAF by species are highest and most variable for chironomid, gastropods and isopods.

Figure 10-35 provides the scatter plot of the BSAF for Aroclor 1054 for each species by the sediment concentrations. The highest BSAF are observed for a geometric mean sediment concentration of 90 ug/g. BSAF for the highest sediment concentrations (above 200 ug/g) are all between 0 and 4.

BSAF for Aroclor 1254: Biota to Sediment Goodness-of-Fit

The model was run by applying the distribution derived above to each geometric mean sediment concentration by river mile. The 10th, 25th, 50th, 75th, 90th percentiles were calculated as well as a maximum. These percentiles were compared to the output from the frequency analysis on the benthic invertebrate data done using the SPSS™ software package. After log-transforming the results, the observed benthic invertebrate concentrations were plotted against the percentiles predicted from the model. Figure 10-36 shows the results of this analysis. The modeled and observed percentiles compare favorably.

BSAF for Total PCBs: Biota to Sediment Calculations

Figure 10-37 shows the BSAF for Total PCBs (all species combined) by river mile. The mean BSAF for river miles 100, 189 and 189.5 are higher and have wider error bars than the other river miles. The BSAF for river mile 189 is about 6; the BSAF for river miles 100 and 189.5 are about 3. The BSAF for the other river miles are about 1, with very narrow error bars.

Figure 10-38 shows the BSAF Total PCBs (all river miles combined) by species. The BSAF for chironomids, about 4, is higher and has wider error bars than the other river miles. The BSAF for Isopods, about 3, also has wide error bars. BSAF for the remaining river miles range between 0 and 2, with narrower error bars.

Figure 10-39 provides the scatter plot of the BSAF Total PCBs for each species by the sediment concentrations. The BSAF for most species and sediment concentrations range between 0 and 5. The highest BSAF are for the Sorted Total and Isopods, about 15 and 13, respectively, at about 450 ug/g. A high BSAF is also shown for Chironomids, about 9 at about 300 ug/g.

BSAF for Total PCBs: Biota to Sediment Goodness-of-Fit

The model was run by applying the distribution derived above to each geometric mean sediment concentration by river mile. The 10th, 25th, 50th, 75th, 90th percentiles were calculated as well as a maximum. These percentiles were compared to the output from the frequency analysis on the benthic invertebrate data done using the SPSS™ software package. After log-transforming the results, the observed benthic invertebrate concentrations were plotted against the percentiles predicted from the model. Figure 10-40 shows the results of this analysis. The modeled and observed percentiles compare favorably.

Summary of Biota-Sediment Accumulation Factors

The modeled PCB distributions compare favorably to the observed distributions of PCB concentrations for individual calibration congeners, Aroclors 1016 and 1254, and total PCBs. The model for benthic invertebrates captures the observed variability in the underlying data. In areas where the sediment concentrations display heterogeneity (such as Thompson Island Pool), the model accurately captures the maximum observed concentrations. However, in the Lower Hudson River, where sediment (and biota) concentrations display far less heterogeneity, the model tends to overpredict the maximum observed concentrations. In this case, the 75th percentiles capture the maximum observed concentrations, while the 90th percentiles overpredict by a factor of 2 or more. It may be more appropriate to use only Lower Hudson River distributions at those locations at which sediment concentrations (and corresponding benthic invertebrate concentrations) do not show much variability.

10.3 Water Column Invertebrate:Water Accumulation Factors (BAFs)

10.3.1 Approach

Water column invertebrates are defined as those that receive most of their exposure to PCBs via the water column. As defined, this group includes zooplankton as well as invertebrates living on substrates such as plants or rock surfaces but are not in direct contact with the sediments. The approach taken relates body burdens in water column invertebrates (on a lipid-normalized basis) to water concentrations (normalized to particulate organic carbon). This was done for the following reasons:

1. It is assumed that PCBs in the particulate phase in the water column and PCBs in the dissolved phase in the water column are in quasi steady-state over time scales of months during the Summer as discussed in Section 8. Thus by establishing relationships between invertebrates and a particular phase (particulate organic carbon in this case), overall accumulation from the water column will be taken into account.

2. The relationship to PCBs normalized to particulate organic carbon was selected because, while water column invertebrates will accumulate PCBs directly from the dissolved phase, the higher chlorinated congeners are predominantly associated with the particulate phase which form the food base for the invertebrates. Partition coefficients derived in the Data Evaluation and Interpretation Report (TAMS/CADMUS/Gradient, 1996 - pending publication) show that as much as 60 percent of PCBs in the water column are associated with the particulate phase for tetra- and higher chlorinated congeners.

Because there are no Phase 2 TAMS/Gradient samples for water column invertebrates, and only a few collocated water column sampling stations and ecological survey stations, several approaches were explored to derive relationships that could be used in the food chain model. The approach described below and alternative approaches (Section 10.3.3) are subject to various data limitations and extrapolation problems. As a result, there is considerable uncertainty in the BAFs that relate water column invertebrate body burdens to particulate water column concentrations of PCBs.

The approach selected for deriving BAF values for water column invertebrates relies upon historical data from the New York State Department of Health studies for the Hudson River PCB Reclamation Demonstration Project (Simpson et al., 1986). NYSDOH conducted long- and short-term biomonitoring studies from 1976 to 1985 using caddisfly larvae, multiplate samples and chironomid larvae.

NYSDOH placed artificial substrate samplers (multiplates) along 17 sites for five weeks in the Hudson river from Hudson Falls to Nyack, New York (Novak et al., 1988). Samplers remained in place for five weeks during July through September collecting a composite of sediment, algae, plankton and various macroinvertebrates. After collection, the samplers were analyzed for Aroclors 1016 and 1254. Invertebrates collected on the samplers included: Chironomidae, Oligochaetes, Trichoptera, Ephemeroptera, Amphipoda and Elmidae. Chironomid larvae and pupae were the most abundant invertebrate component from Fort Edward to Saugerties. In addition, caddisfly larvae were hand-picked from rocks at five designated sites: Hudson Falls, Fort Edward, Fort Miller, Stillwater and Waterford.

The short-term biomonitoring study conducted by NYSDOH involved the chironomid larvae, *Chironomus tentans*. Twenty-five laboratory-raised chironomid larvae in nylon mesh packets were placed, in groups of ten, in steel mesh baskets at four Hudson River locations (one at Bakers Falls, two at Thompson Island Pool, and one at Fish Creek). One set of packets was exposed to the sediment at a collection site on the eastern shore of the Thompson Island Pool. The remainder were placed in the water column.

This study showed that the PCB congener pattern in the chironomid tissue differed significantly from the congener pattern observed in the water (TAMS/Gradient, 1991). Other studies have also found this to be the case (Kadlec and Bush 1994). Water column invertebrates respond on the order of days to changes in water column concentrations of PCBs. Novak (1984) found that chironomids exposed to the water column show concentrations 10^5 times higher than water concentrations within 96 hours. The data show that concentrations in water column invertebrates represent the first important link in the biomagnification of PCBs along the aquatic food chain.

Other studies have shown that kinetic processes are significant even before this stage of the food web (Skoglund et al., 1996). In a model developed for the Great Lakes, Skoglund found that phytoplankton accumulate more PCB than would be predicted by equilibrium partitioning alone. Under low growth conditions, the kinetic model and the equilibrium model results were similar. However, during periods of intense growth, the equilibrium model did not fit the observed data as well as the kinetic model.

The NYSDOH multiplate samples represent the only Hudson River specific information available on the relationship between water column invertebrates and water column concentrations. Under the assumption that the majority of water column PCBs are associated with organic rich particles, we evaluated the relationship of water column invertebrates to the particulate phase in the water column as:

$$BAF_{\text{water}} = C_{\text{invert}}/C_{\text{oc}}$$

where,

BAF_{water} = The bioaccumulation factor between water column invertebrates and particulate bound PCB

C_{invert} = mg PCB per Kg lipid in invertebrate tissue

C_{oc} = mg PCB per Kg organic carbon in suspended particulates.

The equation describes the relationship between individual multiplate biological species and the water column, providing an indication as to how much PCB associated with the organic fraction of the particulate in the water column is likely to partition into the lipid of individual species. To define the relationship between PCB and organic carbon associated with the particulate matter in the water column, the following equation was used:

$$C_{\text{oc}} = C_{\text{solid}} * \text{TSS/POC}$$

where,

C_{oc} = mg PCB per Kg organic carbon in suspended particulates

C_{solid} = mg PCB per Kg solid on multiplate sampler from NYSDOH

TSS = Total Suspended Solids in Kg/l (from TAMS/Gradient Phase 2)

POC = particulate organic carbon in Kg/l (from TAMS/Gradient Phase 2).

Note that TSS and POC were not synoptically measured with C_{solid} . The derivation of a BAF described above, assumes that the relationship between TSS and POC is relatively consistent over time for a given river segment. The average summer TSS and POC measurements were taken from the TAMS/Gradient Phase 2 dataset and paired by location to the C_{solid} found on the multiplate samples from the NYSDOH study.

The NYSDOH data are not available on a congener basis. The long-term monitoring data only provide information on Aroclor 1016 and Aroclor 1254, and total PCBs. The values derived for total PCBs can be used in the model for totals and Aroclors but do not represent individual congeners. Further analysis is required to obtain values of individual congeners. The short-term studies address uptake of specific congeners, but cannot be used in this analysis, as they reflect uptake responses on the order of 48-96 hours, rather than quasi-steady state conditions.

10.3.2 Calculation of BAF_{water} for Water Column Invertebrates

The BAF_{water} between PCB concentrations in individual species from NYSDOH multiplate samples and the mg PCB per kg organic carbon associated with particulate matter in the water column is shown in Table 10-2 for Aroclor 1016, Table 10-3 for Aroclor 1254 and Table 10-4 for total PCBs. Figures 10-41 through 10-43 show the distributional analysis conducted for these data. Distribution fitting was done using Crystal Ball 4.0 for Excel. The data for each Aroclor and total PCBs are matched against a number of known distributions and goodness-of-fit tests conducted using appropriate statistical techniques. The most commonly used tests include Chi-square, Kolmogorov-Smirnov, and Anderson-Darling, but each test may not be appropriate for all distributions. In this case, the results from the Kolmogorov-Smirnov and Anderson-Darling tests are more important to consider, since these tests are more appropriate for data that are asymptotically sensitive, or require a close fit at the tails (Madansky, 1988). Results were compared for all tests as described next.

The Chi-square test breaks the observed distribution down into areas of equal probability and compares the individual data points within each area to the number of expected data points. A p-value of 0.5 or greater generally indicates a close fit when using this test. The Kolmogorov-Smirnov and Anderson-Darling tests weight

the observed and theoretical distributions greater at the tails than at the midranges. A value of less than 0.03 for Kolmogorov-Smirnov and a value of less than 1.5 for Anderson-Darling generally indicate a close fit for the particular distribution.

Figure 10-41 presents the results of the distributional analysis for Aroclor 1016. Values range from slightly above zero to 56. Page 2 of Figure 10-41 shows the calculated percentiles. The widest range of BAF are found between the 90th and 100th percentiles, indicating that only 10 percent of the modeled population experience these higher BAFs. The best fit for a distribution for these data, although they appear lognormal, is actually an extreme value distribution. The Chi-square for the extreme value fit was 10.2 with a *p-value* of 0.68, Kolmogorov-Smirnov was 0.04 and Anderson-Darling was 1.29.

Figure 10-42 presents the results of the distributional analysis conducted for Aroclor 1254. The percentiles calculated for Aroclor 1254 are similar to those for Aroclor 1016 except that the maximum observed BAF for Aroclor 1254 is 70. The best distributional fit for Aroclor 1254 is the Weibull distribution, showing a Chi-square of 20.14 and a *p-value* of 0.13, Kolmogorov-Smirnov is 0.06 and Anderson-Darling was 0.71.

Figure 10-43 presents the results of the distributional analysis conducted for total PCBs. The calculated percentiles ranges from slightly above zero to 58, with the greatest range of BAF between the 90th and 100th percentiles. Goodness-of-fit tests showed that the best distributional fit was the beta distribution with a Chi-square of 15.3 and a *p-value* of 0.429, Kolmogorov-Smirnov was 0.05 and Anderson-Darling was 1.01.

The distributions of bioaccumulation factors for the accumulation of particulate organic carbon normalized PCB water concentrations to water column invertebrates all show similarly elongated right tails, with the greatest spread in accumulation factors between the 90th and 100th percentiles. Only 10% of the population is expected to experience the range of accumulation factors between the 90th and 100th percentiles. The maximum observed BAF was used to truncate each of the distributions described above so that no water column invertebrates accumulated PCBs at greater than the observed maximum. These BAFs are used to model the accumulation of particulate organic carbon normalized PCB water concentrations to water column invertebrates for Aroclors 1016 and 1254, and total PCBs.

10.3.3 Alternative Approaches

Several alternative approaches are being considered to evaluate the BAFs developed in this study. These will be explored further in the next phase but are summarized briefly below. Because there are no data suitable for model validation,

it will be important to evaluate other approaches to quantifying this compartment in the model.

Alternative Approach 1: Oliver and Niimi (1988)

Oliver and Niimi (1988) conducted bioaccumulation field studies in Lake Michigan. They evaluated field results for an aquatic food web on a congener-specific basis, a portion of which may provide useful information for this model compartment. They provide BAFs for whole water to zooplankton and zooplankton to a common water column invertebrate, *Mysis relicta*. They also provide measured suspended sediment values, although they do not provide an indication of the fraction organic carbon. However, "...material in the water column is mainly resuspended bottom sediment...", so it may be possible to use the measured TOC in bottom sediments as a surrogate value.

Oliver & Niimi (1988) estimated BAFs ranging from 2 to greater than 14 on a lipid-normalized basis for individual congeners from total water to plankton. Derived ratios from plankton to mysids ranged from 1 to 10 on a lipid-normalized basis for individual congeners.

The whole water zooplankton BAF may provide enough information on the expected concentration in water column invertebrates. However, the data in Oliver and Niimi (1988) are presented as arithmetic averages and standard deviations, rather than log-space statistics required by the probabilistic model. Given the lognormal distribution of the underlying data, the BAFs predicted by Oliver and Niimi (1988) would tend to overpredict the geometric means utilized in the probabilistic model.

Alternative Approach 2: Great Lake Initiative (GLI) BAF

The Great Lake Water Quality Initiative Technical Support Document provides a procedure for determining bioaccumulation factors in four trophic levels: phytoplankton, zooplankton, small fish and top predator fish. The approach relies on the BAF equation provided in Oliver and Niimi (1988) divided by a laboratory-measured BCF for each trophic level. The result is a food chain multiplier based on the Log K_{ow} of the contaminant in question. For Level 2, zooplankton, food chain multipliers for contaminants with Log K_{ow} greater than 6.5 can range from 0.1 to 19.

Alternative Approach 3: Bivariate Statistical Analyses (Section 9)

Section 9 provides the results of statistical analyses conducted for the NYSDEC fish monitoring results on an Aroclor basis. This section provides BAFs for several fish species, including pumpkinseed, a common forage fish. Embedded in this value is the BAF from water to water column invertebrates, and from water column invertebrates to fish. By combining the information from these analyses

with information derived by comparing pumpkinseed concentrations to those found on the NYSDOH multiplate samplers, it may be possible to disaggregate the relative contribution of the water column to water column invertebrates.

Alternative Approach 4: Flow-Averaged Summer Concentrations to Benthic Chironomids

As discussed in Section 10.2, benthos-associated chironomid show significantly higher PCB concentrations, particularly for the lower chlorinated congeners, than do the remaining benthic invertebrates. It is likely that some, if not all, benthic invertebrates are experiencing potential exposure from water as well as sediment, especially in areas such as Thompson Island Pool. One approach involves considering the BAF from summer flow-averaged total water concentrations to certain benthic invertebrate species, particularly chironomid. The dataset for this approach is limited, and is therefore restricted by small sample sizes. However, an exploratory analysis is included as part of future modeling work (Appendix B).

Alternative Approach 5: Sediment Pore Water to Benthos as a Surrogate for Whole Water to Water Column Invertebrates

This approach involves evaluating the relationship between estimated pore water and benthic invertebrates. It may be that this relationship is indicative of the relationship between whole water column concentrations and invertebrates. This approach requires equilibrium assumptions between PCBs and sediments as generally derived for nonionic organic compounds (e.g. Shea, 1988).

Alternative Approach 6: Evaluating Other Modeling Approaches

Skoglund (1996) recently developed a kinetic accumulation model for PCBs based on data collected from Green Bay, Lake Michigan. Although data from other systems may not be indicative of conditions in the Hudson River, the general dynamics that have been observed in these datasets may provide useful insight into mechanistic processes in the Hudson. One of the most important aspects revealed by the work of Skoglund et al., is that an equilibrium model significantly underestimates observed accumulation. This provides further evidence that significant accumulation occurs at the low end of the food web. The data used in the development of the Skoglund model have been made available and exploratory analyses are included in the plans for future modeling work (Appendix B).

10.4 Forage Fish:Diet Accumulation Factors (FFBAFs)

As discussed in Section 8 and Appendix A, forage fish are treated as a single compartment that reflects the composition and feeding habits of species in the Hudson. As a group, forage fish are expected to have a diet that varies depending on the data available for that given river mile. Individual forage fish will vary from

this percentage. For example, spottail shiners are expected to feed evenly on water column and benthic invertebrates, while pumpkinseed favor water column food sources. An appropriate weighted mean was used in the model depending on the specific species caught at a sampling location. The approach used to develop FFBAFs for forage fish is described below.

Note that there is an important distinction between model development and model implementation. In model development, the full BSAF and BAF distributions are used to estimate the range of expected PCB concentrations in the forage fish diet. The ratio of individual measured forage fish concentrations to the mean expected concentration in the diet (by sampling location) represents the distribution of forage fish bioaccumulation factors. However, in model implementation, the mean and associated standard error are used to represent the distributions derived through model development.

10.4.1 Approach

Forage fish consume both water column and benthic invertebrates. As a result, their dietary exposure to PCBs is represented as a weighted average of the PCB concentration in the diet. Distributions in the FFBAF are derived from measured concentrations of PCBs in forage fish at a river mile divided by the estimated concentrations in their diet. The distributions for the benthic invertebrate and water column invertebrate compartments discussed earlier were used to estimate concentrations in those compartments. Due to the lack of information regarding congener-specific uptake into the water column invertebrate compartment, which comprises a significant portion of forage fish food, only distributions for Aroclors 1016 and 1254 and total PCBs could be derived.

FFBAF values were derived by:

1. Evaluating the available data for forage fish <10 cm for each river mile. Determining feeding preferences for use in the model based on typical species composition at a given river mile combined with abundance data for the Hudson River (Appendix A).
2. Plotting concentrations to identify a) which species contribute most to data variability and b) which river miles show the greatest uncertainty and variability in observed concentrations.
3. Estimating the expected PCB concentrations in benthic invertebrates and water column invertebrates for Aroclors 1016 and 1254 and total PCBs using the distributions described earlier in this section. A congener-specific analysis is still pending based on the results from the water column invertebrate box.

4. Deriving a river-wide distribution of FFBAF by taking the ratio of a measured individual forage fish concentration to the geometric mean dietary concentration. The mean diet is represented by the weighted average of the benthic invertebrate (measured) and water column invertebrate (estimated) compartments.

The method provides a basis for deriving FFBAF values for forage fish as a group as well as for the selected fish species, spottail shiner and adult pumpkinseed sunfish. The Phase 2 data were not adequate for estimating FFBAF values for small pumpkinseed sunfish that may be eaten by other fish species. Other approaches for pumpkinseed are discussed in subsequent sections.

10.4.2 Water Column Concentrations Used to Derive FFBAF Values

Because forage fish feed on water column invertebrates and because there are no synoptic data for these invertebrates in the Phase 2 dataset, body burdens for the invertebrates were estimated from water column measurements and the BAF_{water} distribution relating invertebrates to water as discussed in Section 10.3. A summer average particulate water concentration was used for a given river reach, normalized to fraction organic carbon.

The fraction organic carbon associated with the particulate matter in the water column is described as:

$$FOC = 0.611 \times WLOI@375^{\circ}$$

where,

FOC = fraction organic carbon

0.611 = constant from the Data Evaluation and Interpretation Report (TAMS/CADMUS/Gradient, 1996 - pending publication)

$WLOI$ = weight-loss-on-ignition from TAMS/Gradient Phase 2 dataset

10.4.3 Forage Fish Body Burdens Used to Derive FFBAF Values

Bar charts were developed to show lipid-normalized concentrations in forage fish by river mile. Two charts were prepared for each of the individual congeners, Aroclors 1016 and 1254, and for total PCBs. The boxplots present the average and 50% of observed values contained within each box. The lines extending from the boxes show the upper and lower values with extreme values shown as asterisks and identified by species. Extreme values are those values more than 1.5 times outside the interquartile range represented by the box. The mean forage fish concentration by river mile charts show mean concentrations (all species combined) within an error bar indicating plus and minus one standard error of the mean. The

standard error provides information on how confident one is about the mean estimate.

In general, concentrations show far less variability in the lower river than in the upper river. As a trend, concentrations relatively steadily decline from river mile 169.5 down to 88.9. At river mile 58.7, a slight increase is seen. Within the upper river, concentrations are highest at river mile 189.5. River mile 191.5 shows lower concentrations than river miles 194.1 or 189.5, probably as a result of the specific location chosen for sampling. However, these data show that PCB body burdens in forage fish are highly variable in the Thompson Island Pool area and areas close to sources of PCBs. Forage fish body burdens may also reflect the sediment type of the habitat (i.e. fine-grain sediments tend to accumulate higher levels of PCBs).

Forage Fish Body Burden Data for BZ#4

Figure 10-44 shows that the concentrations of BZ#4 in forage fish do not display much variability from river mile 169.5 on down the river. However, sample sizes were smaller than for the upper river. The upper river, by contrast, displays greater variability in BZ#4 concentrations. Maximum observed concentrations at river miles 189.5 and 194.1 are in the tessellated darter. Figure 10-45 shows that the concentrations of BZ#4 at most river miles ranged from just above 0 to about 5 ug/g. Three river miles had considerably higher means, with wider error bars: River mile 194.1, with a mean just over 20 ug/g, river mile 189.5, with a mean of approximately 18 ug/g, and river mile 191.5, with a mean of 8 ug/g.

Forage Fish Body Burden Data for BZ#28

Figure 10-46 shows that the concentrations of BZ#28 in forage fish are most variable between river miles 189.5 and 194.1. Tessellated darters and spottail shiners represent the species with the highest observed concentrations. Figure 10-47 shows that concentrations at most river miles ranged from just above 0 to just under 20, with narrow error bars. Concentrations at river miles 194.1 and 189.5 were considerably higher, about 80 and 100 ug/g, respectively, with wide error bars, indicating uncertainty in the mean estimate.

Forage Fish Body Burden Data for BZ#52

Figure 10-48 shows that the concentrations of BZ#52 are most variable between river miles 189.5 and 194.1. Tessellated darters and spottail shiners represent the species with the highest observed concentrations. BZ#52 concentrations for most of the river miles range from just above 0 to 20 ug/g. Higher concentrations (around 80 ug/g) and wider error bars are shown for river miles 194.1 and 189.5. A somewhat higher mean concentration (about 40 ug/g) was also shown for river mile 191.5.

Forage Fish Body Burden Data for BZ#101 with BZ#90

Figure 10-50 shows that river miles 189.5 through 194.1 display the greatest variability in forage fish body burdens, with one spottail shiner at river mile 194.1 exceeding the mean by almost a factor of 5. Figure 10-51 shows that forage fish concentrations at most of the river miles ranged from just above 0 to about 15, with narrow error bars. Again, Thompson Island Pool and the area closest to PCB sources, river miles 189.5 through 194.1, show much higher concentrations, with wider error bars.

Forage Fish Body Burden Data for BZ#138

Figure 10-52 shows that PCB concentrations display the greatest variability within the Thompson Island Pool. Figure 10-53 shows that forage fish concentrations at most of the river miles ranged from just above 0 to about 10 ug/g. Thompson Island Pool shows much higher concentrations, with wider error bars.

Forage Fish Body Burden Data for Aroclor 1016

Figure 10-54 presents the boxplots for Aroclor 1016. Individual tessellated darters and spottail shiners show higher concentrations than the remaining fish within the Thompson Island Pool. From river mile 169.5 on down the river, concentrations are tight and steadily decreasing. Figure 10-55 shows that the mean estimates from river mile 169.5 on down the river show narrow error bars, but there is less confidence in the mean estimates for river miles 189.5 and 194.1.

Forage Fish Body Burden Data for Aroclor 1254

Figure 10-56 provides boxplots for Aroclor 1254. High concentrations are observed in individual tessellated darters and spottail shiners. These high concentrations contribute to the wide error bars on the means calculated for river miles 189.5 and 194.1, as presented in Figure 10-57.

Forage Fish Body Burden Data for Total PCBs

Figure 10-58 shows that mean concentrations are similar for river miles 189.5 and 194.1, and significantly higher at these locations than elsewhere in the river. Figure 10-59 shows that forage fish Total PCB concentrations at most of the river miles ranged from just above 0 to about 300 ug/g.

10.4.4 Calculation of FFBAF Values for Forage Fish

The body burden data provide important information on the expected variability in forage fish concentrations. The data show that the greatest variability in fish concentrations exists within the Thompson Island Pool and areas closest to the source of PCBs. This is also the area showing greatest sediment concentration heterogeneity, and an analysis of the water column data show that water column concentrations vary significantly depending on the time of year. Fish in this area experience transient exposures and integrate both "hot spots" and less contaminated area exposures.

The forage fish model was run for Aroclors 1016, 1254, and total PCBs to evaluate the goodness-of-fit between observed and modeled fish body burdens. As described in Appendix A, the expected contribution of benthic and water column invertebrates was estimated based on the forage fish data available for each river mile. For example, there are a number of river miles for which forage fish concentrations are represented by spottail shiners. Data show that spottail shiners consume relatively equal amounts of benthic and water column invertebrates. Other river miles have a number of forage fish species represented, and accordingly a weighted mean was used to estimate an overall feeding preference by river mile. The next phase of work will focus on model verification through a comparative analysis with the Gobas model.

The model calculated 10th, 25th, 50th, 75th, and 90th percentiles as well as a maximum. Percentiles were calculated from the observed forage fish distribution at each river mile using the SPSS™ software package. The modeled concentrations of PCBs in forage fish follow a lognormal distribution, characterized by long right tails. After log-transforming the fish concentration percentiles (both observed and modeled), the observed percentiles were plotted against the model-generated percentiles. This plot is shown in Figure 10-60 for Aroclor 1016, Figure 10-61 for Aroclor 1254, and Figure 10-62 for total PCBs. The center line represents the regression equation with 95% confidence limits. A second set of figures presents individual forage fish observations with modeled output superimposed. These data are presented by river mile, and note that each river mile has anywhere from 3 to 15 individual data points (see Figures 10-54 through 10-59 for the *n* at each river mile).

Figure 10-63 shows individual observed forage fish concentrations at each river mile with the 50th and 90th calculated percentile values from the model. At river mile 194.1, the model 90th percentile estimate exceeds the maximum observed concentration. At river mile 169.5, the 90th percentile calculated from the model falls within the range of the maximum observed forage fish concentrations. In the lower river, the 50th percentile concentrations match the observed values best, while the 90th percentile estimates exceed the maximum observed forage fish concentrations.

Figure 10-64 presents the individual observed forage fish concentrations by river mile ("measured" line) with model outputs superimposed. In the lower river, the modeled 50th percentile represents the most accurate descriptor of observed forage fish concentrations. Due to the variability in the upper river, the 90th percentile modeled output captures most of the observed variability, and the maximum modeled output is high (*i.e.*, 100% of observations are significantly less than predicted).

Figure 10-65 presents the results for total PCBs. Individual observed forage fish concentrations are represented by a dashed line, with modeled outputs superimposed. Again, the modeled maximum exceeds the observed maximum in every instance except one observation at river mile 189.5. The modeled 50th percentile represents the closest fit in most portions of the river.

One of the goals of the probabilistic model is to predict a high-end exposure (*i.e.*, 90% or 100% of the population will experience PCB body burdens at this level). It is important to capture information about the variability of fish concentrations, particularly in the Thompson Island Pool area, in order to more effectively reach management decisions. In areas where variability dominates, the ability to make predictions is confounded. The next phase of this analysis will focus on validating the model through hindcasting and by using recently-collected NYSDEC data that were not used in model development.

10.4.5 Calculation of FFBAFs for Small Pumpkinseed Sunfish

Knowing that pumpkinseed, for example, consume primarily water column invertebrates (Appendix A), the TAMS/Gradient team explored this relationship further. The Phase 2 dataset did not contain many data for pumpkinseed around the 10cm size range, so the NYSDEC data were explored in more detail. Individual pumpkinseed (less than 10 cm) concentrations were compared to the NYSDOH lipid-normalized multiplate data. Multiplate data are available for July and August of a given year while the pumpkinseed were sampled in September. The average multiplate concentration was used as a dietary concentration for pumpkinseed. River Mile 175 (Stillwater) provided the best available dataset. These data are shown in Table 10-5 for Aroclor 1016, Table 10-6 for Aroclor 1254 and 10-7 for total PCBs. These FFBAF values are significantly less than the FFBAF values estimated from the model. This may indicate that the BAF_{water} used to estimate water column invertebrate concentrations in the model is too low and that the bulk of the bioaccumulation occurs already in the water column to water column invertebrate step.

The next phase of this analysis will be to evaluate the distribution between pumpkinseed and the multiplate samplers in more detail.

10.5 Piscivorous Fish:Diet Accumulation Factors (PFBAF)

The Phase 2 dataset imposes limitations on these analyses. There are very few data available for large (greater than 150 cm) piscivorous fish, notably largemouth bass. In fact, yellow perch is one of the only semi-piscivorous fish in the correct size range. In order to demonstrate the method, PFBAF derived through the Phase 2 dataset have been explored using yellow perch. Largemouth bass are discussed in Section 10.5.2.

10.5.1 Approach Used for Yellow Perch

Only larger yellow perch were selected for analysis (greater than 150 cm). This species consumes a small percentage of forage fish (between 10 and 15 percent of its diet), the balance comprised of invertebrates. The PFBAFs for yellow perch were derived as follows:

1. Determine weighted average dietary contribution to yellow perch. This is estimated to be 15 percent forage fish, 20 percent benthic invertebrates, and 65 percent water column invertebrates. These proportions are being evaluated in a sensitivity analysis to determine the impact of changing feeding preferences.
2. Estimate the expected yellow perch accumulation factors by dividing the measured individual yellow perch concentrations by the mean dietary concentrations. The mean dietary concentration is calculated using the percentages shown in step 1 as applied to the measured geometric mean concentration for each compartment (except for water column invertebrates, for which there are no measured data).

Figure 10-66 shows the distribution of PFBAF values for yellow perch for total PCBs. Figure 10-67 shows the predicted distribution of yellow perch concentrations based on these bioaccumulation factors. The results are presented here primarily as a demonstration of the method.

10.5.2 Approach Used for Largemouth Bass

In the TAMS/Gradient Phase 2 dataset, there were no data available for largemouth bass of the correct size (all samples were for largemouth bass less than 16 cm). Largemouth bass do not become piscivorous until at least 20 cm. At the small sizes of the largemouth bass in the Phase 2 dataset, the largemouth bass display feeding patterns equivalent to a typical forage fish, such as pumpkinseed. Therefore, analysis for largemouth bass has to rely on the data from the Phase I NYSDEC dataset. In the absence of suitable Phase 2 data, a preliminary analysis was made relating largemouth bass lipid-normalized concentrations to pumpkinseed lipid-normalized concentrations for measurements reported as Aroclors 1016 and 1254.

Largemouth Bass to Pumpkinseed BAF for Aroclor 1016

Figure 10-68 shows the ratio of largemouth bass greater than 25 cm to pumpkinseed less than 10 cm for Aroclor 1016 by river mile and year. The ratios range from less than one to nearly four, showing a fairly consistent and tight relationship. Pumpkinseed derive between 80 and 90 percent of their PCB body burden from water column sources. Largemouth bass are also closely tied to the water column, and the bivariate statistical analysis of the same dataset showed that largemouth bass are 91 percent explained by the water column.

Largemouth Bass to Pumpkinseed BAF for Aroclor 1254

Figure 10-69 shows the ratio of largemouth bass greater than 25 cm to pumpkinseed less than 10 cm for Aroclor 1254 by river mile and year. These ratios display greater variability than do the ratios for Aroclor 1016. They range from 1 to almost 15, with outliers up to 22. Generally, however, the ratios are near 5, consistent with data from other studies.

Largemouth Bass to Pumpkinseed BAF for Total PCBs

Figure 10-70 shows the ratio of largemouth bass greater than 25 cm to pumpkinseed less than 10 cm for total PCBs by river mile and year. These ratios are similar to those derived for Aroclor 1254, but show lower standard errors and fewer outliers. The range is generally from 1 to 5, except for River Mile 190 during 1990.

Additional Analyses for Largemouth Bass

Additional work is underway to define the relationships between largemouth bass body burdens and their diet. The distributions derived above will be explored in greater detail, and the model will be used to "predict" 1995 data collected by NYSDEC. The use of the Gobas (1993) model is also being explored, as it has been shown that the dynamics of digestion and gastrointestinal absorption may play the most important role in determining PCB body burdens in piscivorous fish.

10.5.3 Approach Used for White Perch

The available white perch data are only for river miles where there are no corresponding water column data. White perch, as described in the fish profiles, tend to exhibit a diet that is 50 percent sediment sources and 50 percent water column sources. Therefore, the necessity for initial water column concentrations precluded a detailed analysis of white perch using the Phase 2 dataset. Work is still underway on the white perch bioaccumulation model and no results are presented in this report.

10.6 Demersal Fish:Sediment Relationships

10.6.1 Approach and Calculations of BAF Values

Brown bullhead accumulation factors were calculated by two methods:

1. Individual brown bullhead PCB concentrations were compared to the geometric mean sediment concentrations at a given river mile;
2. Individual brown bullhead concentrations were compared to the geometric mean benthic invertebrate concentrations at a given river mile.

Table 10-8 shows these results. There are only four individual brown bullhead samples available from the Phase 2 dataset, making detailed statistical analysis of the distribution difficult. The next phase of work will focus on incorporating data from other sources in more accurately defining the distribution, and using NYSDEC data for validation.

10.7 Summary of Probabilistic Food Chain Models

Probabilistic food chain models have or are being developed for six fish species. This work is still in progress. In addition, the models that have been developed are being reviewed and modified on an on-going basis. This report provides an overview of the general structure of the models but should not be considered to reflect the final structure. The models are being used to explore the relationships within the food web in the Hudson River and to evaluate data variability. The status of the food chain models at this writing (August, 1996) is as follows:

Fish Species	Status of Model/Future Work
Spottail Shiner	Model complete for total PCBs and Aroclors 1016 and 1254; next steps involve comparing model outputs to historical data for total PCBs; these results may be used to further tune the model; additional work is required to use the model for individual congeners
Pumpkinseed	Model development is continuing; data issues still need to be resolved
Brown Bullhead	Model complete for total PCBs and congeners; next steps involve comparing model outputs to historical data for total PCBs; these results may be used to further tune the model
Yellow Perch	Model complete for total PCBs; a sensitivity analysis is being performed with regard to effects of different dietary assumptions; next steps include comparing model outputs to historical data for total PCBs; these results may be used to further tune the model; additional work is required to use the model for specific Aroclors and congeners
Largemouth Bass	Preliminary model has been developed for Aroclors and total PCBs; next steps involve comparing model outputs to historical data; these results may be used to further tune the model; data are not sufficient for constructing a model for specific congeners
White Perch	Work has begun on this model but there are a number of data issues still to be resolved

10.8 Illustration of Food Chain Model Application

The yellow perch model has been run under a set of assumptions to illustrate one form in which output would be provided. It should be noted that the model output is for illustrative purposes and that the model is not in final form. All results are based on unvalidated data.

An example of a model run is given in Figure 10-71, the report generated from a Monte Carlo run of the model in Crystal Ball. This model run has taken as input an average water and sediment concentration. The report illustrates the various transfer steps in the process as distributions. Note that because forage fish and yellow perch body burdens will reflect the result of an "average" diet, mean BAF values and associated standard errors of the means are used to represent transfers among the food chain components. Resulting PCB body burdens (on a lipid normalized basis) are represented as a full distribution. The model can also provide output on a whole body or fillet basis but these are not included with the example run.

One way in which the model can be used is to generate look-up tables or nomographs for various combinations of water and sediment PCB levels. The model is run for combinations of water and sediment concentrations (yielding output similar to that shown in Figure 10-71 for each run) and the percentiles extracted from the model output. The result is a look-up table such as presented in Tables 10-9 through 10-12. These tables provide look-up tables for the 15th percentile, the average, the 75th percentile, and the 95th percentile. These look up tables can then be linked with the output of the HUDTOX model. Other percentiles of interest to human health and ecological risk assessors or of regulatory interest could also be specified. The model can be used to identify the fraction of the population expected to fall above or below a selected concentration.

The look-up tables will provide information on how different sediment:water exposure concentrations impact fish body burdens under a specific set of feeding assumptions. Sensitivity analyses are included as part of the future modeling work (Appendix B). These analyses will evaluate the relative contributions of sediment and water exposure pathways.

10.9 Comparison of Bivariate Statistical and Food Chain Models

The Bivariate Statistical Model has been applied to the historical dataset of Aroclors 1016 and 1254 while the food chain models have been applied primarily to the TAMS Phase 2 data. While it is planned to run the food chain models for the historical dataset, this has not yet been done. It is possible to compare the models in terms of the degree to which PCB body burdens are related to water and sediment exposures as well as the general magnitudes of total uptake.

The models have been applied, in common, to three species: yellow perch, largemouth bass, and brown bullhead. The relative contributions of water and sediments to the body burdens of these species is summarized below. It should be noted that sediments and water concentrations are related and that the comparisons reflect the predominance of particular exposure pathways rather than the importance of particular sources.

Fish Species	Bivariate Statistical Model	Probabilistic Food Chain Model
Pumpkinseed Sunfish	Aroclor 1016 61% water 39% sediment Aroclor 1254 72% water 28% sediment	Modeling has not been completed. Dietary analysis (Appendix A) indicates the species feeds 80% in water column and 20% from sediment
Yellow Perch	Aroclor 1016 84% water 16% sediment Aroclor 1254 81% water 19% sediment	Water contributes 18 to 40% under one set of assumptions and 67 to 90% under another set of assumptions; model is being evaluated to determine which combination is more likely
Largemouth Bass	Aroclor 1016 88% water 12% sediment Aroclor 1254 42% water 58% sediment	Water contributes 49 to 80%
Brown Bullhead	Aroclor 1016 73% water 27% sediment Aroclor 1254 14% water 86% sediment	Sediment is considered to represent 100% of the source

A comparison of the two models reveals some similarities and some differences. Both models indicate the importance of water exposure pathways for the pumpkinseed and the yellow perch (under a specific set of assumptions about feeding). Both species rely upon water column invertebrates as a large fraction of their diets.

In the case of largemouth bass, the Bivariate Statistical Model suggests that water was more important for Aroclor 1016 (91%) and sediment was more important for Aroclor 1254 (56%). In comparison, the Probabilistic Food Chain Model suggests that water contributes 49 to 80% of the total PCB body burden. The importance of a sediment component in both models - as compared to yellow perch and pumpkinseed - indicates that they may be reflecting a common exposure pathway. Based on the food chain model, this reflects a higher percentage of forage fish in the diet of largemouth bass combined with a high percentage of benthic invertebrates.

The two models show similarities and differences for the brown bullhead. The Bivariate Model indicates that water is the major source for Aroclor 1016 and sediment the major source for Aroclor 1254. The food chain model is based on a direct relationship between body burdens and either sediments or sediment invertebrates. As a result, brown bullhead body burdens are 100% related to sediments. Because of the differences between the two models, this relationship will be examined further by applying the food chain model to the dataset used for the Bivariate Model.

The results of the Bivariate Model help to define the dietary contribution from water and sediment pathways. The mean estimates from the Bivariate Model are complemented by the distributional analysis provided by the Probabilistic Model. The Probabilistic Model presents a range of expected concentrations. The mean estimate does not address the likelihood that the majority (or what percentage) of fish will experience that concentration. The Probabilistic Model incorporates the observed variability in the extensive Hudson River dataset to better define the percentage of the population that will be at or below a particular PCB concentration.

REFERENCES

- Achman, D.R., K.C. Hornbuckle, and S.J. Eisenreich. 1993. Volatilization of polychlorinated biphenyls from Green Bay, Lake Michigan. *Environmental Science & Technology*, Vol. 27, No. 1, pp.75- .
- Ambrose, R.B., Jr., T.A. Wool, J.P. Connolly and R.W. Schanz. 1988. WASP4, A hydrodynamic and water quality model - Model theory, user's manual, and programmer's guide. EPA/600/3-87/039. U.S. Environmental Protection Agency, Environmental Research Laboratory, Athens, Georgia.
- Anderson, R.C. and D. Brazo. 1978. Abundance, feeding habits and degree of segregation of the spottail shiner (*Notropis hudsonius*) and longnose dace (*Rhinichthys cataractae*) in a Lake Michigan surge zone near Ludington, Michigan. *Mich. Acad.* 10(3):337-346.
- Ankley, G.T., P.M. Cook, A.R. Carlson, D.J. Call, J.A. Swenson, H.F. Corcoran, and R. A Hoke. 1992. Bioaccumulation of PCBs from sediments by oligochaetes and fishes: comparison of laboratory and field studies. *Can. J. Fish. Aquat. Sci.* 49:2080-2085.
- Barron, M. 1990. Bioconcentration. *Environ. Sci. Technol.* 24:1612-1618.
- Bath, D.W. and J.M. O'Connor. 1982. The biology of the white perch (*Morone Americana*) in the Hudson River estuary. *Fish Bull. U.S.* 80:599-610.
- Bierman, V.J., Jr. 1990. Equilibrium partitioning and biomagnification of organic chemicals in benthic animals. *Environ. Sci. Technol.* 24:1407-1412.
- Bierman, V.J., Jr., J.V. DePinto, T.C. Young, P.W. Rodgers, S.C. Martin and R.K. Raghunathan. 1992. Development and Validation of an Integrated Exposure Model for Toxic Chemicals in Green Bay, Lake Michigan. Report prepared for U.S. Environmental Protection Agency, Grosse Ile, Michigan. Cooperative Agreement CR-814885.
- Bierman, V.J., Jr. 1994. Partitioning of organic chemicals in sediments: Estimation of interstitial concentrations using organism body burdens. Chapter 9 in: *Transport and Transformation of Contaminants Near the Sediment-Water Interface*. (Ed. J.V. DePinto, W. Lick and J.F. Paul) CRC Press, pp. 153-175.
- Biscayne, P.E. and C.R. Olsen. 1976. Suspended particulate concentrations and compositions in the New York bight; proceedings of the symposium, special symposia Vol. 2, Middle Atlantic Continental Shelf and the New York Bight. *American Soc. of Limnology and Oceanography*; pp. 124-137.
- Bopp, R.F. 1979. The geochemistry of polychlorinated biphenyls in the Hudson River. Ph.D. Dissertation, Columbia University. Univ. Micro. Intern. 8008704, 191 pp.

- Bopp, R.F. and H.J. Simpson, 1984. Persistent chlorinated hydrocarbon contaminants in the New York Harbor complex, 1st year final report for Contract HUD 1183-A38, by Lamont-Doherty Geological Observatory of Columbia Univ., submitted to Hudson River Foundation; 6 pp. + extensive tables, figures, app.
- Boreman, J. 1981. "Life Histories of Seven Fish Species that Inhabit the Hudson River Estuary." National Marine Fisheries Service, Woods Hole Laboratory, No. 81-34, October.
- Bowman, M.J. 1977. Hydrographic Properties, MESA, New York Bight ATLAS Monograph 1. NY Sea Grant Institute, Albany, N.Y.; 78 pp.
- Brown, M.P., M.B. Werner, R.J. Sloan, and K.W. Simpson. 1985. Polychlorinated biphenyls in the Hudson River, recent trends in the distribution of PCBs in water, sediment and fish. *Environmental Science and Technology* 19(8):656-661.
- Buckley, J. and B. Kynard. 1981. Spawning and rearing of shortnose sturgeon from the Connecticut River. *Prog. Fish-Cult.* 43:74-76.
- Bush, B., S. Dzurica, L. Wood, and E.C. Madrigal. 1994. Sampling the Hudson River Estuary for PCBs using multiplate artificial substrate samplers and congener-specific gas chromatography in 1991. *Environmental Toxicology and Chemistry*, 13(8):1259-1272.
- Butcher, J.B. 1993. Flood frequency analysis, Fort Edward at Roger's Island Gage, Hudson River. Memorandum on Revised Log Pearson Flood Frequency Analysis.
- Carlson, D.M. 1986. "Fish and Their Habitats in the Upper Hudson Estuary." Region 4 Fisheries, Stamford, New York, November.
- Carlson, D.M. 1992. Importance of wintering refugia to the largemouth bass fishery in the Hudson River Estuary. *Journal of Freshwater Ecology* 7:173-180.
- Chiou, C.T. 1985. Partition coefficients of organic compounds in lipid-water systems and correlations with fish bioconcentration. *Environ. Sci. Technol.* 19:57-62.
- Chow, V.T. 1960. Open-Channel Flow. McGraw-Hill. New York, New York.
- Clayton, J.R., S.P. Pavlou, and N.F. Brietner. 1977. Polychlorinated biphenyls in coastal marine zooplankton: bioaccumulation by equilibrium partitioning. *Environ. Sci. Technol.* 11:676
- Cohn, T.A., L.L. DeLong, E.J. Gilroy, R.M.Hirsch, and D.K. Wells. 1989. Estimating constituent loads. *Water Resources Research.* 25(5):937-942.
- Cole, J.J., N.F. Caraco and B.L. Peierls. 1992. Can phytoplankton maintain a positive carbon balance in a turbid, freshwater, tidal estuary?. *Limnology and Oceanography* 37(8):1608-1617.
- Connolly, J.P. and R. Tonelli, 1985. Modelling Kepone in the striped bass food chain of the James River estuary. *Estuarine, Coastal and Shelf Science* 20:349-366.

Connolly, J.P., R.P. Winfield, and J.R. Blasland. NO DATE. "Application of a Food Chain Model of PCB Accumulation to the Striped Bass of the Hudson Estuary." Report to the Hudson River Foundation. 35 pp.

Cook, L. 1994. Usability of Phase 2 and GE Results for BZ#4, BZ#28, BZ#52, BZ#101, BZ#138 and Total PCBs. Technical Memorandum dated November 8, 1994. Gradient Corporation.

Crance, J.H. 1986. Habitat suitability index models and instream flow suitability curves: shortnose sturgeon. U.S. Fish Wildl. Serv. Biol. Rep. S2(10.129) 31 pp.

DiToro, D.M. 1985. A particle interaction model of reversible organic chemical sorption. *Chemosphere* 14(10):1503-1138.

DiToro, D.M. and J.J. Fitzpatrick. 1993. Chesapeake Bay Sediment Flux Model. U.S. Army Corps of Engineers, Waterways Experiment Station, Vicksburg, Mississippi. Contract Report EL-93-June 1993.

Di Toro, D.M., C.S. Zarba, D.J. Hansen, W.J. Berry, R.C. Swartz, C.E. Cowan, S.P. Pavlou, H.E. Allen, N.A. Thomas, and P.R. Paquin. 1991. Technical basis for establishing sediment quality criteria for nonionic organic chemicals using equilibrium partitioning. *Environmental Toxicology and Chemistry* 10(12):1541-1583.

Domermuth, R.B. and R.J. Reed. 1980. Food of juvenile American shad (*Alosa sapidissima*), juvenile blueback herring (*Alosa aestivalis*) and pumpkinseed (*Lepomis gibbosus*) in the Connecticut River below Holyoke Dam, Massachusetts. *Estuaries* 3:65-68.

Dovel, W.L. 1992. Movements of immature striped bass in the Hudson Estuary. In *Estuarine Research in the 1980s: The Hudson River Environmental Society Seventh Symposium on Hudson River Ecology* (Ed: C.L. Smith) State University of New York Press, pp. 276-300.

Dovel, W.L., A.W. Pekovitch, and T.J. Bergren. 1992. Biology of the shortnose sturgeon (*Acipenser brevirostrum* Lesueur, 1818) in the Hudson River Estuary, New York. In *Estuarine Research in the 1980s: The Hudson River Environmental Society Seventh Symposium on Hudson River Ecology* (Ed: C.L. Smith) State University of New York Press, pp. 187-216.

Eadie, B.J. and J.A. Robbins. 1987. The role of particulate matter in the movement of hydrophobic organic compounds in Great Lakes. In: Advances in Chemistry Series No. 216, Sources and Fates of Aquatic Pollutants. R.A. Hites and S.J. Eisenreich (eds.), American Chemical Society. Chapter 11.

Eadie, B.J., N.R. Morehead and P.F. Landrum. 1990. Three-phase partitioning of hydrophobic organic compounds in Great Lakes waters. *Chemosphere*. 20(1-2):161-178.

- Connolly, J.P., R.P. Winfield, and J.R. Blasland. NO DATE. "Application of a Food Chain Model of PCB Accumulation to the Striped Bass of the Hudson Estuary." Report to the Hudson River Foundation. 35 pp.
- Cook, L. 1994. Usability of Phase 2 and GE Results for BZ#4, BZ#28, BZ#52, BZ#101, BZ#138 and Total PCBs. Technical Memorandum dated November 8, 1994. Gradient Corporation.
- Crance, J.H. 1986, Habitat suitability index models and instream flow suitability curves: shortnose sturgeon. U.S. Fish Wildl. Serv. Biol. Rep. 82(10.129) 31 pp.
- DiToro, D.M. 1985. A particle interaction model of reversible organic chemical sorption. *Chemosphere* 14(10):1503-1138.
- DiToro, D.M. and J.J. Fitzpatrick. 1993. Chesapeake Bay Sediment Flux Model. U.S. Army Corps of Engineers, Waterways Experiment Station, Vicksburg, Mississippi. Contract Report EL-93-June 1993.
- Di Toro, D.M., C.S. Zarba, D.J. Hansen, W.J. Berry, R.C. Swartz, C.E. Cowan, S.P. Pavlou, H.E. Allen, N.A. Thomas, and P.R. Paquin. 1991. Technical basis for establishing sediment quality criteria for nonionic organic chemicals using equilibrium partitioning. *Environmental Toxicology and Chemistry* 10(12):1541-1583.
- Domermuth, R.B. and R.J. Reed. 1980. Food of juvenile American shad (*Alosa sapidissima*), juvenile blueback herring (*Alosa aestivalis*) and pumpkinseed (*Lepomis gibbosus*) in the Connecticut River below Holyoke Dam, Massachusetts. *Estuaries* 3:65-68.
- Dovel, W.L. 1992. Movements of immature striped bass in the Hudson Estuary. In *Estuarine Research in the 1980s: The Hudson River Environmental Society Seventh Symposium on Hudson River Ecology* (Ed: C.L. Smith) State University of New York Press, pp. 276-300.
- Dovel, W.L., A.W. Pekovitch, and T.J. Bergren. 1992. Biology of the shortnose sturgeon (*Acipenser brevirostrum* Lesueur, 1818) in the Hudson River Estuary, New York. In *Estuarine Research in the 1980s: The Hudson River Environmental Society Seventh Symposium on Hudson River Ecology* (Ed: C.L. Smith) State University of New York Press, pp. 187-216.
- Eadie, B.J. and J.A. Robbins. 1987. The role of particulate matter in the movement of hydrophobic organic compounds in Great Lakes. In: Advances in Chemistry Series No. 216, Sources and Fates of Aquatic Pollutants. R.A. Hites and S.J. Eisenreich (eds.), American Chemical Society. Chapter 11.
- Eadie, B.J., N.R. Morehead and P.F. Landrum. 1990. Three-phase partitioning of hydrophobic organic compounds in Great Lakes waters. *Chemosphere*. 20(1-2):161-178.

Endicott, D., R. Kreis, D. Griesmer, and L. Mackelburg. 1994. "PCB partitioning and bioaccumulation in Green Bay, Lake Michigan." Presented as a poster at the 15th Annual Meeting of the Society of Environmental Toxicology and Chemistry, October 30 - November 3, 1994, Denver, Colorado.

Ewald, G., and P. Larsson. 1994. Partitioning of ^{14}C -labeled 2,2',4,4'-tetrachlorobiphenyl between water and fish lipids. *Environmental Toxicology and Chemistry* 13(10):1577-1580.

Farrow, D.R.G., F.D. Arnold, M.L. Lombardi, M.B. Main and P.D. Eichelberger, 1986. The National Coastal Pollutant Discharge Inventory. Estimates for Long Island Sound; for Strategic Assessment Branch, Ocean Assessment Div., Office of Oceanography and Marine Assessment, NOD, NOAA; 40 pp.

Federal Emergency Management Agency (FEMA). 1982. Flood Insurance Study for the Town of Ft. Edward, New York, Washington County. Washington, D.C.

Feldman, R.S. 1992. PCB accumulation in Hudson River pumpkinseed sunfish and bullhead: influences of invertebrate prey. Ph.D. Dissertation, State University of New York.

Fish, P.A. and J. Savitz. 1983. Variations in home ranges of largemouth bass, yellow perch, bluegills, and pumpkinseeds in an Illinois lake. *Trans. Am. Fish. Soc.* 112:147-153.

Freeze, R.A., and J.A. Cherry. 1979. *Groundwater*. Prentice-Hall, Inc., Englewood Cliffs, New Jersey.

Gailani, J., C.K. Ziegler, and W. Lick. 1991. Transport of Suspended Solids in the Lower Fox River. *Journal of Great Lakes Research* Vol. 17, No. 4.

Gauthier, T.D. 1994. Aroclor Translation Procedures. Internal memorandum, July 7, 1994. Gradient Corporation, Cambridge, MA.

Geoghegan, P., M.T. Mattson, and R.G. Keppel. 1992. Distribution of the shortnose sturgeon in the Hudson River Estuary, 1984-1988. In *Estuarine Research in the 1980s: The Hudson River Environmental Society Seventh Symposium on Hudson River Ecology* (Ed: C.L. Smith) State University of New York Press, pp. 217-227.

Gerking, S.D. 1958. The restricted movement of fish populations. *Biol. Rev.* 34:221-242.

Gilbert, C.R. 1989. "Species Profiles: Life Histories and Environmental Requirements of Coastal Fishes and Invertebrates: Atlantic and Shortnose Sturgeons." U.S. Fish Wildl. Serv. Biol. Rep. 82(11.122). U.S. Army Corps of Engineers. TR EL-82-4. 28 pp.

Gobas, F.A.P.C. 1993. A model for predicting the bioaccumulation of hydrophobic organic chemicals in aquatic food-webs: Application to Lake Ontario. *Ecological Modelling* 69:1-17.

- Gobas, F.A.P.C., X. Zhang, and R. Wells. 1993. Gastrointestinal magnification: the mechanism of biomagnification and food chain accumulation of organic chemicals. *Environ. Sci. Technol.* 27:2855-2863.
- Gunn, J.M., S.U. Quadri and D.C. Mortimer. 1977. Filamentous algae as a food source for the brown bullhead (*Ictalurus nebulosus*). *J. Fish Res. Board Can.* 34:396-401.
- Harkey, G.A., M.J. Lydy, J. Kukkonen, and P.G. Landrum. 1994. Feeding selectivity and assimilation of PAH and PCB in *Diporeia* spp. *Environmental Toxicology and Chemistry* 13(9):1445-1455.
- Hasler, A.D. and W.J. Wisby. 1958. The return of displaced largemouth bass and green sunfish to a 'home' area. *Ecology* 39:289-293.
- Hjorth, D.A. 1988. Feeding selectivity of larval striped bass and white perch in the Hudson River Estuary. In *Fisheries Research in the Hudson River* (Ed: C.L. Smith) State University of New York Press, Albany, pp. 134-147.
- HydroQual, Inc. The Erosion Properties of Cohesive Sediments in the Upper Hudson River, prepared for the General Electric Company, 1995.
- Hydroscience, Inc. 1975. Development of a steady state water quality model for New York Harbor. Volume I, for ISC; 302 pp.
- Hydroscience, Inc. 1978a. Estimation of PCB reduction by remedial action on the Hudson River ecosystem. For NYS DEC; 107 pp.
- Hydroscience, Inc. 1978b. Seasonal steady state modeling. NYC 208 Task Report, Task 314 for Hazen & Sawyer Engineers, and NYC DWR; 697 pp.
- Jinks, S.M. and M.E. Wrenn. DATE NOT GIVEN. Radiocesium transport in the Hudson River Estuary. pp. 207-227.
- Johnson, J.H. 1983. Summer diet of juvenile fish in the St. Lawrence River. *New York Fish and Game Journal* 30(1).
- Jones, P.A., R.J. Sloan, and M.P. Brown. 1989. PCB congeners to monitor with caged juvenile fish in the Upper Hudson River. *Environ. Toxicol. Chem.* 8:793-803.
- Kadlec, M.J. 1994. Bioconcentration of Congener Specific Polychlorinated Biphenyl (PCB) in Rainbow Trout (*Oncorhynchus mykiss*) Exposed to the Water Column of the St. Lawrence River. M.S. Thesis, State University of New York at Albany
- Kadlec, M.J. and B. Bush. 1994. "Bioconcentration of Congener Specific Polychlorinated Biphenyl (PCB) in Rainbow Trout (*Oncorhynchus mykiss*) Exposed to the Water Column of the General Motors Superfund Site, Massena, N.Y." Presented at the Superfund XIV Conference, Hazardous Materials Research Institute, Washington, DC.

- Karickhoff, S.W., D.S. Brown and T.A. Scott. 1979. Sorption of hydrophobic pollutants on natural sediments. *Water Research*. 13:241-248.
- Karickhoff, S.W. 1984. Organic pollutant sorption in aquatic systems. *Journal of Hydraulic Engineering*. 110:707-735.
- Klauda, R.J., J.B. McLaren, R.E. Schmitt and W.P. Dey. 1988. Life history of white perch in the Hudson River estuary. *American Fisheries Society Monograph* 4:69-88. Also in *Science, Law and Hudson River Power Plants: A Case Study in Environmental Impact Assessment*.
- Kramer, R.H. and L.L. Smith, Jr. 1960. "Utilization of nests of largemouth bass, *Micropterus salmoides*, by golden shiners, *Notemigonus crysoleucas*." *Copeia* (1):73-74.
- Lake, J.L, N.I. Rubinstein, H. Lee II, C.A. Lake, J. Heltsche and S. Pavignano. 1990. Equilibrium partitioning and bioaccumulation of sediment-associated contaminants by infaunal organisms. *Environ. Tox. Chem.* 9:1095-1106.
- Larsson, P. 1984. Transport of PCBs from aquatic to terrestrial environments by emerging chironomids. *Environmental Pollution (Series A)*, 34:283-289.
- Lawler, Matusky & Skelly Engineers. 1992. "1990 Year Class Report of the Hudson River Estuary Monitoring Program." Report to Consolidated Edison Company of New York, Inc.
- LeBlanc, L. and B. Brownawell. 1994. "Tests of Bioaccumulation Models for PCBs: A Study of Young-of-the-Year Bluefish in the Hudson River Estuary." Report to the 1993 Polgar Fellowship Program. pp. VII-1 - VII-42.
- Lick, W., J. McNeil, Y. Xu, and C. Taylor. 1995. Resuspension Properties of Sediments from the Fox, Saginaw, and Buffalo Rivers. *Journal of Great Lakes Research*, International Association for Great Lakes Research. 21(2):257-274.
- Limno-Tech, Inc., 1992. Phase II Screening Model Application to Dioxin (2,3,7,8-TCDD) in the Columbia River. Report prepared for Tetra-Tech, Inc. under EPA Contract No. 68-C9-0013 and submitted to U.S. Environmental Protection Agency, Region X, Seattle, Washing.
- MacDonald, C.R., C.D. Metcalfe, G.C. Balch and T.L. Metcalfe. 1993. Distribution of PCB congeners in seven lake systems: interactions between sediment and food-web transport. *Environ. Toxicol. Chem.* 12:1991-2003.
- Mackay, D. 1979. Finding fugacity feasible. *Environ. Sci. Technol.* 13:1218.
- Madansky, A. 1988. *Prescriptions for Working Statistician*. Springer-Verlag, New York. 295p
- Makarewicz, J.C. 1987. "Hudson River Fisheries Study." Report to Halfmoon Electric Project for Interpower of New York, Inc.
- Mansueti, R.J. 1957. Movements, reproduction and mortality of the white perch in the Patuxent River estuary, Maryland. Diss. for D.SC. Johns Hopkins Univ.

- McBride, N.D. 1985. "Distribution and Relative Abundance of Fish in the Lower Mohawk River." New York State Department of Environmental Conservation, Stony Brook, New York.
- McFadden, J.T. Texas Instruments Incorporated and Lawler, Matusky & Skelly Engineers. 1978. Influence of the proposed Cornwall pumped storage project and steam electric generating plants on the Hudson River Estuary with emphasis on striped bass and other fish populations. Revised. Report to Consolidated Edison Company of New York, Inc.
- McLaren, J.B., J.C. Cooper, T.B. Hoff and V. Lander. 1981. Movements of Hudson River striped bass. *Trans. Am. Fish. Soc.* 110:158-167.
- Mehta, A.J., E.J. Hayter, W.R. Parker, R.B. Krone, and A.M. Teeter. 1989. Cohesive sediment transport. 1. Process Description. *J. of Hydr. Eng.* 115 (8), pp 1076-1093.
- Mehta, A.J., E.J. Hayter, W.R. Parker, R.B. Krone, and A.M. Teeter. 1989. Cohesive sediment transport. 2. Application. *J. of Hydr. Eng.* 115 (8), pp. 1094-1112.
- Menzie, C.A. 1980. The Chironomid (Insecta:Diptera) and other fauna of a *Myrophyllum spicatum* L. plant bed in the lower Hudson River. *Estuaries*, 3(1):38-54.
- Merritt, R.W. and K.W. Cummins. 1978. *An Introduction to the Aquatic Insects of North America.* (Iowa: Kendall/Hunt Publishing Company).
- Mesing, C.L. and A.M. Wicker. 1986. Home range, spawning migrations, and homing of radio-tagged Florida largemouth bass in two central Florida lakes. *Trans. Am. Fish. Soc.* 115:286-295.
- Malcolm Pirnie (MPI). 1984. "New York State Barge Canal Environmental Report Maintenance Dredging Program 1985-1995." Report to New York State Department of Transportation
- Mueller, J.A., J.S. Jeris, A.R. Anderson, C.F. Hughes, 1976. Contaminant Inputs to the New York Bight. Prepared by Manhattan College for MESA, ERL, NOAA; 347 pp.
- Nack, S. and W. Cook. 1986. Characterization of spawning and nursery habitats of largemouth bass (*Micropterus salmoides*) in the Stockport component of the Hudson River National Estuarine Research Reserve. In Polgar Fellowship Reports of the Hudson River National Estuarine Research Reserve Program (Eds: E.A. Blair and J.C. Cooper) New York State Department of Environmental Conservation, The Hudson River Foundation, and The U.S. Department of Commerce.
- National Oceanic and Atmospheric Administration (NOAA). 1984. "Emergency Striped Bass Study, Study V: Biotic Factors Affecting Juvenile Striped Bass Survival in the Hudson Estuary." U.S. Department of Commerce, National Marine Fisheries Service, September.

- Neter, J., Wasserman, W., and Kutner, M.H. 1985. Applied Linear Statistical Models, 2nd Ed., Richard D. Irwin, Inc.
- Novak, M.A., A.A. Reilly, and S.J. Jackling. 1988. Long-term monitoring of polychlorinated biphenyls in the Hudson River (New York) using caddisfly larvae and other macroinvertebrates. Arch. Environ. Contam. Toxicol. 17:699-710.
- Novak, M.A., A.A. Reilly, B. Bush and L. Shane. 1990. In situ determination of PCB congener-specific first order absorption/desorption rate constants using chironomus tentans larvae (insecta: diptera: chironomidae). Wat. Res. 24(3):321-327.
- NUS. April 1984. Volume 1, Feasibility Study, Hudson River PCBs Site, New York, EPA Contract No. 68-01-6699. Table 4-2, pp 4-13.
- O'Brien & Gere Engineers, Inc. 1993a. Hudson River project sampling and analysis program: 1991 sediment sampling and analysis program. Report to General Electric Co., Corporate Environmental Programs. Albany, New York.
- O'Brien & Gere Engineers, Inc. 1993b. 1991 hydrographic survey of the Upper Hudson River Hudson River project sampling and analysis program. General Electric Company, Corporate Environmental Programs. Albany, New York.
- O'Brien and Gere. 1993c. *Data Summary Report, Hudson River Project 1991-1992 Sampling and Analysis Temporal Water Column Monitoring Program*. Report to General Electric Company Corporate Environmental Programs. O'Brien and Gere Engineers, Inc., Syracuse, New York.
- O'Brien and Gere. 1993d. *Data Summary Report, Hudson River Project 1991-1992 Sampling and Analysis Program, 1991-1992 High Flow Water Column Monitoring Program*. Report to General Electric Company Environmental Program. O'Brien and Gere Engineers, Inc., Syracuse, New York.
- O'Brien and Gere. 1994. *Fort Edward Dam PCB Remnant Containment 1993 Post-Construction Monitoring Program*. May 1994. General Electric Co. Albany, New York.
- O'Connor, D.J. 1985. Modeling Frameworks. Toxic Substances Notes, Manhattan College Summer Institute in Water Pollution Control, Manhattan College, Bronx, New York.
- Oliver, B.G. 1987. Biouptake of chlorinated hydrocarbons from laboratory-spiked and field sediments by oligochaete worms. Environ. Sci. Technol. 21:785-790.
- Oliver, B.G., and A. J. Niimi. 1988. Trophodynamic analysis of polychlorinated biphenyl congeners and other chlorinated hydrocarbons in the Lake Ontario ecosystem. Environ. Sci. Tech. 22:388-397.
- Olsen, C.R. 1979. Radionuclides, sedimentation and the accumulation of pollutants in the Hudson Estuary. Ph.D. Dissertation, Columbia Univ. 343 pp.
- Parchure, T.M., and Mehta, A.J., 1985. "Erosion of soft cohesive sediment deposits." *J. Hydr. Engrg.*, ASCE, 111(10), 1308-1326.

- Neter, J., Wasserman, W., and Kutner, M.H. 1985. Applied Linear Statistical Models, 2nd Ed., Richard D. Irwin, Inc.
- Novak, M.A., A.A. Reilly, and S.J. Jackling. 1988. Long-term monitoring of polychlorinated biphenyls in the Hudson River (New York) using caddisfly larvae and other macroinvertebrates. Arch. Environ. Contam. Toxicol. 17:699-710.
- Novak, M.A., A.A. Reilly, B. Bush and L. Shane. 1990. In situ determination of PCB congener-specific first order absorption/desorption rate constants using chironomus tentans larvae (insecta: diptera: chironomidae). Wat. Res. 24(3):321-327.
- NUS. April 1984. Volume 1, Feasibility Study, Hudson River PCBs Site, New York, EPA Contract No. 68-01-6699. Table 4-2, pp 4-13.
- O'Brien & Gere Engineers, Inc. 1993a. Hudson River project sampling and analysis program: 1991 sediment sampling and analysis program. Report to General Electric Co., Corporate Environmental Programs. Albany, New York.
- O'Brien & Gere Engineers, Inc. 1993b. 1991 hydrographic survey of the Upper Hudson River Hudson River project sampling and analysis program. General Electric Company, Corporate Environmental Programs. Albany, New York.
- O'Brien and Gere. 1993c. *Data Summary Report, Hudson River Project 1991-1992 Sampling and Analysis Temporal Water Column Monitoring Program*. Report to General Electric Company Corporate Environmental Programs. O'Brien and Gere Engineers, Inc., Syracuse, New York.
- O'Brien and Gere. 1993d. *Data Summary Report, Hudson River Project 1991-1992 Sampling and Analysis Program, 1991-1992 High Flow Water Column Monitoring Program*. Report to General Electric Company Environmental Program. O'Brien and Gere Engineers, Inc., Syracuse, New York.
- O'Brien and Gere. 1994. *Fort Edward Dam PCB Remnant Containment 1993 Post-Construction Monitoring Program*. May 1994. General Electric Co. Albany, New York.
- O'Connor, D.J. 1985. Modeling Frameworks. Toxic Substances Notes, Manhattan College Summer Institute in Water Pollution Control, Manhattan College, Bronx, New York.
- Oliver, B.G. 1987. Biouptake of chlorinated hydrocarbons from laboratory-spiked and field sediments by oligochaete worms. Environ. Sci. Technol. 21:785-790.
- Oliver, B.G., and A. J. Niimi. 1988. Trophodynamic analysis of polychlorinated biphenyl congeners and other chlorinated hydrocarbons in the Lake Ontario ecosystem. Environ. Sci. Tech. 22:388-397.
- Olsen, C.R. 1979. Radionuclides, sedimentation and the accumulation of pollutants in the Hudson Estuary. Ph.D. Dissertation, Columbia Univ. 343 pp.
- Parchure, T.M., and Mehta, A.J., 1985. "Erosion of soft cohesive sediment deposits." *J. Hydr. Engrg.*, ASCE, 111(10), 1308-1326.

- Partheniades, E. 1965. Erosion and deposition of cohesive soils. J. Hydraulic Div., ASCE, 91 (HY1), pp 105-138.
- Piavis, P.G. 1991. Yellow Perch. Habitat Requirements for Chesapeake Bay Living Resources, Chesapeake Research Consortium, Inc. Solomons, Maryland. 2nd Edition. pp 14-15.
- Pizza, J.C. and J.M. O'Connor. 1983. PCB dynamics in Hudson River striped bass. II. Accumulation from dietary sources. Aquatic Toxicology 3:313-327.
- Preston, S.D., V.J. Bierman, Jr., and S.E. Silliman. 1989. An evaluation of methods for the estimation of tributary mass loads. Water Resources Research. 25(6):1379-1389
- Raney, E.C. and D. A. Webster. 1940. The food and growth of the young common bullhead, *Americurus nebulosus* (LeSueur) in Cayuga Lake, New York. Trans. Am. Fish. Soc. 69:205-209.
- Raney, E.C. 1952. The life history of the striped bass, *Roccus saxatilis* (Walbaum). Bull. Bingham Oceanog. Coll. 14:5-110.
- Raney, E.C. 1967. Some catfishes of New York. Conservationist 21(6):20-25.
- Raudkivi, A.J. 1990. Loose Boundary Hydraulics. 3rd edition. Pergamon Press.
- Riley, G.A. and H.M. Schurr, 1959. Transparency of Long Island Sound waters; bulletin of the Bingham Oceanographic Collection, Peabody Museum of Natural History, Yale University; Vol. 17, Article I. pp. 66-82.
- Sadzikowski and Wallace. 1976. A comparison of food habits of size classes of three sunfishes (*Lepomis macrochirus* [Rafinesque], *L. gibbosus* [Linnaeus] and *L. cyanellus* [Rafinesque]). Am. Midl. Nat. 95:220-225.
- Schaefer, R.H. 1970. "Feeding habits of striped bass from the surface waters of Long Island, NY." NY Fish and Game Journal, 17:1-17.
- Schlichting, H. 1979, Boundary-Layer Theory. McGraw-Hill, New York, New York.
- Scott, W.B. and E.J. Crossman. 1973. Freshwater Fishes of Canada. Bulletin 184. Fisheries Board of Canada, Ottawa.
- Setzler, E.M., W.R. Boynton, K.V. Wood, H.H. Zion, L. Lubbers, N.K. Mountford, P. Frere, L. Tucker, and J.A. Mihursky. 1980. Synopsis of biological data on striped bass, *Morone saxatilis* (Walbaum). NOAA Technical Report NMFS Circular 433, FAO Synopsis No. 121, U.S. Dept. of Commerce, Rockville, MD. 69 pp.
- Setzler-Hamilton, E.M. 1991. White Perch. Habitat Requirements for Chesapeake Bay Living Resources, Chesapeake Research Consortium, Inc. Solomons, Maryland. 2nd Edition. pp 12-20.
- Shaw, G.R. and D.W. Connell. 1984. Factors controlling bioaccumulation of PCBs. In PCBs and the Environment Volume 1 National Technical Information Service, pp. 501-516.

Shea, D. 1988. Developing national sediment quality criteria. *Environ. Sci. Technol.* 22:1256-1261.

Shindel, H.L. 1969. Time-of-Travel Study, Upper Hudson River, Fort Edwatd, New York to Troy Lock and Dam, New York. Report of Investigation RI-10, prepared by U.S. Geological Survey in cooperation with NYSDOH. State of New York, Conservation Department, Water Resources Commission.

Shoemaker, H.H. 1952. Fish home areas of Lake Myosotis, New York. *Copeia* 2:83-87.

Simpson, K.W. and R.W. Bode. 1980. Common Larvae of Chironomidae (Diptera) from New York State Steams and Rivers. Bulletin No. 439, New York State Museum, The University of the State of New York.

Simpson, K.W., M.A. Novak, and A.A. Reilly. 1986. Final report, biomonitoring of PCBs in the Hudson River. New York State Department of Health.

Skoglund, R.S., Stange, K., and D.L. Swackhamer. 1996. A Kinetics Model for Predicting the Accumulation of PCBs in Phytoplankton. *Environmental Science and Technology* 30:7, pp 2113-2120.

Sloan, R.J., M. Brown, R. Brandt and C. Barner. 1984. Hudson River PCB relationships between resident fish, water and sediment. *Northeastern Environmental Science*, 3(3/4): 137-151.

Smith, V.E., J.M. Spurr, J.C. Filkins, and J.J. Jones. 1985. Organochlorines contaminants of wintering ducks foraging on Detroit River sediments. *J. Great Lakes Res.* 11:231-246.

Smith, C.L. 1985. The Inland Fisheries of New York State. New York, New York State Department of Environmental Conservation, 522 pp.

Smith, S. 1987. Trophic status of the spottail shiner, (*Notropis hudsonius*) in Tivoli North Bay's Hudson River fresh tidal marsh. Polgar Fellowship Reports of the Hudson River National Estuarine Research Reserve Program.

TAMS/Gradient. 1991. Phase I Report Interim Characterization and Evaluation Hudson River PCB Reassessment RI/FS EPA Work Assignment No. 013-2N84 August 1991.

TAMS/Gradient. 1992. Final Phase 2 Work Plan and Sampling Plan Hudson River PCB Reassessment RI/FS EPA Work Assignment No. 013-2N84. September 1992.

TAMS/Gradient, 1992. Phase 2A Sampling & Analysis Plan-Quality Assurance Project Plan Hudson River PCB Reassessment RI/FS.

TAMS/Gradient. 1995. Further Site Characterization and Analysis Database Report. Phase 2 Report - Review Copy. TAMS Consultants, Inc. and Gradient Corporation. October 1995.

TAMS/CADMUS/Gradient. 1996. Further Site Characterization and Analysis Data Interpretation and Evaluation Report. Phase 2 Report - Draft Copy. TAMS Consultants, Inc., The CADMUS Group, Inc. and Gradient Corporation. August 1996.

Texas Instruments. 1976. Hudson River ecological study in the area of Indian Point. Thermal effects report. Dallas, Texas.

Texas Instruments. 1980. "1978 Year Class Report for the Multiplant Impact Study: Hudson River Estuary." Report to Consolidated Edison Company of New York, Inc., September.

Thomann, R.V. 1981. Equilibrium model of fate of microcontaminants in diverse aquatic food chains. Can. J. Fish. Aquat. Sci. 38:280-296.

Thomann, R.V. and J.P. Connolly. 1984. Model of PCB in Lake Michigan lake trout food chain. Environ. Sci. Technol. 18:65-71.

Thomann, R.V. and Salas, H.J., 1986. Manual on Toxic Substances in Surface Waters, Pan American Health Organization, CEPIS, Lima, Peru.

Thomann, R.V. and J.A. Mueller. 1987. *Principles of Surface Water Quality Modeling and Control*. Harper Row, Publishers, Inc., New York, New York.

Thomann, R.V. 1989. Bioaccumulation model of organic chemical distribution in aquatic food chains. Environ. Sci. Technol. 23:699-707.

Thomann, R.V., J.A. Mueller, R.P. Winfield and C.R. Huang. 1989. "Mathematical model of the long-term behavior of PCBs in the Hudson River estuary." prepared for the Hudson River Foundation, Grant #007/87A/030, 011/88A/030, June.

Thomann, R.V., J.A. Mueller, R.P. Winfield, and C.R. Huang. 1991. Model of fate and accumulation of PCB homologues in Hudson Estuary. Journal of Environmental Engineering, Vol. 117, No.2.

Thomann, R.V., J.P. Connolly, and T.F. Parkerton. 1992. An equilibrium model of organic chemical accumulation in aquatic food webs with sediment interaction. Environmental Toxicology and Chemistry 11:615-629.

Thomas, W. A. and W.H. McNally, Jr. 1990, User's manual for the generalized computer program system: open-channel flow and sedimentation, TABS-2. US Army Engineer Waterways Experiment Station, Vicksburg, Mississippi.

U.S. EPA. 1984. Technical Guidance Manual for Performing Waste Load Allocations, Book II: Streams and Rivers, Chapter 3, Toxic Substances. Office of Water Regulations and Standards, Monitoring and Data Support Division. EPA-440/4-84-022.

U.S. EPA. 1991. Proposed technical basis for establishing sediment quality criteria for nonionic organic chemicals using equilibrium partitioning. August 1991. Office of Science and Technology, Health and Ecological Criteria Division, Washington, DC.

U.S. EPA. 1994. Great Lakes water quality initiative technical support document for the procedure to determine bioaccumulation factors. EPA-822-R-94-002. Office of Water, Office of Science and Technology, Washington, DC.

van der Oost, R., H. Heida, and A. Oppenhuizen. 1988. Polychlorinated biphenyl congeners in sediments, plankton, molluscs, crustaceans, and eel in a freshwater lake: Implications of using reference chemicals and indicator organisms in bioaccumulation studies. *Arch. Environ. Contam. Toxicol.* 17:721-729.

Velleux, M. and D. Endicott. 1994. Development of a mass balance model for estimating PCB export from the lower Fox River to Green Bay. *Journal of Great Lakes Research*, Vol. 20, No. 2.

Waldman, J.R. 1988a. 1986 Hudson River striped bass tag recovery program. The Hudson River Foundation, New York, NY 48 pp + Append.

Waldman, J.R. 1988b. Private Communication

Whittle, D.M. and J.D. Fitzsimmons. 1983. The influence of the Niagara River on contaminant burdens of Lake Ontario biota. *J. Great Lakes Res.* 9(2):295-302.

Wood, L.W. G.Y. Rhee, B. Bush and E. Barnard. 1987. Sediment desorption of PCB congeners and their bio-uptake by dipteran larvae. *Water Res.* 21:875-884

Woolfolk, M., M. Barta, and G. Drendel. 1994. "Modeling the Accumulation of PCBs in Largemouth Bass from Lake Hartwell, South Carolina." Presented at SETAC.

Wrenn, M.E., S.M. Jinks, L.M. Hairr, A.S. Paschoa, and J.W. Lentsch. 1972. Natural activity in Hudson River Estuary samples and their influence on the detection limits for gamma emitting radionuclides using NaI Gamma Spectrometry. *Proc. Second Int. Symp. on the Natural Rad. Environ.* Rice Univ., Houston, TX, onf-720805-P2, pp. 897-916.

Xu, Y. 1991. Transport properties of fine-grained sediments. Ph.D. dissertation. University of California at Santa Barbara.

Young, R.A. and B.F. Hillard. 1984. Suspended matter distributions and fluxes related to the Hudson-Raritan Estuarine plume; NOAA Tech. Memo NOS OMA 8, Rockville, MD, 32 pp.

Young. 1988. A report on striped bass in New York marine water. NYS Marine Fisheries, Stony Brook, NY.

Zimmie. 1985. Assessment of erodibility of sediments in the Thompson Island Pool of the Hudson River. Final Report to the Office of Special Projects, New York State Department of Environmental Conservation. US EPA Grant No. C-36-1167-01.

GLOSSARY

Abbreviations and Acronyms

BAF	Bioaccumulation Factor
BCF	Bioconcentration Factor
BSAF	Benthic Invertebrate: Sediment Accumulation Factors
CD-ROM	Compact Disc - Read Only Memory
cfs	Cubic feet per second
cm	Centimeter
Corp.	Corporation
deg. C	Degree Celsius
DOC	Dissolved Organic Carbon
e.g.	For example
EPA	Environmental Protection Agency
et al.	and others
FA	Flow Average (Phase 2 Water Column Monitoring Program)
FEMA	Federal Emergency Management Agency
FFBAF	Forage Fish: Diet Accumulation Factors
FGET	Food and Gill Exchange of Toxic Substances Model
foc	Fraction organic carbon
fps	Feet per second
g	Gram
GBTOX	Green Bay Mass Balance Model
GE	General Electric
GIS	Geographic Information System
GLI	Great Lake Initiative
HEC-2	US Army Corps of Engineers, Hydraulic Engineering Center, Surface Water Profile Model
HOC	Hydrophobic Organic Chemicals
HUDTOX	Hudson River Mass Balance Model
i.e.	That is
kg	Kilogram
m/s	Meters per second
mg/l	Milligrams per liter
mi ²	Square miles
MT	Metric Ton
MVUE	Minimum Variance Unbiased Estimator
NAPL	Non-aqueous Phase Liquid
ng/m ³	Nanograms per cubic meter
ng/L	Nanograms per liter
NGVD	National Geodetic Vertical Datum
NOAA	National Oceanic and Atmospheric Administration
NYSDEC	New York State Department of Environmental Conservation
NYSDOH	New York State Department of Health
NYSDOT	New York State Department of Transportation

OC	Organic Carbon
PCBs	Polychlorinated Biphenyls
PFBAF	Piscivorous Fish: Diet Accumulation Factors
RI/FS	Remedial Investigation/Feasibility Study
RMA-2V	Thompson Island Pool Hydrodynamic Model
ROD	Record of Decision
RPI	Rensselaer Polytechnic Institute
TIN	Triangulated Irregular Network
TIP	Thompson Island Pool
TSF (tsf)	Temperature slope factor
TSS	Total Suspended Solids
ug/g (ppm)	Micrograms per gram (parts per million)
μg/L	Micrograms per liter
USEPA	United States Environmental Protection Agency
USGS	United States Geological Survey
WASP4	USEPA, Water Quality Analysis Simulation Program, Version 4
TOXI4	Toxic Chemical Module in WASP4
WASTOX	USEPA toxic chemical modeling framework
WY	Water year